

# 1 APPENDIX F

## 2 PROPOSED GUIDE SPECIFICATION 3 APPLICATION EXAMPLES

### 4 F.1 Introduction

5 Based on the work performed to characterize the redundancy of the bridges studied, a set of requirements  
6 was developed so an Engineer can establish whether a steel bridge possesses an adequate level of  
7 redundancy after the failure of a main tension member. Given that the characterization of redundancy  
8 requires the consideration of every alternate load path and complex interactions between the components  
9 of a bridge, 3-D finite element analysis (FEA) is considered as the most suitable analysis tool.

10 The FEA methodology developed in NCHRP Project 12-87a is applicable to typical steel bridges that  
11 contained members designated as fracture critical members (FCMs): simple span and continuous I-girder  
12 and tub-girder bridges, through-girder bridges, truss bridges, and tied-arch bridges. The methodology has  
13 not been thoroughly benchmarked for non-typical steel bridges, i.e., cable stayed bridges, suspension  
14 bridges, etc. However, the overall methodology discussed hereafter may be used to evaluate non-typical  
15 bridges at the discretion of the Owner and/or Engineer. For a bridge superstructure which has one or more  
16 members that may be considered as fracture critical members (FCMs), the redundancy analysis consists of  
17 the following required steps:

- 18
- 19 1. Selection of an adequate finite element analysis tool as described in section F.1.1.
- 20 2. Construction of a three-dimensional finite element model capable of simultaneously capturing  
21 material and geometrical non-linearity and the formation of alternative load paths. The  
22 construction of these model requires the analyst to:
  - 23 • Construct the geometry, meshes and of the different components of the superstructure  
24 steelwork as described in section F.1.2.
  - 25 • Construct the geometry, meshes and of the concrete slab and concrete barriers as described  
26 in section F.1.3.
  - 27 • Model the connections between the steelwork components, including connection failure  
28 and/or flexibility when required. This requirement is described in section F.1.4.
  - 29 • Model the frictional contact interaction between the slab and the steelwork, and model  
30 shear stud behavior when required, as described in section F.1.5.
  - 31 • Include the effect of the flexibility of the substructure as described in section F.1.6.
- 32 3. Identification of steel members that are subjected to net tension across its entire or a portion of its  
33 cross-section, and which failure is suspected to result in collapse or loss of serviceability. At the  
34 very least, the Engineer must include that least the following, considering one complete member  
35 failure, i.e., the entire cross-section of the member is failed,, at a time:
  - 36 • In girder bridges (I-girder, tub-girder, wide flange girder, and through-girder bridges), at  
37 least, the following member failures shall be investigated:

- In continuous spans of girder bridges, member failure shall be assumed in both an end span and at least one interior span at the most critical location in the positive moment region of each span.
  - In simple-span girder bridges, member failure shall be assumed at the most critical location for positive moment within the span.
  - In continuous I-girder bridges, in regions with high shear and negative moment, e.g., interior supports, member failure shall be assumed at the most critical location.
  - In truss bridges, at least, the following member failures shall be investigated: In simple-span truss bridges, member failure shall be assumed in at least one tension shear diagonal and one tension chord.
    - In continuous spans of truss bridges, member failure shall be assumed in at least one tension chord in the positive and negative moment regions in both an end and an interior span.
    - In continuous spans of truss bridges, member failure shall be assumed in at least one shear diagonal in the positive and negative moment regions in both an end and an interior span.
    - In multi-span truss bridges, where an interior span is to be considered, the member failure scenarios shall be considered for the longest interior span.
    - In all truss bridges, member failure shall be assumed in a single truss hanger.
  - In tied-arch bridges, at least, the following member failures shall be investigated:
    - In tied-arch bridges, member failure shall be assumed in the tension tie at a critical location within the span. This location may be at midspan or at a location where the deck and stringers are discontinuous, such as at a deck joint at some location near mid span.
    - In tied-arch bridges, member failure shall be assumed in the tension tie near the intersection with the arch.
  - Regarding floor beam systems in girder bridges, in single interior floor beams, member failure shall be assumed at mid span of the floor beam. Floor beams located where stringers are not continuous and/or where deck joint are present shall be investigated.
  - Regarding cross-girders, also known as integral pier caps, steel bent caps, etc., the failure of a cross-girder must be assumed at mid span and near the support or column.
4. Analysis of the failure of each steel tension member in the constructed finite element model. In the analysis, the structure must be subjected to load conditions representative of two scenarios: (1) the occurrence of the member failure (Redundancy I), and (2) an extended period of service between the failure event and the structure being repaired or replaced (Redundancy II). The required analysis procedures are described in section F.1.8.
  5. Comparison of the results of each individual analysis with a set of minimum performance requirements. This includes satisfaction of strength and serviceability requirements as described in section F.1.9.

These analysis steps are summarized in the flowchart shown in Figure F-1. The requirements are further explained in section F.1.1 through section F.1.9.

Additionally, the following examples of the application of the analysis methodology can be found for further clarification of the analysis methodology:

- a. A continuous two span curved twin tub girder bridge is analyzed in section F.2.
- b. A simple span through-girder is analyzed in section F.3.
- c. A simple span tied-arch bridged is analyzed in section F.4.
- d. A continuous three span plate girder bridge with a three girder cross section is analyzed in section F.5.

87 In these examples the behavior of the bridge after the failure of a primary steel tension member (that may  
88 be designated as a fracture critical member) is evaluated. If the faulted structure is able to meet the  
89 requirements described in the proposed guide specification in Appendix E, the member which failure is  
90 assumed may be re-designated as a system redundant member (SRM); otherwise, such member shall be  
91 designated as a fracture critical member (FCM).  
92

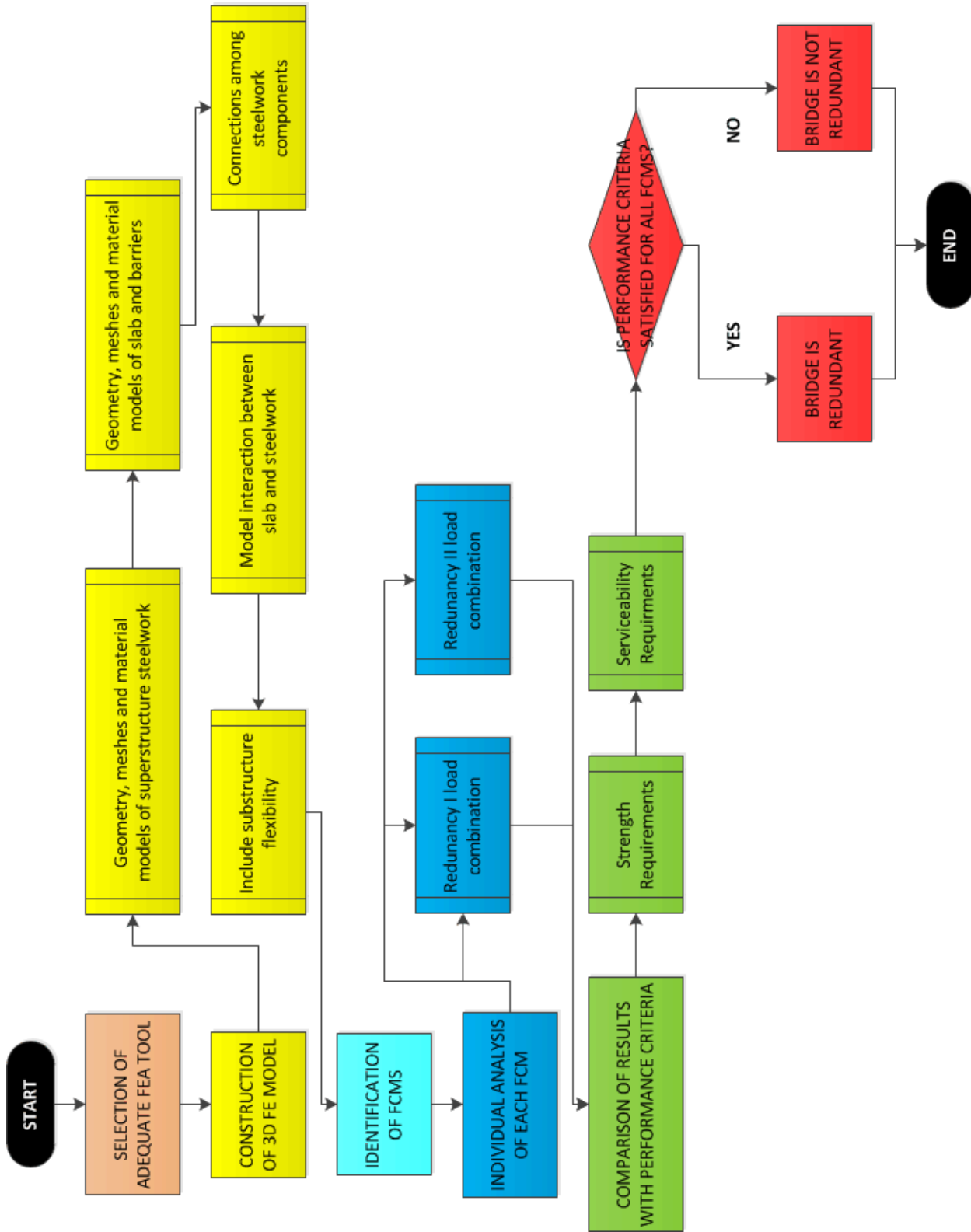


Figure F-1. Flowchart showing overall system analysis procedure.

## 95 **F.1.1 Analysis Software and Solution Procedure Requirements**

96 Although the methodology that has been developed was implemented using Abaqus, the Engineer may  
97 utilize any software and solution procedure provided that:

- 98 a. The geometry of the finite element model is three-dimensional.
- 99 b. Inertial effects are either neglected (static analysis) or negligible (quasi-static analysis). The kinetic  
100 energy shall not be larger than 5% of the strain energy of the system.
- 101 c. The system is stable for the time increments specified. For an implicit analysis the system will be  
102 unconditionally stable. For an explicit analysis the system stability will be conditional to a stable  
103 time increment that depends on the size, mass and stiffness of the utilized methods.
- 104 d. Non-linear geometry, or, in other words, large deformation theory with finite strains and finite  
105 rotations is considered.
- 106 e. The pouring sequence of the slab is considered. Particularly, the finite element analysis must  
107 consider:
- 108 • The slab does not carry any significant portion of dead loads prior to hardening.
  - 109 • When dead loads are applied, the slab does not provide any significant stiffness prior to  
110 hardening.
  - 111 • The slab must deform in accordance with the deformation of the structural steel during the  
112 application of dead load. The slab shall not sag nor slump between girders excessively,  
113 although minor deformations reasonably consistent with real in-situ behavior are  
114 acceptable.
  - 115 • Once dead load is applied, and the slab has deformed appropriately, it must be able to carry  
116 live loads and contribute to the stiffness of the system after it has hardened.
- 117 f. Gradual failure of a primary member can be modeled without significantly increasing kinetic  
118 energy. Stress and displacement amplifications are considered through the use of fracture  
119 amplification factors. The Engineer shall not model the dynamic behavior of the structure due to  
120 sudden failure of a primary steel member; but shall model how failure of a main member alters  
121 static load distribution. In order to achieve that, the structure shall be subjected to its own factored  
122 dead load in the undamaged state and then subjected to failure of a primary member. Factored live  
123 loads and dynamic load allowance, and amplification of load per the dynamic amplification factor  
124 are applied after the failure of a primary steel tension member is modeled.
- 125 g. Material non-linearity, particularly plasticity of steel and concrete inelasticity, can be explicitly  
126 modeled.
- 127 h. The software is capable of modeling kinematic constraints. Particularly the following constraints  
128 must be performed:
- 129 • Embedment: For a truss or beam element embedded in a host solid element, the  
130 translational degrees of freedom of the nodes of the embedded element are constrained to  
131 the interpolated values of the corresponding degrees of freedom of the host element. This  
132 constraint is used to model the interaction between rebar and concrete.
  - 133 • Tie: The motion of a slave surface or node group is set equal to the motion of a master  
134 surface.
  - 135 • Coupling: The motion of a slave surface or node group is constrained to the motion of a  
136 master node.
- 137 i. The software is capable of modeling the contact interaction between the slab and the steelwork.  
138 This includes normal contact and frictional behavior.
- 139 j. The following finite elements are implemented in the software:
- 140 • 8-node linear bricks with reduced integration (ideally with hourglass control).
  - 141 • 4-node shells with reduced integration and finite membrane strains (ideally with hourglass  
142 control).

- 143                   • 2-node linear shear-flexible (Timoshenko) beam elements.
- 144                   • 2-node truss elements with linear displacement.
- 145                   • 2-node three-dimensional spring elements. Coupled force-displacement and moment-rotation relations, elastic and inelastic behavior shall be available in these elements.
- 146
- 147           k. Surface tractions, body forces and prescribed displacements can be applied to the geometries of the
- 148           finite element model.

## 149 **F.1.2 Requirements for Modeling the Behavior of Steel Components**

150       All steel components must follow a linear elastic-kinematic hardening plastic material constitutive  
151       model. Unless shown otherwise through material testing, the following assumptions can be made regarding  
152       steel material properties:

- 153           a. The modulus of elasticity can be assumed to be 29,000 ksi and the Poisson's ratio shall be 0.3.
- 154           b. Hardening shall be linear, with yield onset at nominal yield strength and reaching nominal ultimate  
155           strength at a plastic strain of 0.05.
- 156           c. The steel element shall fail or be deleted once a plastic strain of 0.05 is reached to simulate ductile  
157           fracture.

158       Depending on the type of member modeled, the following elements and meshing procedures shall be  
159       followed:

- 160           a. The following steel members shall be modeled with 4-node shells with reduced integration and  
161           finite membrane strains (ideally with hourglass control):
  - 162                   • All steel members in contact with the slab.
  - 163                   • Tub girders in tub girder systems.
  - 164                   • Plate girders and stringers in plate girder systems.
  - 165                   • Truss members for primary truss members (i.e., not cross bracing between plate girders).
  - 166                   • Fabricated plate floor beams.

167       At least four elements must be used in the along the component width, flange width and/or along  
168       the web height must be used. The element maximum aspect ratio shall be kept under 5, and corner  
169       angles kept between 60 and 120 degrees.

- 170           b. Other members shall be modeled with 2-node linear shear-flexible (Timoshenko) beam elements.  
171           At least three elements must be used along the length of the element. Examples of other steel  
172           members are:
  - 173                   • Lateral bracing.
  - 174                   • Truss floor beams.
  - 175                   • Other secondary slender elements not typically designed to carry primary loads.

176       Vertical stiffeners in plate and tub girder may be either explicitly modeled with shell elements or through  
177       a coupling constraint. If shell elements are used, one element through the width of the stiffening element  
178       is sufficient, but maximum aspect ratio shall be kept under 5, and corner angles kept between 60 and 120  
179       degrees. If coupling constraints are used, they shall be applied to prevent cross-sectional distortion at the  
180       location of the stiffener.

## 181 **F.1.3 Requirements for Modeling the Behavior of Concrete Slabs**

182       The geometry of the concrete slab shall be modeled per one or a combination of the following approaches:

- 183           a. With truss (wire) elements embedded in solid elements:
  - 184                   • The elements modeling the concrete slab shall be 8-node linear brick elements with reduced  
185                   integration. The material model of the solid elements shall model the behavior of concrete.
  - 186                   • A minimum of eight elements shall be used through the thickness of the slab in the regions  
187                   close to the fracture, which is generally within a distance of one half the width of the deck

188 on each side of the failure location. Fewer elements may be used through the thickness in  
189 other regions, but no fewer than four shall be used. The maximum element aspect ratio  
190 shall be less than 5. Unless prohibited by the geometry of the slab, corner angles shall be  
191 kept between 40 and 140 degrees. At the locations in contact with steelwork, e.g., bottom  
192 slab haunches, the mesh density should be higher than the mesh density of the steelwork  
193 to ensure proper enforcement of the contact interaction.

194 • The reinforcing steel within the slab shall be modeled by using wire elements embedded  
195 within the solid elements. The material model of the wire elements shall model the  
196 behavior of the steel rebar. The elements shall be 2-node linear truss elements. The length  
197 of the wire elements shall be approximately equal to the largest dimension of the concrete  
198 element.

199 • Concrete barriers and their reinforcement may be included as part of the slab system.

200 b. With shell elements that implicitly consider the effect of the steel reinforcement layers:

201 • The elements modeling the reinforced concrete slab shall be 4-node linear shells with  
202 reduced integration, finite membrane strains, and a minimum of 5 Simpson thickness  
203 integration points.

204 • The effect of the reinforcement shall be included as a material property or in the integration  
205 of the shell section.

206 • The Engineer shall test the performance of the shell element when the effects of the  
207 reinforcement are included in the element formulation, and verify that the nominal shear  
208 resistance of the slab is not exceeded.

209 • In general, the mesh density shall be similar to the one utilized for the steel elements. At  
210 the locations in contact with steelwork, e.g., bottom slab haunches, the mesh density should  
211 be higher than the mesh density of the steelwork to ensure proper enforcement of the  
212 contact interaction. Haunches may be modeled with additional superimposed layers of  
213 shell elements.

214 The material behavior of rebar shall follow a linear elastic-kinematic hardening plastic material  
215 constitutive model. Unless shown otherwise through material testing, the following assumptions can be  
216 made regarding steel material properties:

217 a. The modulus of elasticity of the rebar shall be assumed to be 29,000 ksi and the Poisson's ratio  
218 shall be 0.3.

219 b. Hardening shall be linear, with yield onset at nominal yield strength and reaching nominal ultimate  
220 strength at a plastic strain of 0.05. Once a plastic strain of 0.05 is reached the steel element shall  
221 fail or be deleted.

222 The material behavior of concrete is based on its nominal compressive strength ( $f'_c$ ) in ksi. Initially, the  
223 material shall be linear elastic, with modulus of elasticity as follows:

$$224 E_c = 33,000(w_c)^{1.5}(f'_c)^{0.5} \leq 1802.5(f'_c)^{0.5}$$

225 where  $w_c$  is the density of concrete in kcf, and Poisson's ratio of 0.3.

226 Concrete inelasticity shall be different for tension and compression. The tension behavior is based on  
227 the provisions in the fib Model Code for Concrete Structures (2010). In tension, the behavior is linear  
228 elastic until tensile the strength of concrete,  $f_t$ , defined as follows:

$$229 f_t = \begin{cases} 0.158(f'_c)^{2/3} & \text{for } f'_c \leq 7.25 \text{ ksi} \\ 0.307 \ln(f'_c + 2.61) - 0.114 & \text{for } f'_c > 7.25 \text{ ksi} \end{cases}$$

230 is reached. At that point failure shall occur with a fracture energy,  $G_t$  (in ksi-in), defined as follows:

$$231 G_t = 5.9 \cdot 10^{-4}(f'_c + 1.16)^{0.18}$$

232 In compression, the elements modeling concrete cannot reach compressive stress in excess of  $f'_c$ , and  
233 should follow the stress-strain Popovics' stress-strain relation, which is:

234

$$f(\varepsilon) = f'_c \left( \frac{\varepsilon}{\varepsilon_c} \right) \left[ \frac{n}{n - 1 + \left( \frac{\varepsilon}{\varepsilon_c} \right)^n} \right]$$

235 where  $f'_c$  is the compressive strength of concrete,  $\varepsilon_c$  is the total strain at compressive strength, and  $n$  is a  
 236 parameter calculated from experimental data. It should be noted that  $\varepsilon$  is the total strain ( $\varepsilon = \varepsilon_{elastic} +$   
 237  $\varepsilon_{plastic}$ ). The total strain at compressive strength,  $\varepsilon_c$ , the experimental parameter,  $n$ , and the plastic strain,  
 238  $\varepsilon_{plastic}$ , may be calculated as:

239

$$n = 0.4f'_c + 1.0$$

240

$$\varepsilon_c = 0.00124 \sqrt[4]{f'_c}$$

241

$$\varepsilon_{plastic} = \varepsilon - \frac{f(\varepsilon)}{E_c}$$

#### 242 **F.1.4 Requirements for Modeling Attached Steel Components**

243 Connections between individual steel components shall transfer forces in accordance with the behavior  
 244 of the connection. When calculated capacities of the connected members are lower than the calculated  
 245 capacity of the connection, it shall be sufficient to model the attachment through appropriate constraints.  
 246 In the cases in which the connection capacity is lower than member capacity, the connection capacity shall  
 247 be considered either by reducing member capacity or by explicitly modeling connection failure. When  
 248 connection plates exist and they increase the flexibility of the connection, their effect shall be considered.  
 249 Eccentricity that may exist due to the configuration of the connection shall also be considered, such as when  
 250 only one leg of an angle is connected to another component. The capacity of the connection shall be  
 251 computed in accordance with the provisions in the AASHTO LRFD BRIDGE Design Specifications (2014)  
 252 (AASHTO LRFD BDS), which nominal (unfactored) values are to be input in the finite element model as  
 253 needed. For bolted connections, it is recommended to consult the provisions in Eurocode 3 (CEN, 2007)  
 254 and/or Henriques et al. (2014) to calculate the stiffness the connection assembly, and the work of Sarraj  
 255 (2007) to determine the maximum displacement at failure.

#### 256 **F.1.5 Requirements for Modeling Interactions between Slab and Steelwork**

257 Normal and tangential behavior of the contact interaction between slab and structural steel shall be  
 258 considered in the analysis. Any contact enforcement method and contact algorithm may be used by the  
 259 Engineer provided that:

260

a. Elements in contact shall be allowed to separate and/or slip.

261

b. The normal behavior follows a hard pressure-overclosure relation. This means that elements in  
 262 contact are not allowed to penetrate each other (although negligible penalty penetrations are  
 263 acceptable), and that the contact pressure is only limited by the bearing capacity of the elements in  
 264 contact. If the elements are not in contact, the contact pressure shall be zero.

265

c. The tangential behavior shall be Coulomb's friction. The coefficient of friction shall be 0.55 with  
 266 a maximum interfacial shear stress of 0.06 ksi.

267

268

269

270

271

When shear studs exist between the slab and the steelwork, both the axial and shear behavior for the  
 shear studs shall be modeled. The prescribed force-displacement behavior shall be calculated in accordance  
 with the governing failure mode of the shear stud group. E.g., the shear force-displacement curve shall  
 capture the shear stud yielding or concrete crushing; the axial force-displacement curve shall capture the  
 concrete breakout or split out. Shear stud modeling recommendations are detailed in Appendix A.



272 **F.1.6 Requirements for Modeling Substructure Flexibility**

273 At the locations in which the superstructure transverse and/or longitudinal displacements are constrained  
274 by the substructure, the flexibility of the structure must be considered as well as the strength of the support  
275 or bearing. It is not necessary to model the substructure in detail, but, at least, a linear elastic relations  
276 between horizontal reaction forces and horizontal displacements shall be applied at the support point. It  
277 shall be noted that transverse and longitudinal force-displacement relations are coupled if either the  
278 superstructure or the substructure are asymmetric, or if the bridge is skewed. When calculating the stiffness  
279 of the substructure, the loads due to self-weight of the superstructure shall be considered to account for the  
280 effects on stability and load stiffening.

281 The flexibility of the substructure in the vertical direction may be neglected (the substructure may be  
282 assumed to be rigid in the vertical direction). Uplift of the superstructure should be allowed if the  
283 connection between superstructure and substructure does not provide resistance against uplift.

284 **F.1.7 Required Minimum Loads in Analysis**

285 Two load combinations, Redundancy I and Redundancy II, must be evaluated to ensure that a bridge has  
286 sufficient capacity after the failure of a main tension component. The appropriate load factors depend upon  
287 whether the steel bridge under analysis is constructed in accordance to the Fracture Control Plan (FCP) or  
288 not. For bridges constructed to Section 12 of the AWS D1.5 (FCP), the load combinations are as follows:

289 
$$\text{Redundancy I (FCP): } (1 + DA_R)(1.05DC + 1.05DW + 0.85LL)$$

290 
$$\text{Redundancy II (FCP): } 1.05DC + 1.05DW + 1.30(LL + IM)$$

291 For bridges that do not meet FCP requirements, the load combinations are as follows:

292 
$$\text{Redundancy I (Non - FCP): } (1 + DA_R)(1.15DC + 1.25DW + 1.00LL)$$

293 
$$\text{Redundancy II (Non - FCP): } 1.15DC + 1.25DW + 1.50(LL + IM)$$

294 In these combinations  $DC$  is the dead load of structural components and nonstructural attachments,  $DW$   
295 is the dead load of wearing surfaces and utilities,  $LL$  is vehicular live load,  $DA_R$  is the dynamic amplification  
296 during the fracture event, and  $IM$  is vehicular dynamic load allowance.

297 The vehicular live load ( $LL$ ) applied in the Redundancy I and Redundancy II load combinations is the  
298 HL-93 live load model. This load model is composed of the design truck (or tandem) and a lane load of  
299 0.64 klf distributed over a 10 feet width.

300 The application of the vehicular live load is different for Redundancy I and Redundancy II load  
301 combinations:

302 a. For Redundancy I:

- 303 • Only the striped or normal travel lane(s) shall be considered.
- 304 • The design truck or design tandem and the design lane load of the HL-93 vehicular live  
305 load model shall be centered within the striped or normal travel lane(s).

306 b. For Redundancy II:

- 307 • The number of lanes to be considered shall be taken as specified in Article 3.6.1.1.1 in the  
308 AASHTO LRFD BDS.
- 309 • The design lanes shall be positioned transversely to produce the largest demands on the  
310 remaining intact components of the bridge.
- 311 • The HL-93 live load model shall be transversely place within the design lanes to produce  
312 the largest demands on the remaining components of the structure.
- 313 • The design truck or design tandem shall be positioned transversely such that the center of  
314 any wheel load is not closer than 2.0 ft from the edge of the design lane.

315 The longitudinal positioning of live load for the redundancy evaluation of longitudinal primary members  
316 shall be as follows:

- 317 • Where the failure section is in a region of positive moment under dead load, the design tandem  
318 or centroid of the design truck of the HL-93 vehicular live load model shall be positioned  
319 longitudinally coincident with the location of the assumed damage in the faulted member.
- 320 • When the failure section is in a region of negative moment under dead load, the HL-93 vehicular  
321 live load model shall be applied as described in the third bullet of Article 3.6.1.3.1 in the  
322 AASHTO LRFD BDS.

323 Multiple presence factors shall be applied as specified in Article 3.6.1.1.2 in the AASHTO LRFD BDS  
324 in both, Redundancy I and Redundancy II, load combinations.

325 For the Redundancy I load combination, the applied dead and live loads shall be amplified by a fracture  
326 amplification factor,  $DA_R$ . The dynamic amplification during the fracture event must be 40% of the  
327 combined and factored  $DC$ ,  $DW$  and  $LL$ , unless the structure is a continuous twin tub girder with individual  
328 span shorter than 225 ft where it must be 20% of the combined and factored  $DC$ ,  $DW$  and  $LL$ . Other values  
329 may be used when backed by the comprehensive and detailed dynamic analysis.

330 For the Redundancy II load combination, the vehicular live loads shall be amplified by a vehicular  
331 dynamic load allowance,  $IM$ . The vehicular dynamic load allowance must be 15% of the factored design  
332 truck or design tandem portion of the HL-93 vehicular live load.

333 The HL-93 live load model, subjected to the appropriate load factors, multiple presence factors,  $DA_R$   
334 and/or  $IM$  shall be applied to minimize any possible inertial effects. It is recommended to apply them  
335 through a smooth amplitude curve such as the following:

336 
$$LR(t) = 6 \left(\frac{t}{T}\right)^5 - 15 \left(\frac{t}{T}\right)^4 + 10 \left(\frac{t}{T}\right)^3$$

337 where  $LR(t)$  is the fraction of load at a load application time  $t$ , and  $T$  is the duration of the load application.  
338 The duration of the load application must be larger than the fundamental period of the structure to minimize  
339 oscillatory behavior in the final explicit dynamic analysis.

340 **F.1.8 Required Analysis Procedure**

341 The analysis procedure shall be static or quasi-static. If a quasi-static analysis procedure is utilized,  
342 experience has shown that the kinetic energy of the system shall not be greater than 5% of the strain energy  
343 of the system. The required analysis procedure for Redundancy I and Redundancy II load combinations  
344 shall be follow the following four steps:

- 345 1. Application of factored dead load of structural components and nonstructural attachments,  $DC$ . This  
346 step must follow these requirements:
  - 347 • Dead loads shall be applied as body forces.
  - 348 • The slab shall not contribute to the stiffness of the system and shall not carry any significant  
349 portion of the dead load.
  - 350 • The slab deformation shall conform to the deformation of the steelwork.
- 351 2. The stiffness of the slab elements shall be changed to their final values assuming the concrete is  
352 fully cured. This step must follow this requirements:
  - 353 • The slab must retain the deformed shape computed in step 1 and not carry any significant  
354 portion of dead load.
  - 355 • The steelwork must retain the stresses and deformations computed in step 1.
- 356 3. Application of factored dead load of wearing surfaces and utilities,  $DW$ . The load effect of the  
357 pavement may be modeled by specifying a layer of relatively soft solid or shell elements (Engineer  
358 should refer to SHRP-A-388 as asphalt stiffness varies very significantly with temperature) and  
359 apply the correspondent body force.
- 360 4. The appropriate section of the main member is fractured and the system is allowed to redistribute  
361 the factored dead load. The amount of material that is removed or softened shall match that portion  
362 which would actually fail as closely as possible. In other words, if a crack is simulated, the width

363 of the member that shall be deleted or softened shall correspond to a very narrow width. Removal  
364 of a large portion of the member in this case is not acceptable. Removal can be accomplished by  
365 gradually softening the behavior of the elements that form the failing section. It is noted that at this  
366 point the slab does contribute to the stiffness of the system and is able to carry load.

- 367 5. Application of the dynamic amplification factor ( $DA_R$ ) to  $DC$  and  $DW$ . This step is only carried  
368 out in the Redundancy I load combination.
- 369 6. Application of factored and amplified vehicular live loads,  $LL$ . It shall be noted that  $LL$  is subjected  
370 to loads factors and multiple presence factors, as well as dynamic amplification ( $DA_R$ ) in the  
371 Redundancy I load combination or dynamic load allowance ( $IM$ ) in the Redundancy II load  
372 combination. These shall be applied as surface tractions normal to the slab surface. Details  
373 regarding the application and positioning of the live loads are described in section F.1.7.
- 374 7. Application of an additional 15% of live loads. This is not to be confused with the 15% related to  
375 vehicular dynamic load allowance.

### 376 **F.1.9 Minimum Required Performance in the Faulted State**

377 In order to establish whether the primary steel tension member which failure is introduced in the analysis  
378 is a fracture critical members (FCM) or a system redundant member (SRM) it is necessary to evaluate the  
379 faulted structure subjected to the loads described for the Redundancy I and Redundancy II load  
380 combinations. If the system meets all of the requirements described in Section F.1.9.1 and Section F.1.9.2,  
381 the member which failure is introduced in the analysis may be re-designated as a SRM, otherwise it shall  
382 remain as a FCM. It shall be noted that the system must previously be subjected to a screening criteria, as  
383 described in Appendix C and in the proposed guide specification in Appendix E.

#### 384 *F.1.9.1 Strength Criteria*

385 All of the strength requirements described hereof are to be checked at the end of step 6 in the analysis  
386 procedure described in Section F.1.8 for both load combinations, Redundancy I and Redundancy II, unless  
387 otherwise noted. A set of requirements apply to primary members of the superstructure, these are:

- 388 • In a component, such as a web or a flange of a primary steel member, the average strain is less than  
389 five times the material yield strain.
- 390 • In a component, such as a web or a flange of a primary steel member, the average strain is less than  
391 0.01.
- 392 • The maximum strain anywhere in a primary steel tension member is less than of 0.05 is reached.  
393 Higher strain limits are permitted when supported by experimental testing.
- 394 • The combined flexural, torsional and axial force effects computed in primary compression  
395 members is below the nominal compressive resistance of the member, unless these limit states are  
396 predicted by the FEA.
- 397 • Although localized crushing in the slab is allowed, the slab shall not reach 0.003 compression strain  
398 in a portion sufficiently large to compromise the overall system load carrying capacity.
- 399 • The system fails shall support, i.e., satisfy static equilibrium, an additional 15% of the factored live  
400 load at the end of step 8.

401 Additionally, the substructure must meet the following requirements:

- 402 • At any support location, the reaction forces and moments is less than the nominal resistance of a  
403 substructure element or the support system.
- 404 • The substructure can safely accommodate the displacements and reactions of the superstructure in  
405 the faulted state.

406

407 *F.1.9.2 Serviceability Criteria*

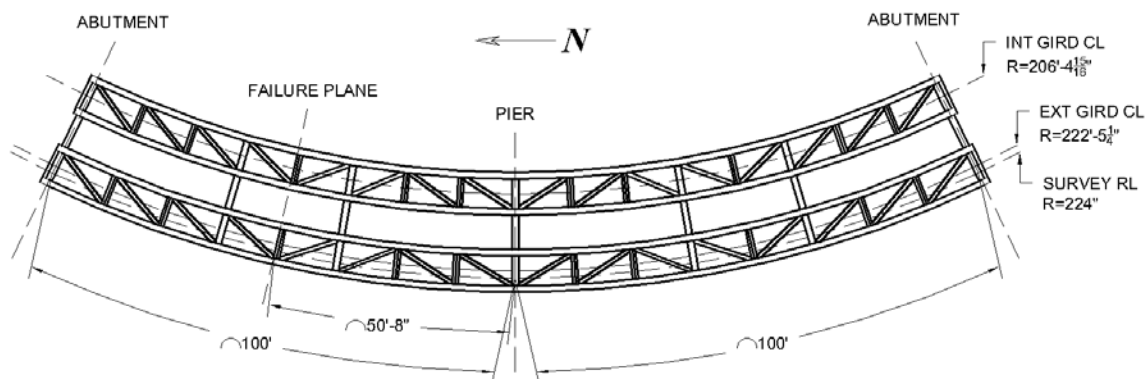
408 The serviceability requirements described hereof are to be checked at the end of step 4 in the analysis  
409 procedure described in Section F.1.8 for the Redundancy II load combination only, these are the following:

- 410 • The maximum vertical deflection is less than  $L/50$ , where  $L$  is the span length for primary members  
411 oriented longitudinally.  
412 • When considering a scenario in which failure of a floor beam is assumed, the maximum vertical  
413 deflection of the floor beam is larger than  $L/50$ , where  $L$  is the distance between floor beams that  
414 are assumed not to have failed.

415 Additionally, the Owner and/or the Engineer may considered other serviceability related parameters such  
416 as uplift at slab joints, changes in the cross-slope of the structure, and other phenomena that negatively  
417 impacts the ability of the structure to provide service in a safe manner.

418 F.2 Continuous Curved Twin Tub Girder Bridge

419 The redundancy of a continuous two span twin tub girder bridge is analyzed by developing a finite  
420 element model in accordance with the methodology described in the proposed guide specification in  
421 Appendix E. It is assumed that the structure does not possess any of the detrimental attributes described in  
422 the screening criteria and that it is built to Section 12 of the AWS D1.5. In this case, the failing tension  
423 member is assumed to be the exterior tub girder. The entire cross-section of the exterior girder is assumed  
424 to have failed at a cross section located 50'-8" north of the continuous support (pier) as shown in Figure  
425 F-2.  
426

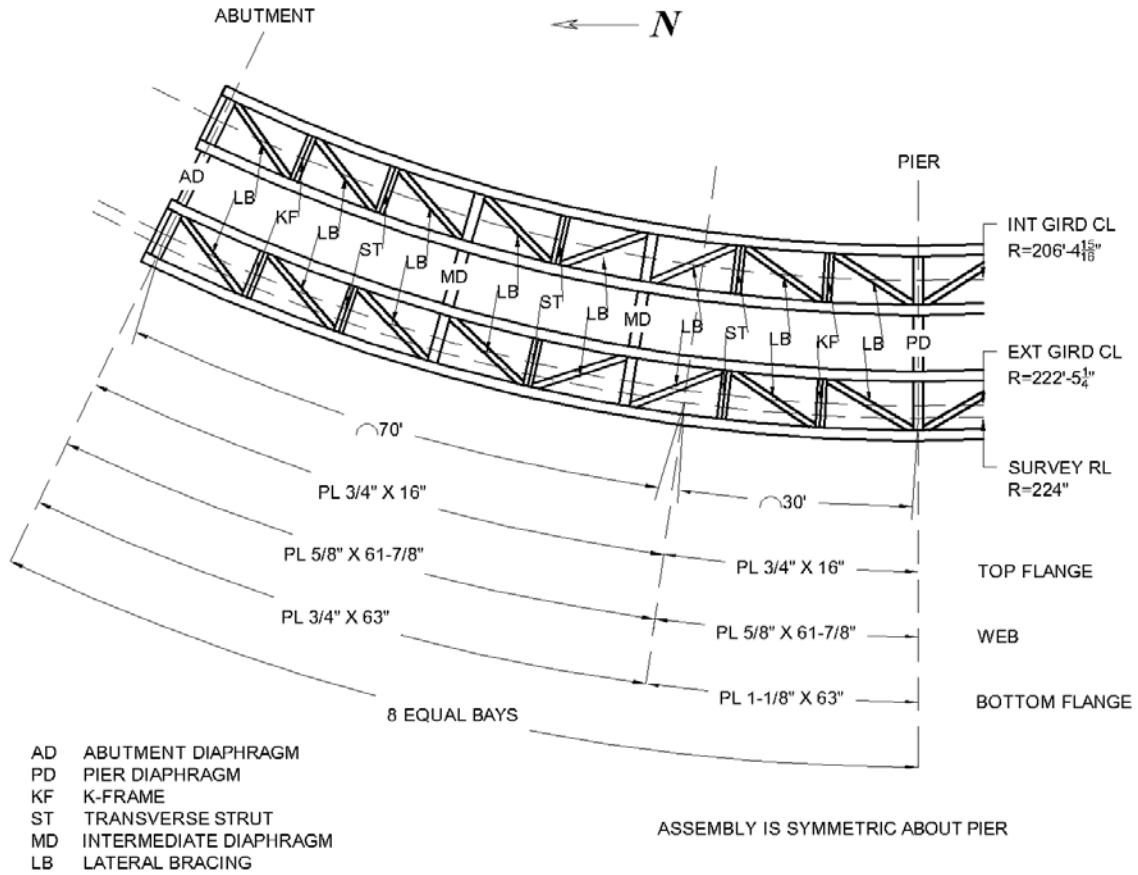


427  
428

**Figure F-2. Steelwork geometry and failure location.**

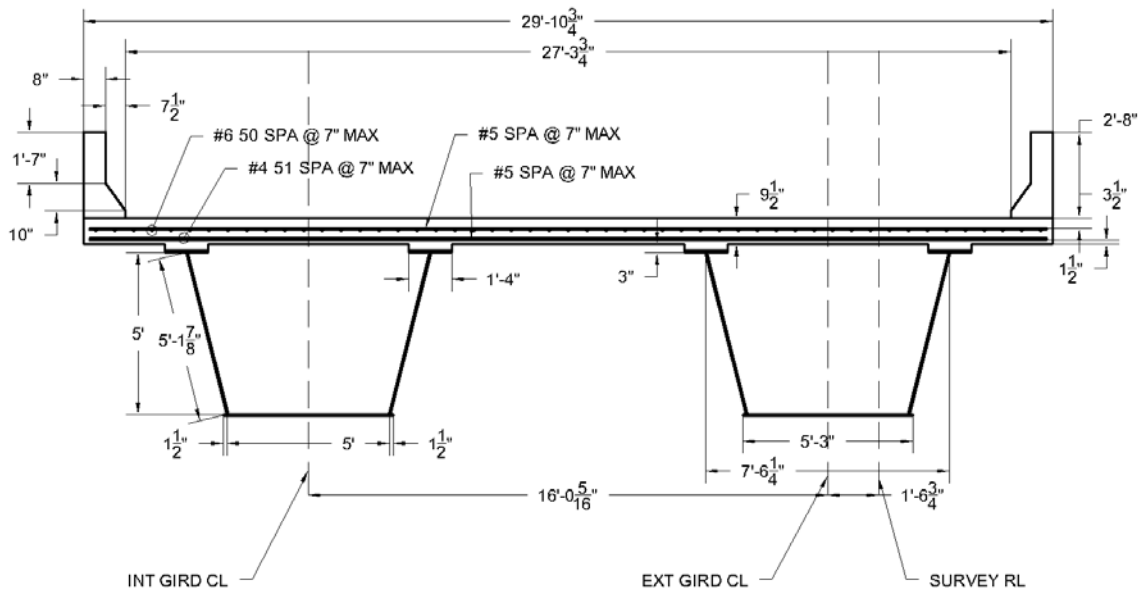
429 The structure has two spans measuring 100 feet long, and it is uniformly curved with a radius of 224 feet  
430 (measured along the surveying reference line). The two trapezoidal box girders have 63 inch wide bottom  
431 flanges, 61.875 inch high webs and 16 inch wide top flanges; with variable plate thicknesses. Stability of  
432 the girders is provided by seven diaphragms joining both girders and a system of K-frames, struts and braces  
433 within each girder. Figure F-3 shows the steelwork framing plan and Figure F-5 provides details of the  
434 different diaphragms and internal bracing members.

435 The reinforced concrete slab is approximately 27 feet wide between interior edges of concrete barriers  
436 (approximately 30 feet wide between the outer exterior edges of concrete barriers) and is fully composite  
437 with the girders' top flanges through shear studs. The end supports are multi-rotational unidirectional  
438 bearings, and the support over the pier is a multi-rotational fixed bearing. All steel plates, used in the  
439 girders and diaphragms are made of ASTM A709 HPS 50W. All rolled sections, used in interior stability  
440 system are made of ASTM A709 Grade 50. All concrete has a minimum specified compressive strength  
441 of 4ksi and all rebar has 60 ksi yield strength. In the analysis of this structure, longitudinal and transverse  
442 slopes, as well as camber adjustments will be neglected. Figure F-4 shows the cross section of the structure  
443 with the slab, barrier and reinforcement details.



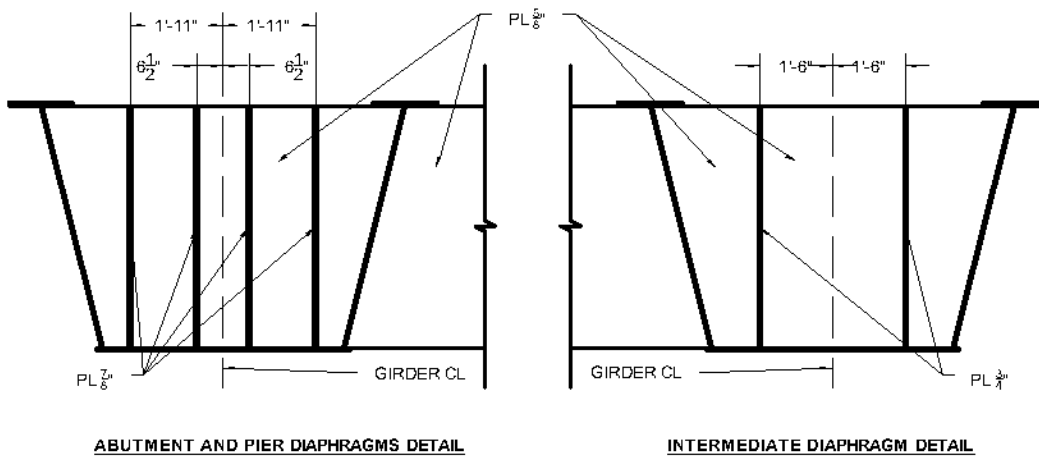
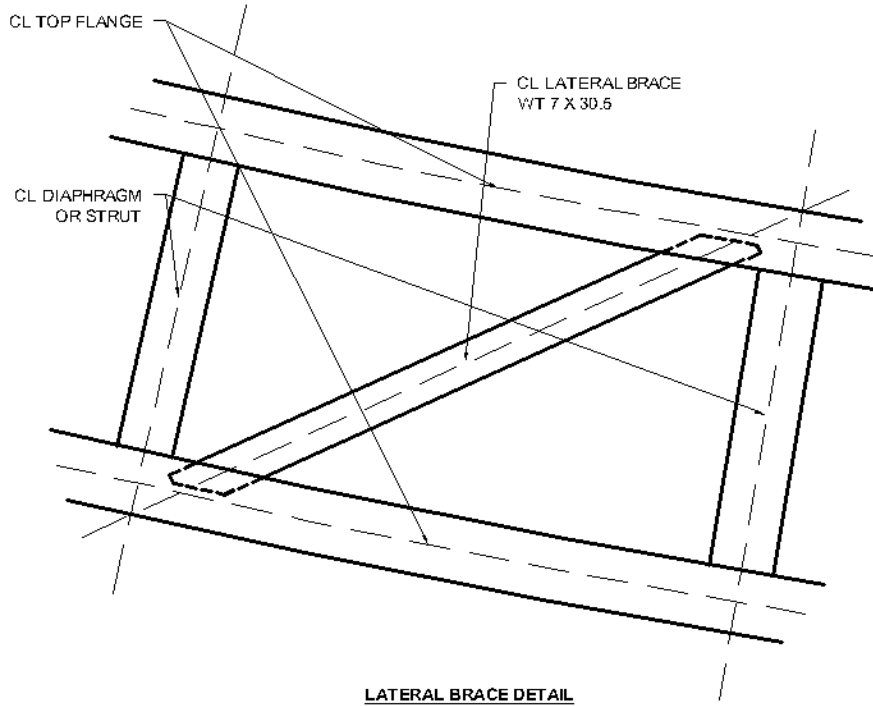
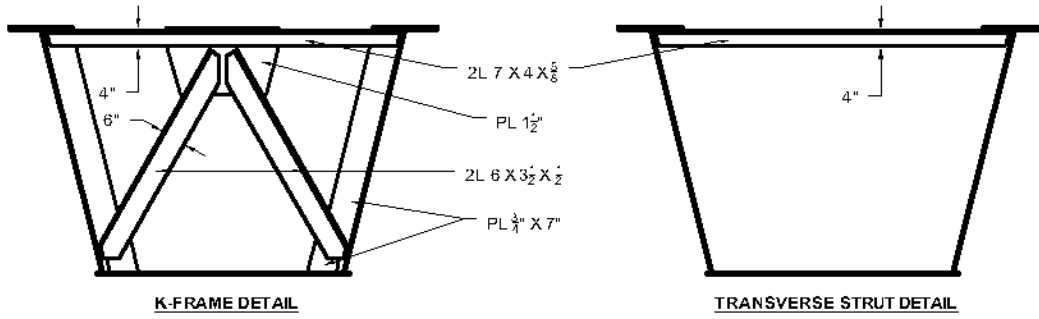
444  
445

**Figure F-3. Girders, diaphragms and internal bracing plan.**



446  
447

**Figure F-4. Typical cross-section and slab reinforcement details.**



448  
449

**Figure F-5. Internal bracing and diaphragm details.**

## 450 **F.2.1 Analysis Procedure**

451 The analysis is performed to establish if the system demonstrates acceptable performance in the faulted  
452 condition. In the example, the term “faulted condition” specifically refers to the case in which a primary  
453 steel tension member is assumed to have failed. For this analysis, load factors for both dead and live load  
454 are applied as described in the proposed guide specification in Appendix E. In this example, the described  
455 analysis procedure is composed of an initial implicit static analysis and a final explicit dynamic analysis,  
456 into which the results from the initial implicit static analysis are imported. While it is not mandatory for  
457 the Engineer to follow these particular steps, it has been found that this procedure optimizes the  
458 computational time required.

### 459 *F.2.1.1 Initial Implicit Static Analysis*

460 Implicit static analysis was utilized to calculate the state of the structure prior to hardening of the concrete  
461 in the slab. An implicit static analysis was used for the initial steps because, although non-linearity is  
462 considered in the analysis, the bridge behavior is linear and inertial effects can be neglected as the bridge  
463 is in the undamaged condition. As the slab does not carry any load and does not contribute to the stiffness  
464 of the system before concrete hardening, two modifications are required in the finite element analysis during  
465 this initial implicit static analysis as follows:

- 466 • A very low stiffness is specified for the elements composing the slab, i.e., the elements modeling  
467 concrete and rebar. A reduced stiffness of 1/1,000 of the respective modulus of elasticity of each  
468 material was used. This is done so the load carried by the slab and rebar have negligible  
469 contribution to the stiffness of the system. No modifications to the stiffness should be applied to  
470 the steelwork.
- 471 • Instead of defining contact interaction between the slab and the steelwork, a mesh tie was specified.  
472 The nodal displacements of the concrete slab elements are tied to the displacements of the top  
473 flanges of girders, floor beams, and stringers which occur due to dead load. As a result, the slab  
474 deforms with the steelwork and does not ‘sag’ between the girders, floor beams, and stringers.

475 It is worth noting that the remainder of the finite element modeling is identical between the initial implicit  
476 static analysis and the final explicit dynamic analysis. The specific steps in the initial implicit static analysis  
477 are described as follows:

- 478 1. Apply load due to self-weight of the structural steel components as a body force.
- 479 2. Apply load due to self-weight of the wet slab components as a body force.
- 480 3. The system is then fixed in terms of position, that is, the displacement degrees of freedom are not  
481 allowed to change.
- 482 4. The elements composing the slab (elements modeling rebar and concrete) are then deactivated.
- 483 5. The elements composing the slab are then reactivated. During this reactivation the strain in the  
484 elements composing the slab is reset to zero.

485 Steps 3 through 5 are necessary since even though very low stiffness was specified for the slab, these  
486 elements do undergo strain. Setting the strains to zero eliminates “locked in” artificial stresses in later steps.

### 487 *F.2.1.2 Final Explicit Dynamic Analysis*

488 As contact algorithms, softening material behavior, and non-linear geometry are required to be part of  
489 the finite element analysis, implicit solution procedures present unavoidable convergence problems in most  
490 FEA solvers. In order to calculate the capacity of the bridge after sudden failure of a tension component, a  
491 dynamic explicit analysis needs to be carried out. Therefore, the results obtained from the initial implicit  
492 static analysis are imported into the final explicit dynamic analysis. In other words, the state of the system  
493 (stresses, strains, displacements and forces) at the beginning of the final explicit dynamic analysis is defined  
494 by the state of the system computed at the end of the initial implicit static analysis.



495 As previously stated, during the initial implicit static analysis, the slab was modeled with largely reduced  
 496 stiffness to reflect that it is not hardened and a mesh tie constraint was used to assure that the slab deformed  
 497 with the steelwork. This approach also prevents excessive sag of the soft slab. After the state of the system  
 498 is imported, the following changes are made to capture the response of the structure after the concrete has  
 499 hardened:

- 500 • The modulus of elasticity of the concrete and rebar elements in the slab is changed to their final  
 501 actual values. It is noted that no modifications need to be applied for the steelwork.
- 502 • The mesh tie constraint between the slab concrete elements and the top flanges of the steelwork is  
 503 replaced by a frictional contact interaction. Additionally, since the structure under analysis is  
 504 composite, elements which accurately model the behavior of shear studs are added.

505 All of the body forces applied during the initial implicit static analysis (i.e., the dead load of the structure)  
 506 are maintained throughout the final explicit dynamic analysis.

507 To evaluate the capacity of the structure in the faulted state, the following steps were carried out in the  
 508 final explicit dynamic analysis:

- 509 6. The stiffness of the elements located at the fracture location under consideration were slowly  
 510 reduced. The stiffness was slowly reduced in order to minimize any dynamic effects. It is noted  
 511 that the actual fracture and subsequent vibration of the structure is not modeled. This dynamic  
 512 effect is accounted for using the  $DA_R$  factor as discussed before. If dynamic effects are found to  
 513 be significant even if the stiffness is slowly reduced, the system must be allowed to oscillate until  
 514 these effects are dampened.
- 515 7. Factored loads due to traffic are applied as surface tractions. For the Redundancy I load  
 516 combination all loads are amplified by  $DA_R$ , for the Redundancy II load combination the dynamic  
 517 load allowance (IM) is applied. These loads were applied very slowly to minimize any dynamic  
 518 effects, as well. If dynamic effects are significant, the system must be allowed to oscillate until  
 519 these effects are dampened.
- 520 8. An additional 15% of live load is gradually applied.

521 **F.2.2 Material Models**

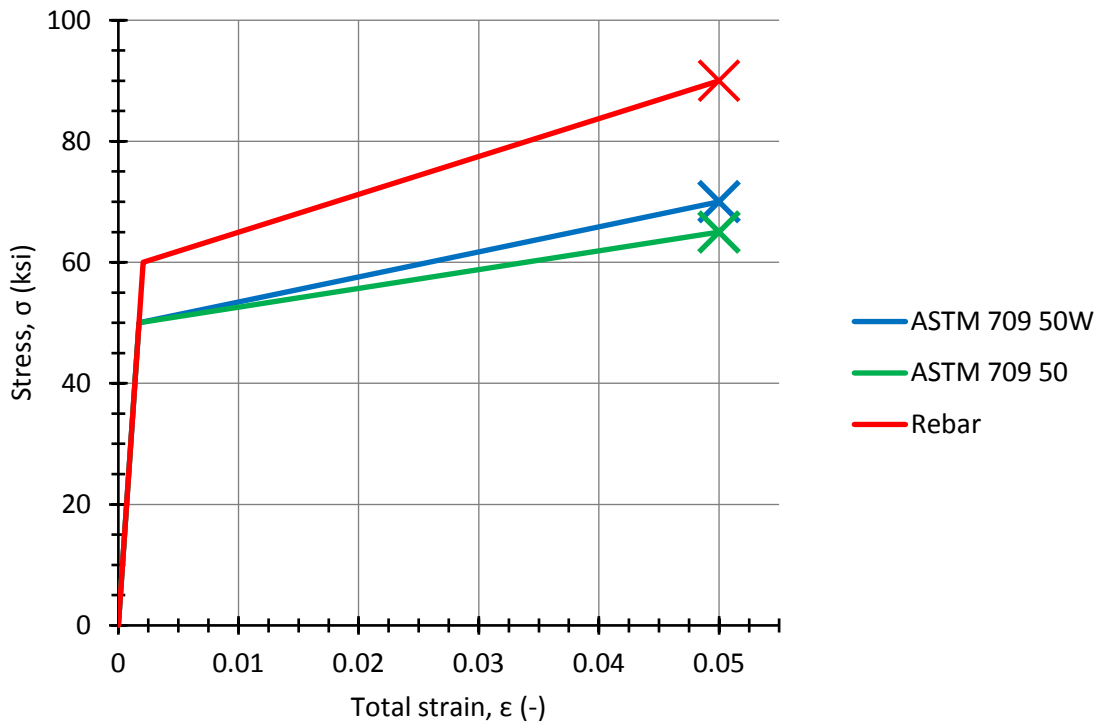
522 Four material models are needed in the finite element model. Three of those are utilized to model  
 523 different steel types, and one is utilized to model the response of concrete. For the development of the steel  
 524 material models, it is necessary to know the yield strength and ultimate strength of each steel type. In this  
 525 example, since no test values are known to the Engineer, nominal values specified in the respective  
 526 standards are utilized. These are summarized in Table F-1. A mass density of 0.494 kcf was specified for  
 527 all steel types.

528 **Table F-1. Material properties for steel material models.**

Material	Nominal Yield Strength	Nominal Ultimate Strength	Standard
ASTM A709 HPS 50W	50 ksi	70 ksi	ASTM A709/A709M
ASTM A709 Gr. 50	50 ksi	65 ksi	ASTM A709/A709M
Grade 60 Rebar	60 ksi	90 ksi	ASTM A615/A615M

529  
 530 The stress-strain relation for all steel components will follow an initial linear elastic steel with a Young's  
 531 modulus of 29,000 ksi and Poisson's ratio of 0.3. Once the nominal yield strength is reached the stress-  
 532 strain relation is defined by Von Mises (J2) plasticity with kinematic linear hardening, until the nominal  
 533 ultimate strength is reached at a total strain of 0.05. Once the nominal ultimate strength or a total strain of

534 0.05 is reached, the material is assumed to fail. Figure F-6 shows the uniaxial material response for the  
 535 steel employed in this finite element model with the 'X' denoting the stress at the failure strain of 0.05.  
 536



537  
 538 **Figure F-6. Stress-strain curves of steel material models.**

539 The material model used in concrete is defined entirely by the specified compressive strength, which in  
 540 this case is 4 ksi. This quantity is also used to calculate the tensile strength, the total strain at compressive  
 541 strength,  $\epsilon_c$ , and the material parameter,  $n$ . Table F-2 summarizes the calculation of these values. A mass  
 542 density of 0.150 kcf was specified for concrete.

543 **Table F-2. Material properties for concrete material model.**

Quantity	Symbol	Equation	Result
Young's modulus	$E_c$	$E_c = 33,000w_c^{1.5}\sqrt{f'_c} \leq 1,802.5\sqrt{f'_c}$	3,600 ksi
Tensile strength	$f_t$	$f_t = 0.158(f'_c)^{\frac{2}{3}}$ for $f'_c \leq 7.25\text{ksi}$ $f_t = 0.307 \ln(f'_c + 2.61) - 0.114$ for $f'_c > 7.25\text{ksi}$	0.398 ksi
Fracture energy	$G_t$	$5.9 \cdot 10^{-4}(f'_c + 1.16)^{0.18}$	$7.93 \cdot 10^{-4}$ kip/in
Total strain at compressive strength	$\epsilon_c$	$\epsilon_c = 0.00124^4\sqrt{f'_c}$	0.00175
Material parameter	$n$	$n = 0.4f'_c + 1.0$	2.6

544

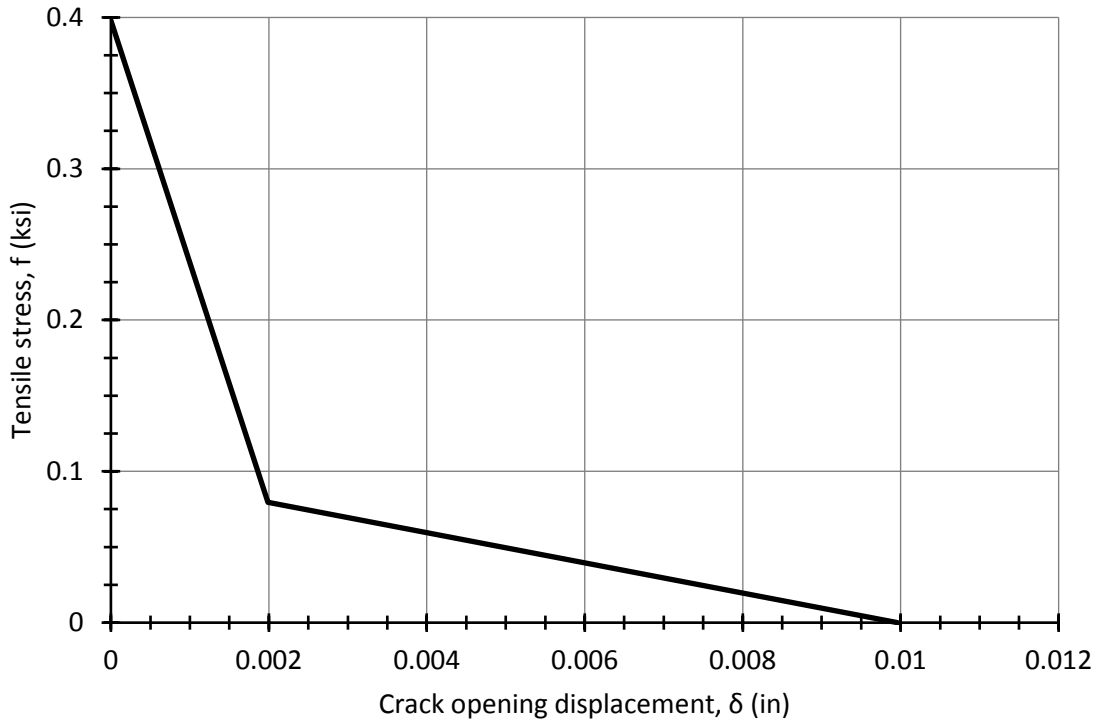
545 The concrete material model is initially linear elastic, defined by a Young's modulus of 3,600 ksi and  
 546 Poisson's ratio of 0.2, followed by concrete damage plasticity. In tension, once the material reaches its  
 547 tensile strength, set at 0.398 ksi in this case, a tensile stress-displacement relation characterized by a fracture  
 548 energy,  $G_t$ , of  $7.93 \cdot 10^{-4}$  kip-in is followed. This fracture energy is applied through a bi-linear tensile stress-  
 549 displacement relation as shown in Figure F-7, and defined by the following quantities:

550 
$$f_{t1} = \frac{f_t}{5} = 0.0796 \text{ ksi}$$

551 
$$\delta_t = \frac{5G_t}{f_t} = 0.00996$$

552 
$$\delta_{t1} = \frac{G_t}{f_t} = 0.00199$$

553



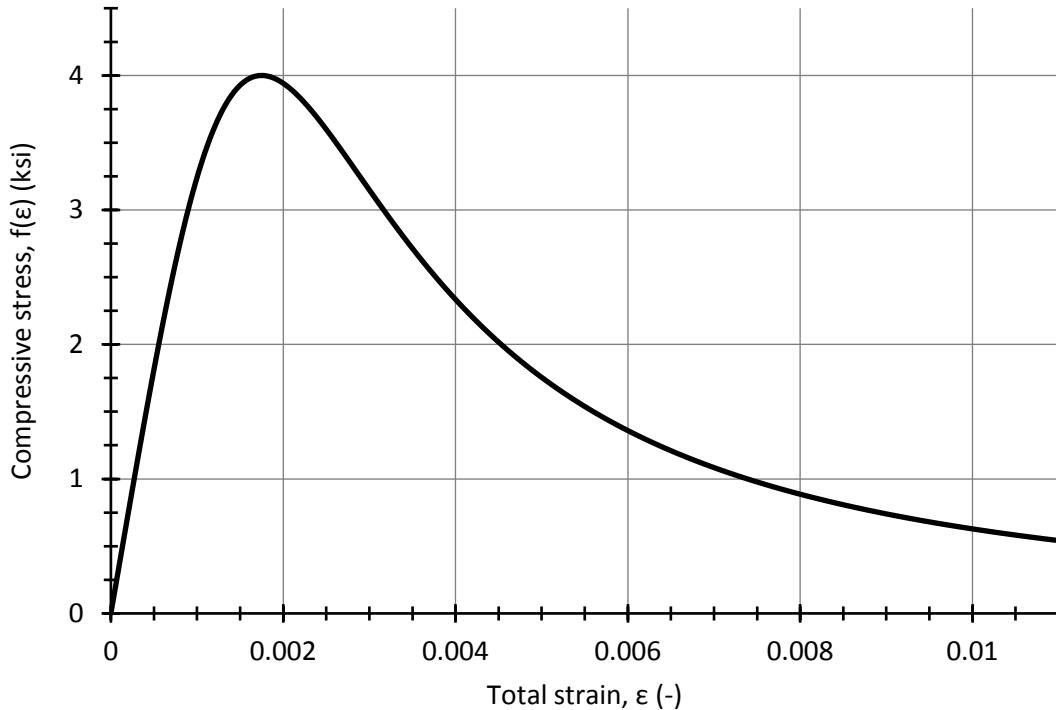
554  
 555 **Figure F-7. Tensile stress-crack opening displacement curve for concrete material model.**

556 In compression the material follows the following stress-strain relations:

557 
$$f(\varepsilon) = f'_c \left( \frac{\varepsilon}{\varepsilon_c} \right) \left[ \frac{n}{n - 1 + \left( \frac{\varepsilon}{\varepsilon_c} \right)^n} \right]$$

558 
$$\varepsilon_{plastic} = \varepsilon - \frac{f(\varepsilon)}{E_c}$$

559 Where  $\varepsilon$  is total (elastic + plastic) strain,  $f(\varepsilon)$  is the compressive stress at a given total strain,  $f'_c$  is the  
 560 specified compressive strength,  $\varepsilon_c$  is the total strain at compressive strength,  $n$  is a material parameter,  
 561  $\varepsilon_{plastic}$  is the plastic strain, and  $E_c$  is the concrete Young's modulus. Figure F-8 shows the resulting  
 562 compressive stress-strain relation.



563  
564

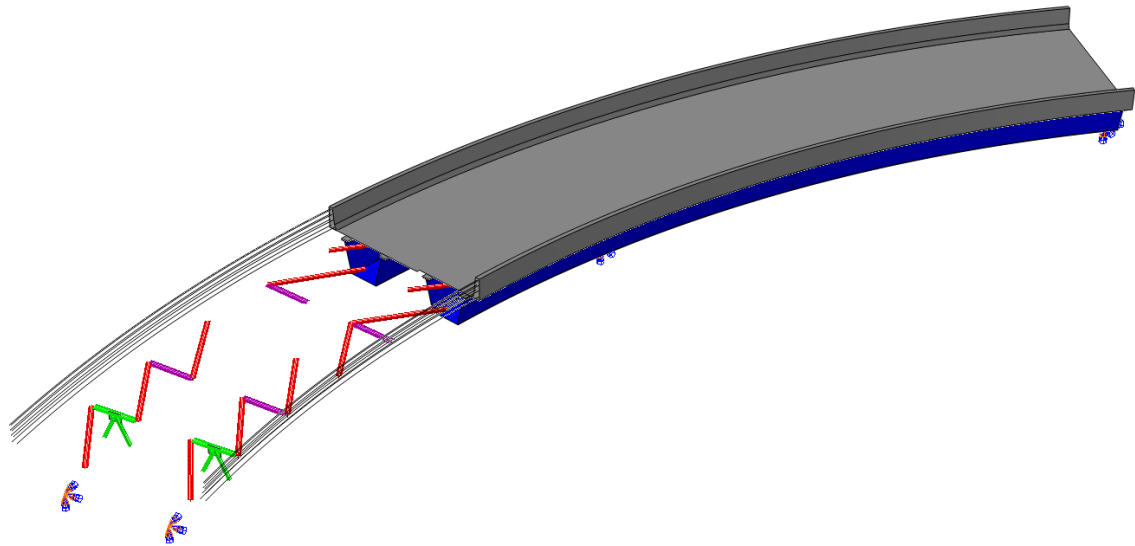
**Figure F-8. Compressive stress-strain curve for concrete material model.**

565 **F.2.3 Geometries, Meshes and Constraints**

566 The geometry of the structure is based on available design plans and is composed of the following  
567 components that must be explicitly modeled:

- 568 1. Two horizontally curved trapezoidal tub girders.
- 569 2. Seven diaphragms connecting both tub girders:
  - 570 a. Two abutment diaphragms.
  - 571 b. One pier diaphragm.
  - 572 c. Four intermediate diaphragms.
- 573 3. A system of internal K-frame within the tub girders (total of 4 frames per girder).
- 574 4. A system of transverse struts within the tub girders (total of 6 struts per girder).
- 575 5. A system of diagonal bracings within the tub girder (total of 16 braces per girder).
- 576 6. A reinforced concrete slab with concrete barriers.

577 When generating the finite element model, splices, holes, access hatches, etc. are neglected. The  
578 structure is assumed to be flat in the vertical plane, in other words, camber and superelevation are ignored.  
579 Figure F-9 shows the assembly of all bridge components.

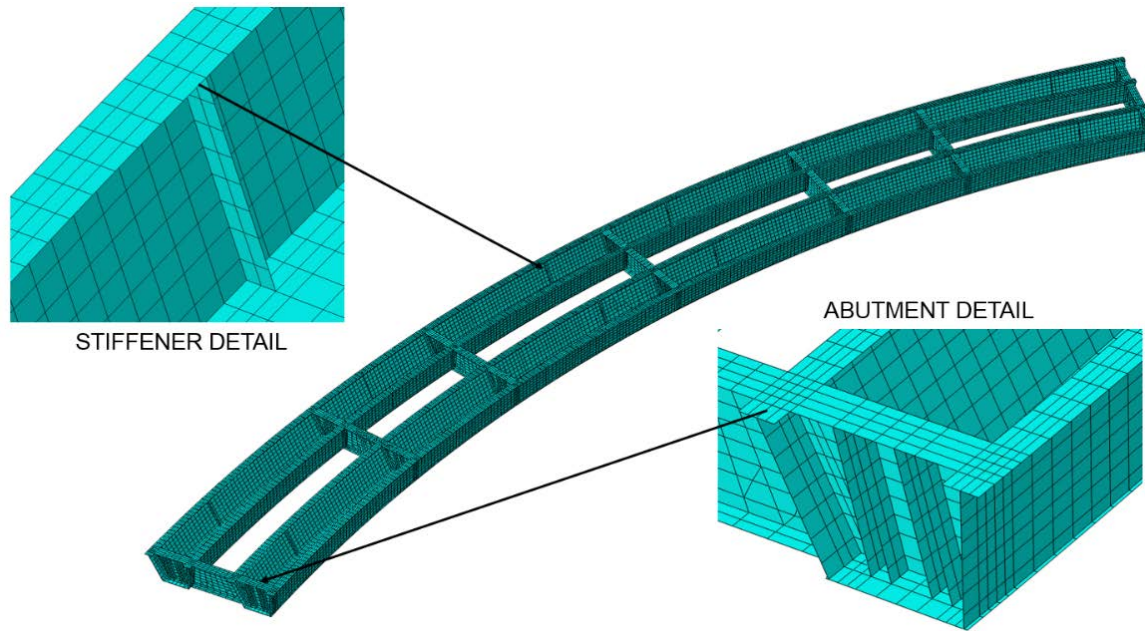


580  
581  
582  
583

**Figure F-9. Twin tub girder bridge geometries. Concrete slab and barriers (grey), tub girders (blue), K-frames (green), transverse struts (magenta), lateral bracing (red), slab reinforcement (black).**

584  
585  
586  
587  
588  
589  
590  
591  
592  
593  
594

Tub girders and diaphragms are modeled with 4-node shell elements with reduced integration. A minimum of four elements are used along flange widths and along web heights. The stiffeners to which the K-frames are attached are modeled with shell elements as well. In this case, the tub girders, diaphragms and stiffeners constitute a single geometry. The maximum aspect ratio was kept below five and corner angles were kept between 60 and 120 degrees. Figure F-10 shows two details of the mesh employed to model the tub girder, diaphragm and stiffener system. The K-frames, transverse struts and diagonal bracings are modeled with 2-node linear shear-flexible (Timoshenko) beam elements. A minimum of three elements are used along the length of the elements. Mesh ties, which are constraints that slave the motion of a surface or node set to the motion of a master surface or node set, are utilized to connect the K-frames to the stiffeners and the struts and diagonals to the webs of the tub girders.



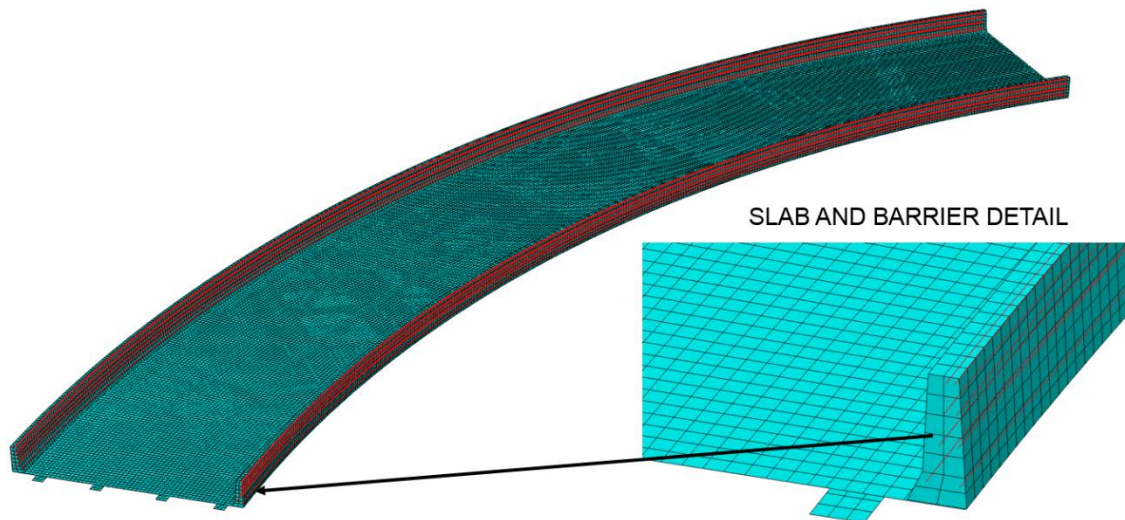
595  
596

**Figure F-10. Mesh details of the tub girders.**

597 The slab is modeled with four-node linear shell elements with reduced integration, finite membrane  
598 strains, and a minimum of five Simpson thickness integration points. The transverse and lateral  
599 reinforcement in the concrete slab is implicitly included in the section integration of the shell elements, as  
600 rebar layers that follow the radial (for transverse reinforcement) and tangential (for longitudinal  
601 reinforcement) characteristic of the curvature of the slab.

602 The barriers are defined using eight-node linear bricks (hexahedral elements) with reduced integration  
603 are used to model concrete, and two-node truss (wire) elements with linear displacement to model steel  
604 reinforcement. Seven solid concrete elements are used through the height of the parapet with maximum  
605 aspect ratio (length of longest edge divided by length of shortest edge) of 5, and corner angles (angle at  
606 which two element edges meet) between 40 and 140 degrees. The length of the truss elements used to  
607 model the parapet reinforcement were approximately equal to the length of the longest edge of the solid  
608 concrete elements. These truss elements are embedded within the solid concrete elements. At the nodes of  
609 the embedded truss elements, the translational degrees of freedom are eliminated and the nodal translations  
610 were constrained to interpolated values of the nodal translations of the host solid concrete element. The  
611 barriers were attached to the slab by mesh ties. Figure F-11 shows a detail of the mesh used for the concrete  
612 barrier and slab.

613



614  
615

**Figure F-11. Mesh details of the reinforced concrete slab and barriers.**

616 **F.2.4 Slab-Structural Steel Interaction**

617 As stated, the interaction between the bottom of the concrete slab and the top of the flanges of the tub  
 618 girders is modeled differently in the two steps described above. In the initial implicit static analysis, when  
 619 the elements comprising the slab and barriers have  $1/1,000^{\text{th}}$  of the modulus of elasticity to model the “wet”  
 620 condition, a mesh tie is used to slave the motion of the slab to the motion of the surface comprising the top  
 621 of the steel work. With this procedure, it is ensured that the slab deformation will conform to the  
 622 deformation of the steelwork while unrealistic sagging of the slab between supporting elements and tipping  
 623 of the barrier is prevented.

624 In the final explicit dynamic analysis, when the stiffness of the elements comprising the slab and barriers  
 625 has been changed to their final real values, the mesh tie previously used is deleted and replaced by a contact  
 626 interaction and modeling of shear studs. The normal behavior of the contact interaction is modeled through  
 627 a penalty stiffness. The penalty stiffness is several orders of magnitude larger than the normal stiffness of  
 628 the underlying contacting elements and allows a very small penetration so a pressure can be calculated.  
 629 The tangential behavior of the contact interaction is modeled through an algorithm based on Coulomb  
 630 friction with a limit on the allowable shear. A friction coefficient of 0.55 and an interfacial shear strength  
 631 of 0.06 ksi are specified.

632 The simplified stud model, as described in the Appendix A is used to model composite action between  
 633 the slab and the steelwork. In the simplified stud model, the shear studs were modeled using connector  
 634 elements which were used to define the axial and interfacial shear interaction between the shear studs and  
 635 concrete slab. Connector elements are special purpose elements with zero length. These elements model  
 636 discrete physical connections between deformable or rigid bodies, and are able to model linear or nonlinear  
 637 force-displacement behavior in their unconstrained relative motion components.

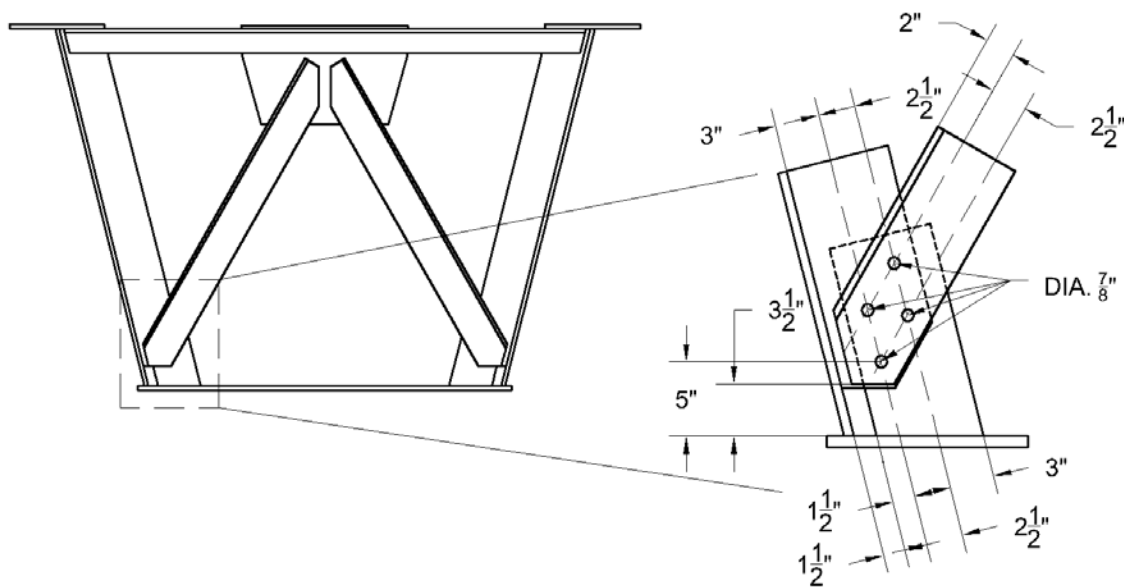
638 The recommendations of Appendix A were used to define the shear and tensile behavior of shear studs.  
 639 The shear stud group is composed of three transversely grouped studs which shear strength is 108 kips,  
 640 following the shear force-displacement relation proposed by Ollgaard et al. (1971) up to maximum shear  
 641 displacement of 0.2 inches. In tension, the governing failure mode is concrete break-out, resulting in a  
 642 initial stiffness of 1632 kip/in, and tensile strength of 12.5 kips, and a maximum tensile displacement at  
 643 failure of 0.049 inches. The tensile behavior follows the characteristic triangular response for transversely  
 644 grouped shear studs which governing failure mode is concrete break-out or shear stud pullout, as described

645 in the recommendations of Appendix A. The tension-shear interaction procedure presented in Appendix A  
646 is used to combine the effects of shear and tension acting simultaneously on a shear stud group.

### 647 **F.2.5 Connection Failure Modeling**

648 When a connection is likely to fail before yielding of the member, in addition to the use of mesh ties to  
649 attach the components, an additional step may be necessary to capture connection failure. Although it is  
650 possible to develop force/moment-displacement/rotation relations which can be applied to a connector  
651 element, a simpler approach was developed and utilized herein. In this particular example, it was not  
652 necessary to include to model connection failure as the forces developed in the member did not exceed the  
653 capacity of the connections. However, fuse elements were included in the finite element model to model  
654 the stiffness, capacity, and ductility of the connection shown in Figure F-12. The behavior was modeled  
655 by a linear-elastic perfectly-plastic relationship defined by the following:

- 656 • An initial elastic stiffness which is defined as a series sum of the contributions due to the axial  
657 flexibility of the connection plate, the bearing stiffness of the connection plate, and the shear  
658 stiffness of the bolts. The calculation procedure is based on the provision in Eurocode 3 (CEN,  
659 2007) and Henriques et al. (2014).
- 660 • The capacity of the connection is calculated per the provision in the AASHTO LRFD BDS. The  
661 nominal (unfactored) tensile capacity was specified.
- 662 • Once the capacity of the connection is reached, the fuse element behaves perfectly plastic until a  
663 maximum failure displacement is reached. This maximum failure displacement is the largest of  
664 2.5 times the ratio of the capacity to the stiffness and 0.18 times the diameter of the bolt, in  
665 accordance with Sarraj (2007).  
666



667  
668

**Figure F-12. K-frame connection detail.**

### 669 **F.2.6 Substructure Flexibility Model**

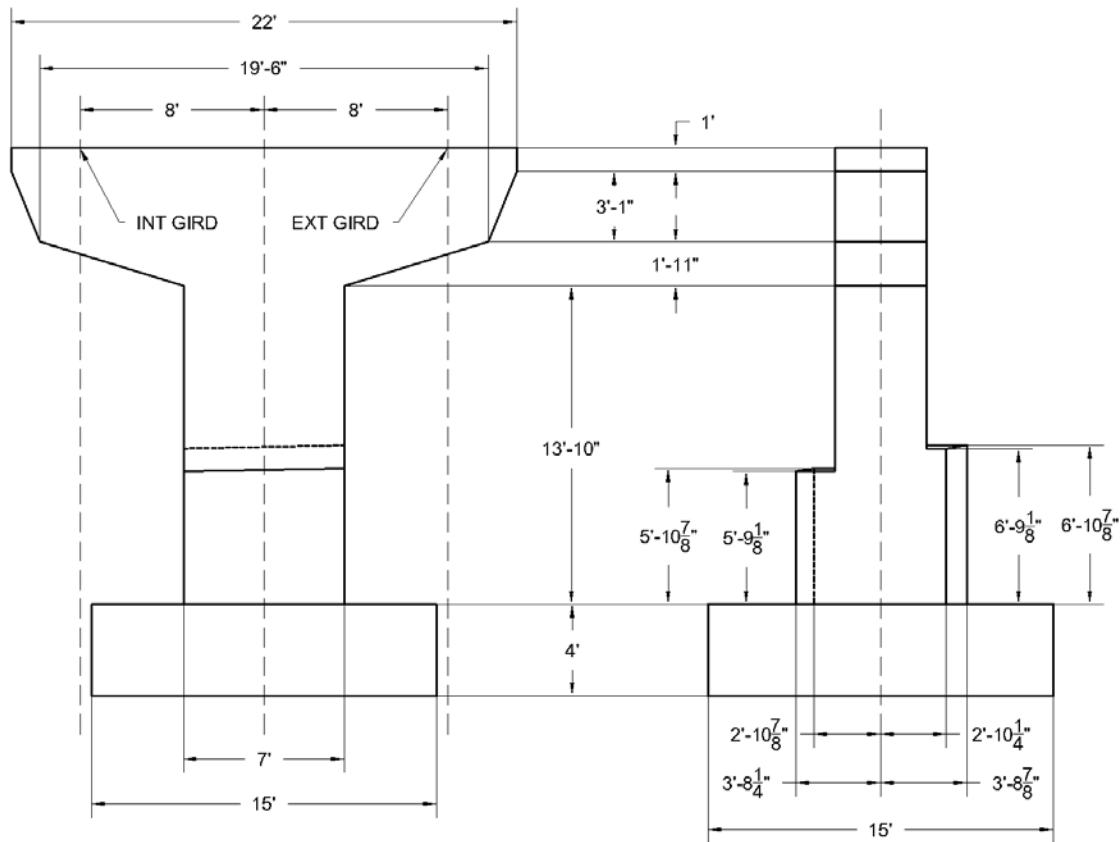
670 In order to account for longitudinal and transverse flexibility of the substructure, connector elements  
671 were utilized. These elements allow for the definition of coupled force-deformation relations. The type  
672 that was determined to best capture the intended behavior was a Cartesian connector. These elements



673 provide a connection between two nodes where the change in position is measured in three directions local  
 674 to the connection. One of the nodes is fixed (or connected to ground) and the other node is the support  
 675 point in the superstructure. The connector element is rigid in the vertical direction, and has a coupled linear  
 676 elastic relation in the two horizontal directions (longitudinal and transverse).

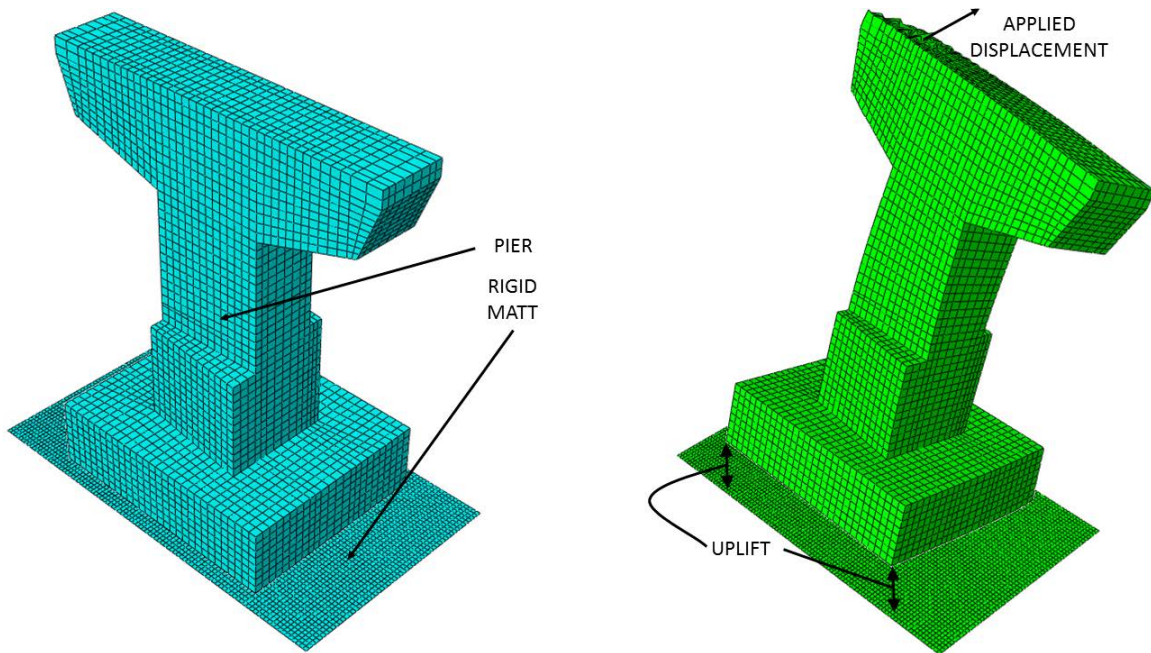
677 In the current case, the structure is assumed to be vertically supported and allowed to translate in the  
 678 horizontal plane at the abutments; hence the vertical translation at the ends of the structure will be set to  
 679 zero. At the continuous support, the structure is assumed to be fixed to the pier. As a result, the vertical  
 680 translation at the pier will be set to zero, while the horizontal stiffness of the pier will be incorporated  
 681 through connector elements.

682 In order to obtain the coupled elastic force-displacement relation, a simple finite element analysis of the  
 683 pier is conducted. The geometry of the pier is drawn according to the design plans, as shown in Figure  
 684 F-13 and meshed with 8-node linear bricks with reduced integration as shown in Figure F-14. The pier was  
 685 modeled as linear elastic with modulus of elasticity of 1,800 ksi (in order to account for possible cracking  
 686 due to combined compression and bending), Poisson's ratio of 0.2 and a density of 0.150 kcf. The base of  
 687 the pier bears on a rigid mat, prohibiting sliding but allowing uplift as shown in Figure F-14.  
 688



689  
 690

**Figure F-13. Geometry of the pier support.**



691  
 692 **Figure F-14. Detail of mesh geometry used (left) and deformed configuration after application of**  
 693 **displacement (right, displacements scale by a factor of 25).**

694 During the first analysis step, dead loads are applied. These are due to (1) the self-weight of the pier,  
 695 applied as a body force, and (2) bearing of the superstructure on the pier, which were calculated to be 380  
 696 kips for the exterior girder and 350 for the interior girder. These are applied as surface tractions over a 28”  
 697 by 28” patch, the size of the patch is based on the size of the bearings. Once the first step is completed,  
 698 displacements are applied at the bearing locations so the reaction forces can be calculated. In this case,  
 699 displacements of 6 inch were applied in the longitudinal and transverse directions (positive and negative  
 700 signs) so the reaction forces and described in Table F-3 were obtained.

701 **Table F-3. Reaction forces and displacements at support points.**

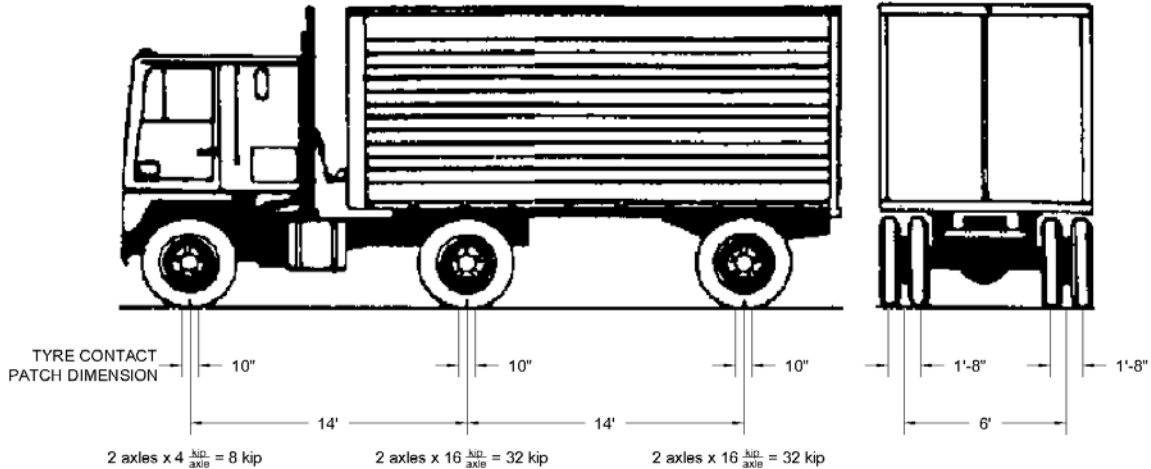
Interior Girder Support				Exterior Girder Support			
U <sub>TRAN</sub>	U <sub>LONG</sub>	R <sub>TRAN</sub>	R <sub>LONG.</sub>	U <sub>TRAN</sub>	U <sub>LONG</sub>	R <sub>TRAN</sub>	R <sub>LONG</sub>
in	in	kips	kips	in	in	kips	kips
6.00	-0.0620	925	-	6.00	-0.0595	971	-
-6.00	0.108	-1020	-	-6.00	1030	-1060	-
-0.771	6.00	-	787	-0.0738	6.00	-	822
0.141	-6.00	-	-786	0.135	-6.00	-	-823

702  
 703 These are used to build the force deformation relations shown hereof, which are incorporated as the  
 704 properties of the connector element in the global model to model the flexibility of the pier:

$$\begin{aligned}
 \begin{bmatrix} F_{TRANSVERSE} \\ F_{LONGITUDINAL} \end{bmatrix}_{INT\ GIRDER\ SUPPORT} &= \begin{bmatrix} 162 & 2.38 \\ 2.38 & 131 \end{bmatrix} \frac{kips}{in} \begin{bmatrix} U_{TRANSVERSE} \\ U_{LONGITUDINAL} \end{bmatrix}_{INT\ GIRDER\ SUPPORT} \\
 \begin{bmatrix} F_{TRANSVERSE} \\ F_{LONGITUDINAL} \end{bmatrix}_{EXT\ GIRDER\ SUPPORT} &= \begin{bmatrix} 170 & 2.38 \\ 2.38 & 137 \end{bmatrix} \frac{kips}{in} \begin{bmatrix} U_{TRANSVERSE} \\ U_{LONGITUDINAL} \end{bmatrix}_{EXT\ GIRDER\ SUPPORT}
 \end{aligned}$$

707 **F.2.7 Loads and Boundary Conditions**

708 Two types of loads were applied in the finite element models: body forces and surface tractions as  
 709 required by the proposed guide specification in Appendix E. Body forces were applied for component dead  
 710 loads (“DC” and “DW” per AASHTO designations). These are simply the product of mass, gravity and  
 711 applicable load factors. Surfaces tractions were applied for traffic live loads (“LL” per AASHTO  
 712 designation). The traffic live load is based on the HL-93 load model described in the AASHTO LRFD  
 713 BDS, which is a combination of the truck loads, shown in Figure F-15, and a 0.64 klf load distributed over  
 714 a width of 10 ft. The current structure does not include any bituminous pavement (i.e., DW is zero).  
 715



716  
 717 **Figure F-15. Truck load components and dimensions of the HL-93 vehicular live load model.**

718 The Redundancy I and Redundancy II loading combinations were used to evaluate the structure in the  
 719 faulted state. The load factors for these two combinations are as in Table F-4 are based on the provisions  
 720 in Appendix E for bridges built to Section 12 in the AWS D1.5. The live load (LL) factors are modified by  
 721 the appropriate multiple presence factors as described in Article 3.6.1.1.2 of the AASHTO LRFD BDS. It  
 722 must be noted that dynamic amplification factor is equal to 0.2 because the structure is a continuous twin  
 723 tub girder system, which is applied to DC and LL in the Redundancy I load combination only. Also, the  
 724 dynamic load allowance is 0.15 of the truck axle loads, and is only applied in the Redundancy II load  
 725 combination.

726 **Table F-4. Load factors used for Redundancy I and Redundancy II load combinations.**

Load Combination	Load Factors				Notes
	DC	LL	DA <sub>R</sub>	IM	
Redundancy I	1.05	0.85	0.20	N. A.	$\beta = 1.5$
Redundancy II	1.05	1.30	N. A.	0.15	$\beta = 1.5$

727  
 728 Longitudinally, the loads are positioned in the most critical positions in both the Redundancy I and  
 729 Redundancy load combinations. For the failure scenario considered in the current case (failure of the  
 730 exterior girder near mid span on the north span as shown in Figure F-2 and Figure F-16), the most critical  
 731 position of the truck axle loads which results in the truck facing south with its middle axis positioned at the  
 732 failure plane, as shown in Figure F-16. The distributed load portion of the HL-93 load is applied along the  
 733 northernmost span, from the north abutment to the pier.

734 As described in the proposed guide specification in Appendix E, the transverse positioning of the HL-93  
 735 live load model differs between the Redundancy I and Redundancy II load combinations, as illustrated in  
 736 Figure F-17. Since the vehicular loads in the Redundancy I load combination are meant to represent the  
 737 applied load at the instant in time in which the assumed member failure occurs, the HL-93 vehicular live  
 738 load model is transversely positioned centered (both the 10 ft loaded width and the truck axle loads) within  
 739 the marked (striped) lanes, in this case one lane. Hence, as the bridge is only striped for one lane, there is  
 740 only one load case for the Redundancy I load combination.

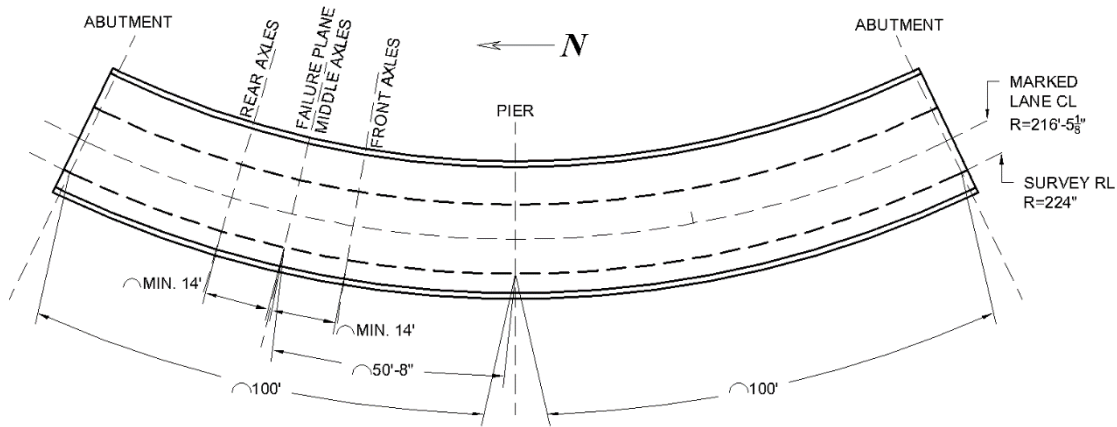
741 On the other hand, the objective of the Redundancy II load combination is to evaluate the strength of the  
 742 system after the failure of the primary steel tension member has occurred, so the number of design lanes is  
 743 established in accordance with Article 3.6.1.1.1 in the AASHTO LRFD BDS, which in this case results in  
 744 two design lanes with a width of 12 ft. In the Redundancy II load combination, the HL-93 vehicular live  
 745 load model is transversely positioned (both the 10 ft loaded width and the truck axle loads) to produce  
 746 extreme force effects within each design lane; however, the truck axle loads are transversely positioned  
 747 such that the center of any wheel load is not closer than 2 ft from the edge of the design lane. Hence, there  
 748 are two load cases for the Redundancy II load combination: two design lanes loaded, or one design lane  
 749 loaded.

750 Component dead loads were linearly applied in the initial implicit static analysis. Traffic live loads were  
 751 applied in the final explicit dynamic analysis. Their dynamic effects were minimized by applying them  
 752 slowly through the use of smooth step, as in the following equation:

753 
$$LR(t) = 6 \left(\frac{t}{T}\right)^5 - 15 \left(\frac{t}{T}\right)^4 + 10 \left(\frac{t}{T}\right)^3$$

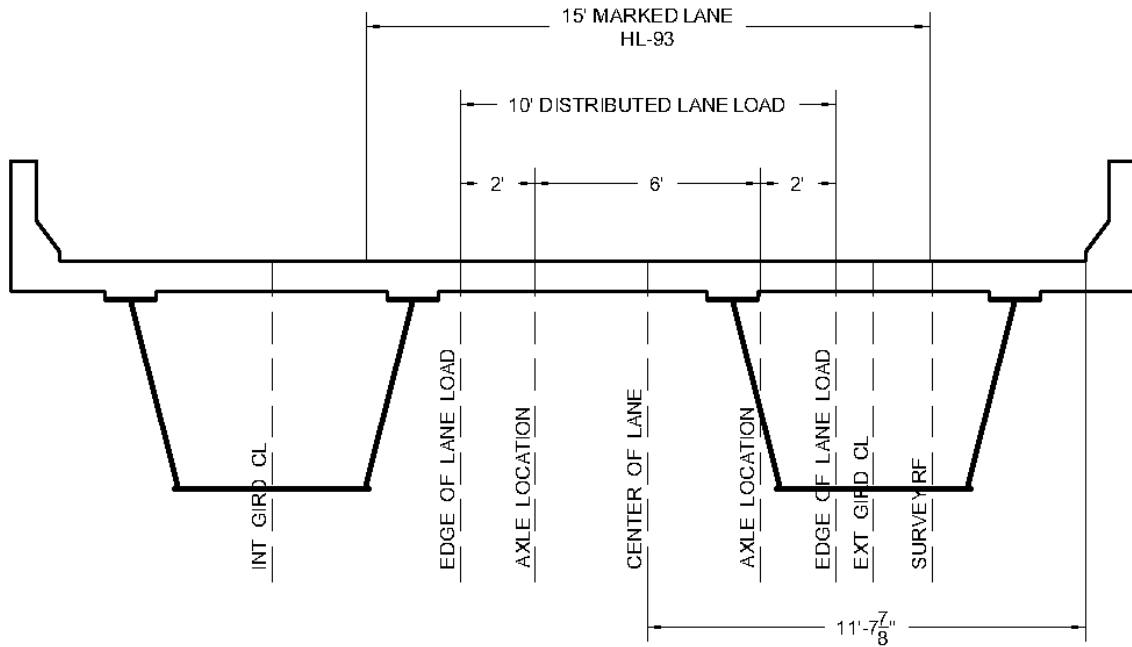
754 where  $LR(t)$  is the fraction of load at a load application time  $t$ , and  $T$  is the duration of the load application.  
 755 The duration of the load application must be larger than the fundamental period of the structure to minimize  
 756 oscillatory behavior in the final explicit dynamic analysis.

757 Regarding prescribed boundary conditions, vertical translation is prescribed to be zero at all support  
 758 location since uplift would not occur under the loading employed in the current case. Horizontal  
 759 translations are discussed in Section F.2.6 as they are enforced through connector elements that model the  
 760 flexibility of the substructure.  
 761

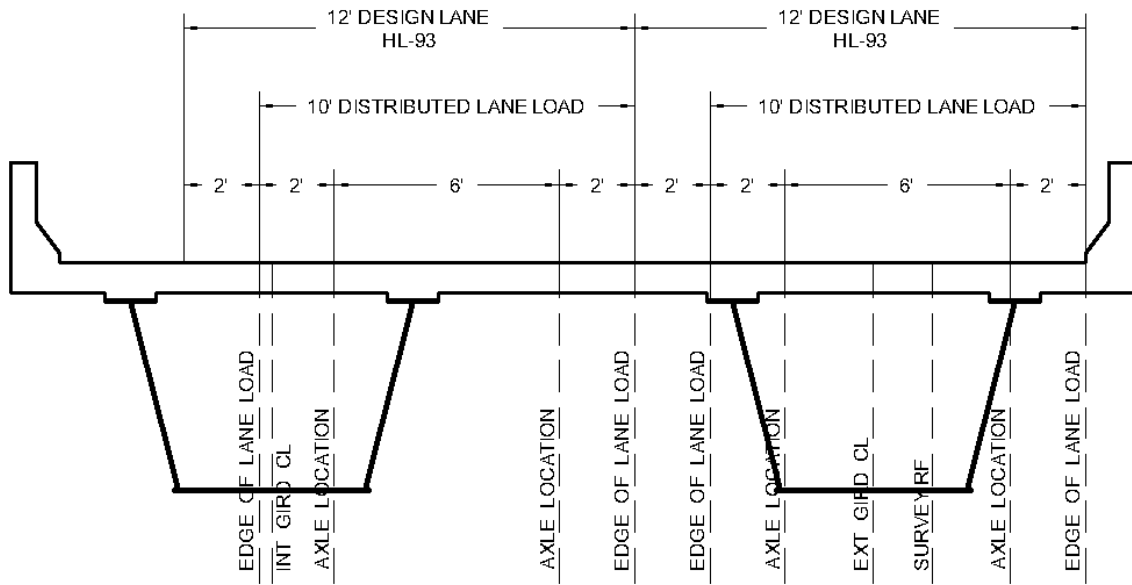


762 **Figure F-16. Longitudinal position of the HL-93 live load model.**  
 763

764



**TRANSVERSE LOAD POSITION FOR REDUNDANCY I**



**TRANSVERSE LOAD POSITION FOR REDUNDANCY II**

765  
766

**Figure F-17. Transverse position of the HL-93 live load model.**

767 **F.2.8 Analysis of Results for Redundancy**

768 Once the analysis is completed the obtained results are evaluated using the requirements described in  
769 Article 8 of the proposed guide specifications in Appendix E. It was found that the structure met the strength

770 and serviceability requirements and is considered redundant against failure of the exterior tub girder.  
 771 Specific details regarding the performance requirements and the results are summarized in Table F-5.

772 **Table F-5. Summary of the redundancy evaluation.**

Performance Requirement		Most Critical Load Combination	Result	Acceptable?
Strength Requirements	Strain Primary Steel Members	-	No plasticity in primary members	<b>YES</b>
	Slab Concrete Crushing	-	No concrete crushing in the slab	<b>YES</b>
Serviceability Requirements	Vertical Deflection	Only Redundancy II DL considered	0.516 in	<b>YES</b>
Notes: 1. The analysis showed that the structure was capable of resisting an additional 15% of the applied factored live load. 2. In order to complete the evaluation, the displacements and reaction forces calculated at support locations should be used as factored demands to check against the nominal capacity of the supports and substructure members.				

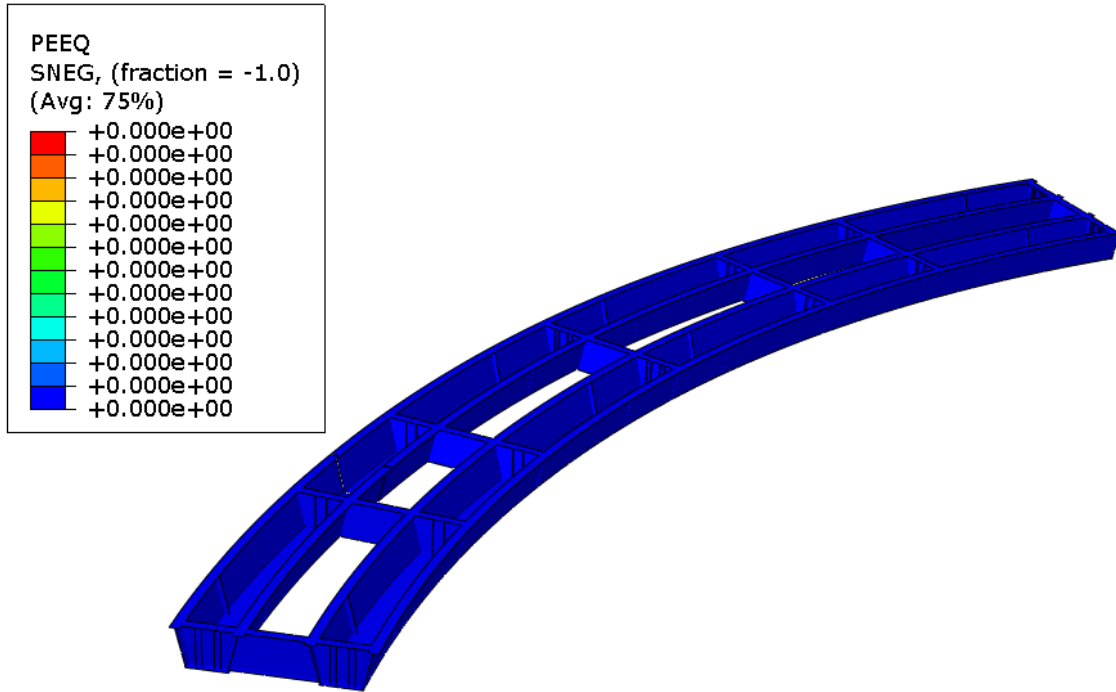
773 **F.2.8.1 Minimum Strength Requirements**

774 All of the strength requirements were met by the system in the faulted state while subjected to any one  
 775 of the load cases included in the Redundancy I and Redundancy II load combinations. Since the system  
 776 met all of the strength requirement it may be re-designated as a system redundant member (SRM) as soon  
 777 as the minimum serviceability requirements are met; otherwise it shall remain designated a fracture critical  
 778 member (FCM).

779 The first set of strength requirements apply to any primary member of the superstructure, which in this  
 780 case are the tub girders, diaphragms, and concrete slab. These requirements are the following:

- 781 • In a component, such as a web or a flange of a primary steel member, the average strain is less than  
 782 five times the material yield strain.
- 783 • In a component, such as a web or a flange of a primary steel member, the average strain is less than  
 784 0.01.
- 785 • A strain level of 0.05 is not reached anywhere in a primary steel member.
- 786 • The combined flexural, torsional and axial force effects computed in primary compression  
 787 members are below the nominal compressive resistance of the member (these limit states are  
 788 predicted by the FEA).
- 789 • If a compression strain greater than 0.003 is reached in the slab, the portion where that limit is  
 790 exceeded does not compromise the overall system load carrying capacity.
- 791 • The system in the faulted condition is able to support an additional 15% of the factored live load.

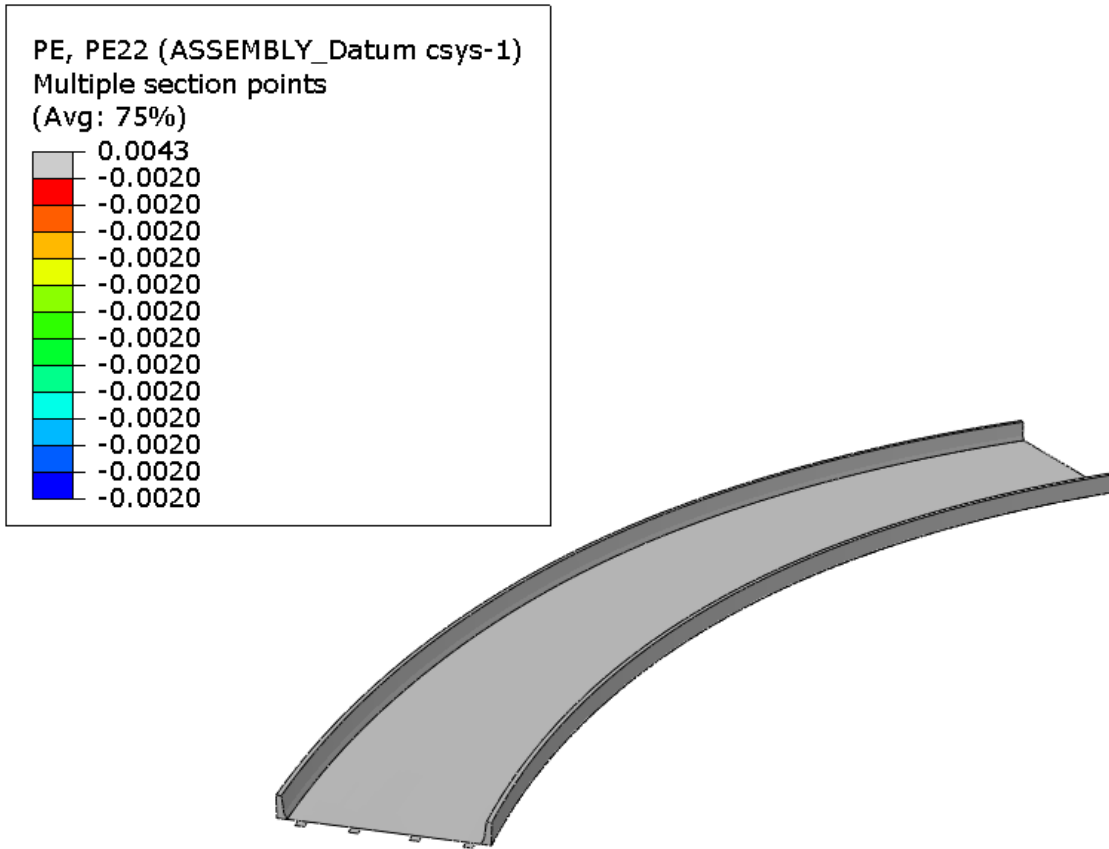
792 No yielding was observed in the primary steel members, further critical buckling loads were not reached  
 793 in any primary steel member. No plastic strains were calculated in the tub girders or the diaphragms after  
 794 the failure of the exterior girder for the Redundancy I or Redundancy II load combinations; therefore, the  
 795 strain requirements on primary steel members are met, as illustrated in Figure F-18. As the FEA accurately  
 796 predicts potential failure of primary steel compression member subjected to combined flexural, torsional,  
 797 and axial force effects, and quasi-static equilibrium is reached for both load combinations, the requirements  
 798 of primary steel compression members are met.  
 799



800  
801

**Figure F-18. Absence of plastic equivalent strain in primary steel members.**

802        Regarding the concrete slab, concrete crushing and tension cracking is allowed and expected to take  
 803 place. However, if the portion of the slab where a total compressive strain of 0.003 has been exceeded is  
 804 large enough to compromise the overall system load carrying capacity or if significant hinging occurs, the  
 805 structure should not be considered as sufficiently redundant. In this example, the Redundancy II load  
 806 combination resulted in the largest compressive strains in the slab, which were located in the haunches over  
 807 the exterior tub girder at the failure location, as shown in Figure F-19. Although there is some localized  
 808 compressive damage in the slab it was extremely confined to a small area. Thus, it was not enough to result  
 809 in a reduction in load carrying capacity.  
 810



811  
812

**Figure F-19. Absence of concrete crushing in slab.**

813 Although the substructure is not explicitly included in the finite element model, the reaction forces at  
 814 support locations are calculated in the analysis. These should be taken as the factored demands that the  
 815 substructure must be able to safely sustain, which are summarized in Table F-6. In this example, the  
 816 Redundancy I load combination resulted in the largest vertical reaction forces, except for the vertical  
 817 reaction at exterior girder support in the north abutment which largest value was calculated under the one  
 818 loaded lane case of the Redundancy II load combination. On the other hand the largest transverse reaction  
 819 forces take place under the two loaded lanes case of the Redundancy II load combination at the pier. The  
 820 unfactored nominal capacity of the abutments and the pier need to be checked against these load demands.  
 821 Similarly the pier and abutments must accommodate the horizontal displacements that are calculated in the  
 822 analysis at the support locations. In this example, Redundancy I and Redundancy II load combinations  
 823 resulted in similar small horizontal displacements which are summarized in Table F-7.  
 824



825

**Table F-6. Calculated reaction forces for redundancy evaluation.**

Support	Girder	Reaction Force	Result for Redundancy I (1 Lane)	Result for Redundancy II (1 Lane)	Result for Redundancy II (2 Lanes)
South Abutment	Interior	Vertical	107.3 kips	86.3 kips	91.0 kips
	Exterior	Vertical	160.8 kips	105.1 kips	116.9 kips
Pier	Interior	Vertical	596.7 kips	581.5 kips	508.9 kips
		Longitudinal	0.0 kips	0.0 kips	0.0 kips
		Transverse	15.2 kips	15.9 kips	18.7 kips
	Exterior	Vertical	578.2 kips	567.9 kips	551.9 kips
		Longitudinal	0.0 kips	0.0 kips	0.0 kips
		Transverse	-15.2 kips	-15.9 kips	-18.7 kips
North Abutment	Interior	Vertical	123.2 kips	108.9 kips	47.0 kips
	Exterior	Vertical	233.1 kips	284.4 kips	283.7 kips
Notes					
<ol style="list-style-type: none"> <li>1. Longitudinal direction is normal to the radius of the curve. Positive longitudinal direction points south.</li> <li>2. Transverse direction is parallel to the radius of the curve. Positive transverse direction points away from the origin of the curve.</li> </ol>					

826

827

**Table F-7. Calculated displacements at support locations for redundancy evaluation.**

Support	Girder	Displacement	Result for Redundancy I (1 Lane)	Result for Redundancy II (1 Lane)	Result for Redundancy II (2 Lanes)
South Abutment	Interior	Longitudinal	0.167 in	0.112 in	0.143 in
		Transverse	0.146 in	0.101 in	0.126 in
	Exterior	Longitudinal	0.180 in	0.141 in	0.173 in
		Transverse	0.147 in	0.102 in	0.125 in
Pier	Interior	Longitudinal	0.000 in	0.000 in	0.000 in
		Transverse	0.093 in	0.098 in	0.115 in
	Exterior	Longitudinal	0.000 in	0.000 in	0.000 in
		Transverse	-0.089 in	-0.094 in	-0.110 in
North Abutment	Interior	Longitudinal	0.290 in	0.251 in	0.319 in
		Transverse	-0.367 in	-0.449 in	-0.474 in
	Exterior	Longitudinal	0.397 in	0.446 in	0.510 in
		Transverse	-0.362 in	-0.447 in	-0.472 in
Notes:					
<ol style="list-style-type: none"> <li>1. Longitudinal direction is normal to the radius of the curve. Positive longitudinal direction points south.</li> <li>2. Transverse direction is parallel to the radius of the curve. Positive transverse direction points away from the origin of the curve.</li> </ol>					

828

829

830

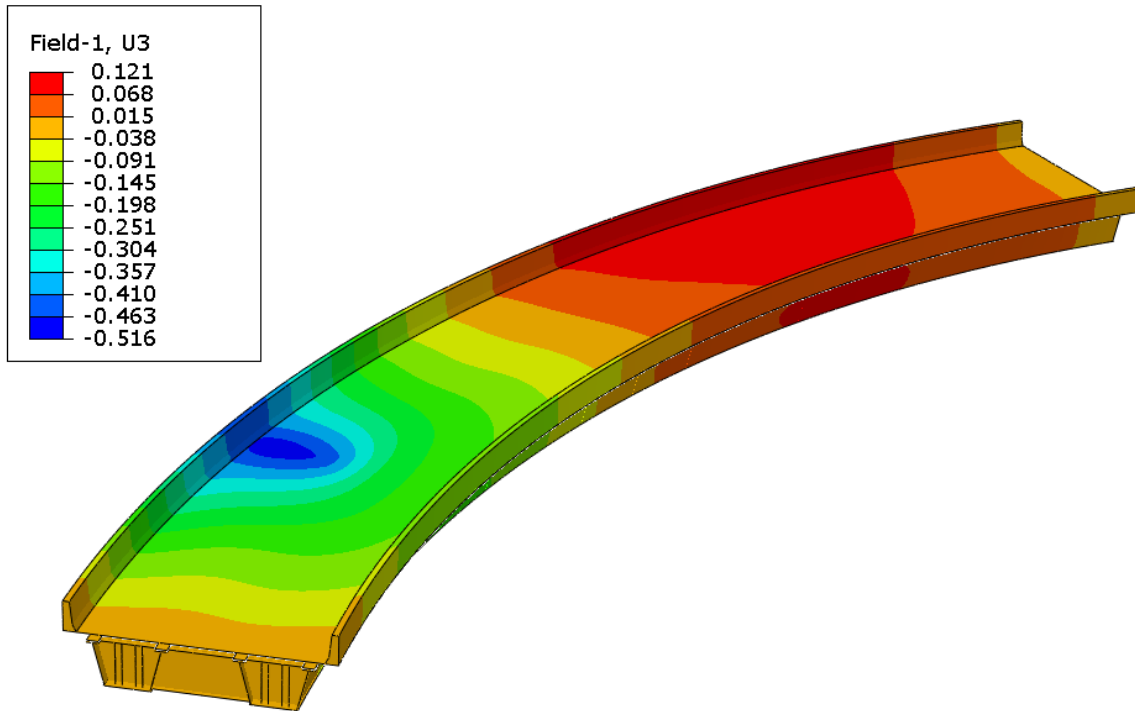
831

832

Additionally, the system demonstrated a reserve margin of at least 15% of the applied live load in the Redundancy I and II load combinations. Effectively, this requirement ensures the slope of the load vs displacement curve for the system structure remains positive (i.e., there is still significant remaining reserve capacity).

833 **F.2.8.2 Minimum Serviceability Requirements**

834 The only serviceability requirement in the Appendix E is that the increase of deflection after the failure  
835 of a primary steel tension member cannot be greater than  $L/50$ . This requirement is to be checked in the  
836 Redundancy II load combination under factored dead load only. In the current case, the limit is 24 inches,  
837 which was not surpassed since the maximum additional deflection computed in the FEA was 0.516 inches.  
838 This is illustrated in Figure F-20. Figure F-20. Deflection after failure of primary steel tension member.  
839



840  
841

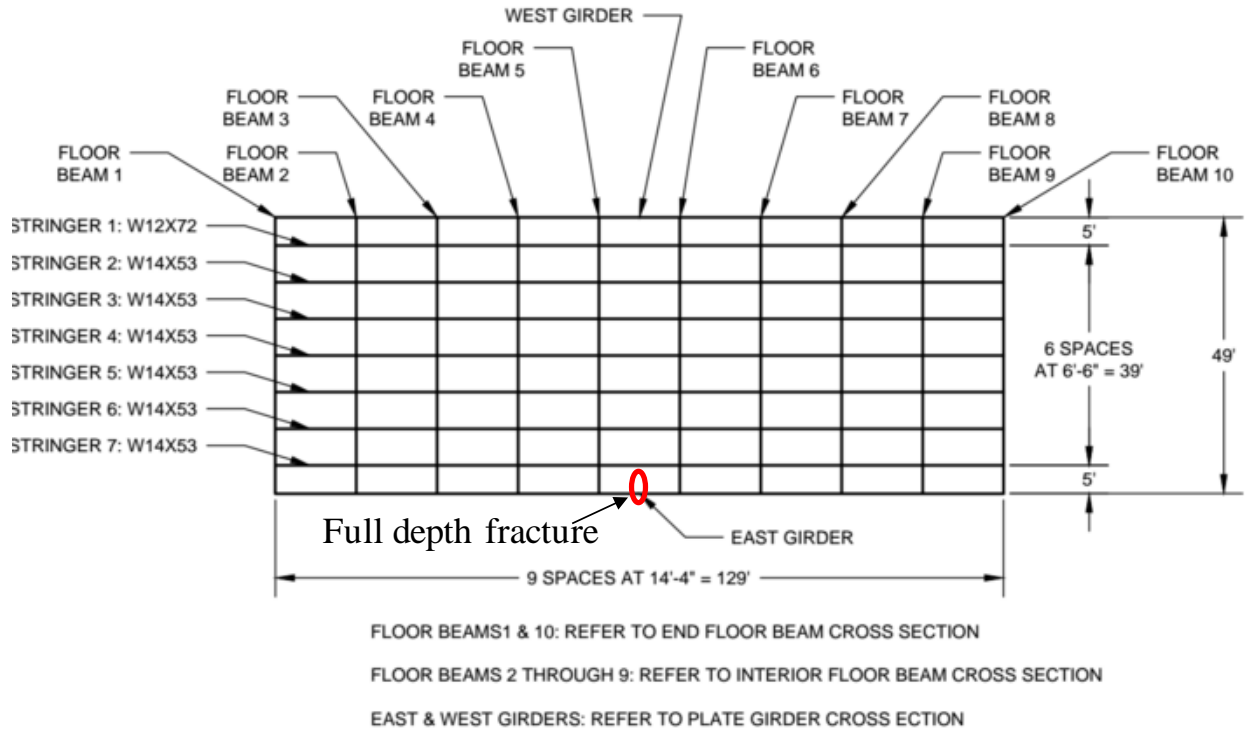
**Figure F-20. Deflection after failure of primary steel tension member.**

842 **F.2.9 Conclusions**

843 The redundancy of a curved continuous two span twin tub girder bridge after the failure of the exterior  
844 tub girder was analyzed in accordance with the methodology described in the proposed guide specification  
845 in Appendix E. Based on the comparison between the obtained results and the minimum performance  
846 requirements, the structure is not likely to fail nor undergo a significant serviceability loss as result after  
847 the failure of the exterior tub girder. Hence the exterior tub girder may be re-designated as a system  
848 redundant member (SRM).

849 F.3 Single Span Through Girder Bridge

850 The redundancy of a single span straight through girder bridge is analyzed by developing a finite element  
 851 model in accordance with the methodology described in the proposed guide specification in Appendix E.  
 852 It is assumed that the structure does not possess any of the detrimental attributes described in the screening  
 853 criteria and that it is built to Section 12 of the AWS D1.5. In this case, the failing tension member is the  
 854 east girder. The entire cross-section, including the compression flange, is assumed to fail at mid span as  
 855 shown in Figure F-21.  
 856



857  
858

**Figure F-21. Steelwork geometry and failure location.**

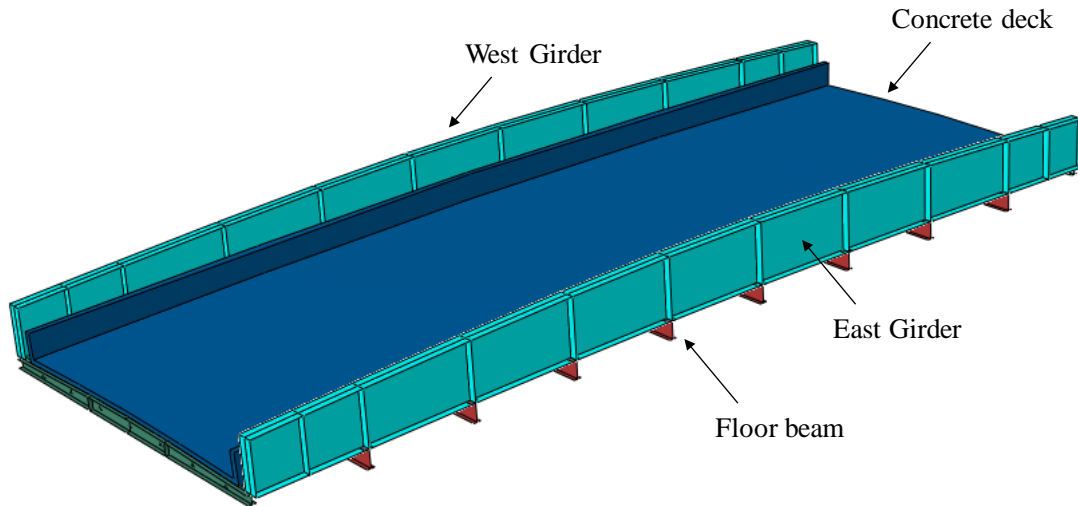


**Figure F-22. Overview of the bridge.**

859  
860

861 The structure is a through girder bridge with girders spaced at 49 feet and a single span measuring 129  
 862 feet long. Figure F-21 shows an overall sketch of the structure. As shown in Figure F-22, the bridge consists  
 863 of the steel girder system and a reinforced concrete slab with railings. The steel girder system is composed  
 864 of two plate girders (west and east), 10 floor beams, and seven stringers, as shown in Figure F-21. The  
 865 concrete slab is 44.5 feet wide. The cross section of the bridge is shown in Figure F-23. Figure F-24 shows  
 866 the connection details between the floor beams and plate girders. Figure F-25 shows the connection details  
 867 between the stringers and floor beams. As can be seen, this connection is a typical of through girder bridges.  
 868 The bridge is composite by using shear studs to connect the concrete slab to the steel system. Three shear  
 869 studs are placed in each row on the top flange of the floor beams, with a typical spacing of 10 in. Two  
 870 shear studs are placed in each row on the top flange of the stringers, with a typical spacing of 6 in. All steel  
 871 plates, used in the girders are made of ASTM A709 Grade 50. Slab reinforcement is made of ASTM A706  
 872 Grade 60. The concrete compressive strength of the slab is 4 ksi. The cross slope and girder camber were  
 873 ignored in the development of the geometry used in the model.  
 874

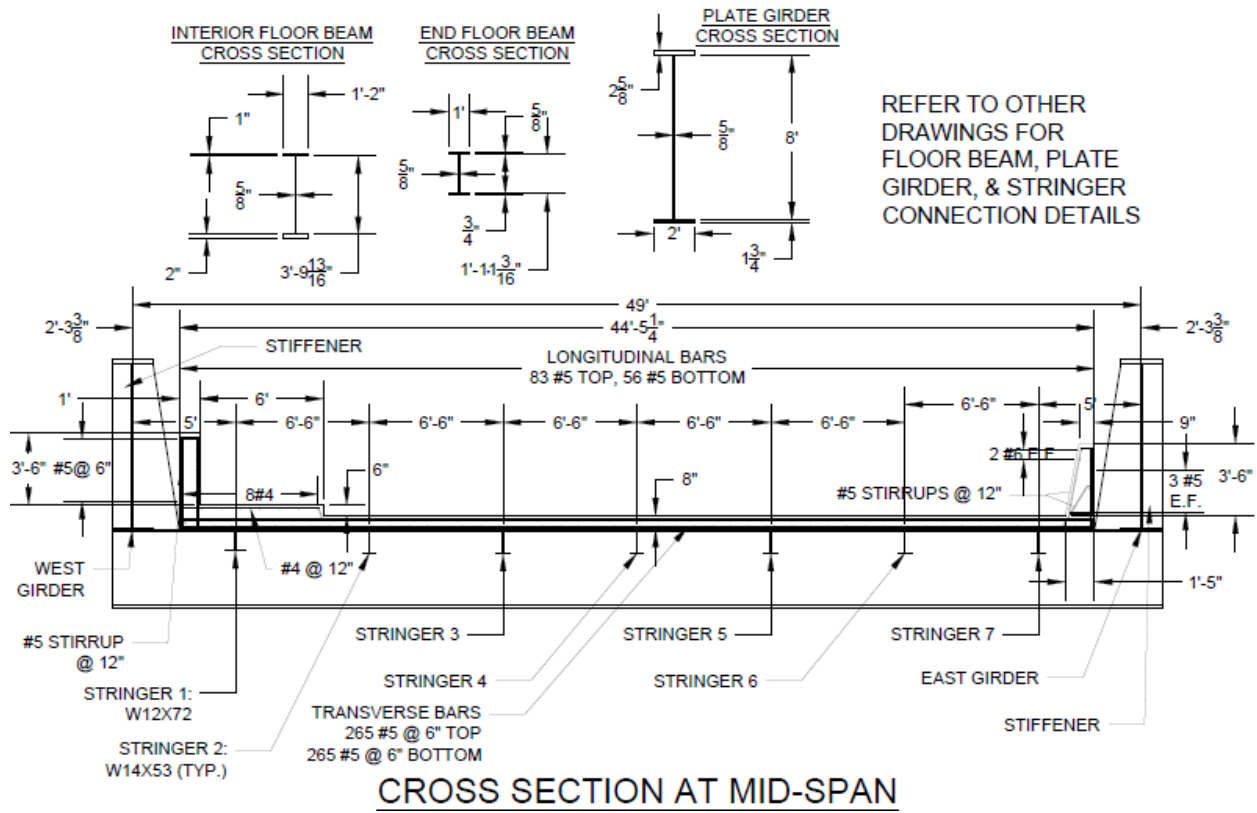


**Figure F-23. Typical cross-section and slab reinforcement details.**

875  
876

877

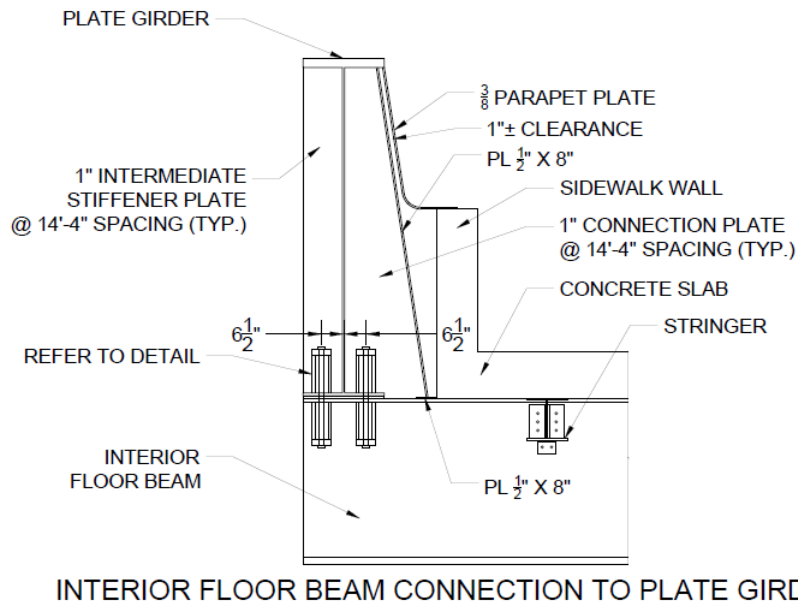
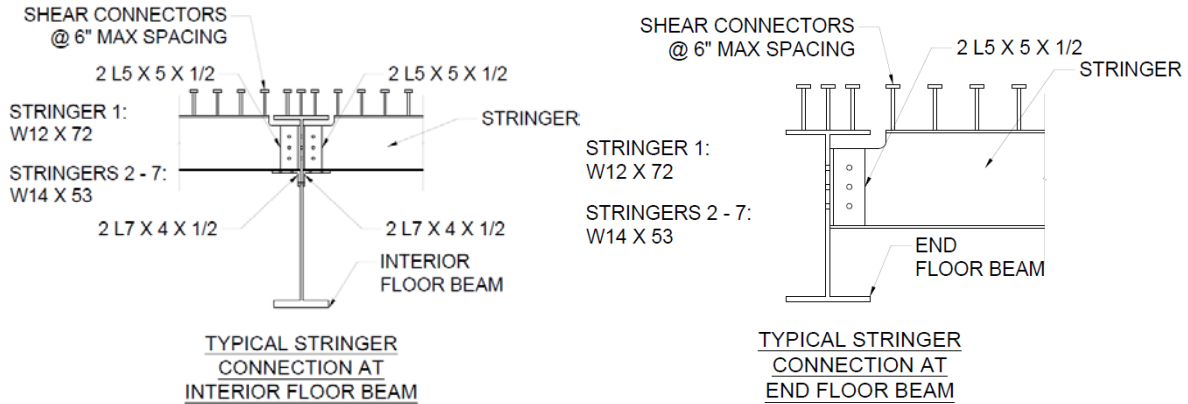


**Figure F-24. Connection details between the floor beams and the plate girder.**

878  
879

880



881  
882 **Figure F-25. Connection details between the stringers and the floor beams.**

883 **F.3.1 Analysis Procedure**

884 The analysis is performed to establish if the system demonstrates acceptable performance in the faulted  
885 condition. In the example, the term “faulted condition” specifically refers to the case in which a primary  
886 steel tension member is assumed to have failed. For this analysis, load factors for both dead and live load  
887 are applied as described in the proposed guide specification in Appendix E. In this example, the described  
888 analysis procedure is composed of an initial implicit static analysis and a final explicit dynamic analysis,  
889 into which the results from the initial implicit static analysis are imported. While it is not mandatory for  
890 the Engineer to follow these particular steps, it has been found that this procedure optimizes the  
891 computational time required.

892 **F.3.1.1 Initial Implicit Static Analysis**

893 Implicit static analysis was utilized to calculate the state of the structure prior to hardening of the concrete  
894 in the slab. An implicit static analysis was used for the initial steps because, although non-linearity is  
895 considered in the analysis, the bridge behavior is linear and inertial effects can be neglected as the bridge  
896 is in the undamaged condition. As the slab does not carry any load and does not contribute to the stiffness  
897 of the system before concrete hardening, two modifications are required in the finite element analysis during  
898 this initial implicit static analysis as follows:

- 899 • A very low stiffness is specified for the elements composing the slab, i.e., the elements modeling  
900 concrete and rebar. A reduced stiffness of 1/1,000 of the respective modulus of elasticity of each  
901 material was used. This is done so the load carried by the slab and rebar have negligible  
902 contribution to the stiffness of the system. No modifications to the stiffness should be applied to  
903 the steelwork.
- 904 • Instead of defining contact interaction between the slab and the steelwork, a mesh tie was specified.  
905 The nodal displacements of the concrete slab elements are tied to the displacements of the top  
906 flanges of girders, floor beams, and stringers which occur due to dead load. As a result, the slab  
907 deforms with the steelwork and does not ‘sag’ between the girders, floor beams, and stringers.

908 It is worth noting that the remainder of the finite element modeling is identical between the initial implicit  
909 static analysis and the final explicit dynamic analysis. The specific steps in the initial implicit static analysis  
910 are described as follows:

- 911 1. Apply load due to self-weight of the structural steel components as a body force.
- 912 2. Apply load due to self-weight of the wet slab components as a body force.
- 913 3. The system is then fixed in terms of position, that is, the displacement degrees of freedom are not  
914 allowed to change.

- 915 4. The elements composing the slab (elements modeling rebar and concrete) are then deactivated.  
916 5. The elements composing the slab are then reactivated. During this reactivation the strain in the  
917 elements composing the slab is reset to zero.  
918 Steps 3 through 5 are necessary since even though very low stiffness was specified for the slab, these  
919 elements do undergo strain. Setting the strains to zero eliminates “locked in” artificial stresses in later steps.

### 920 *F.3.1.2 Final Explicit Dynamic Analysis*

921 As contact algorithms, softening material behavior, and non-linear geometry are required to be part of  
922 the finite element analysis, implicit solution procedures present unavoidable convergence problems in most  
923 FEA solvers. In order to calculate the capacity of the bridge after sudden failure of a tension component, a  
924 dynamic explicit analysis needs to be carried out. Therefore, the results obtained from the initial implicit  
925 static analysis are imported into the final explicit dynamic analysis. In other words, the state of the system  
926 (stresses, strains, displacements and forces) at the beginning of the final explicit dynamic analysis is defined  
927 by the state of the system computed at the end of the initial implicit static analysis.

928 As previously stated, during the initial implicit static analysis, the slab was modeled with largely reduced  
929 stiffness to reflect that it is not hardened and a mesh tie constraint was used to assure that the slab deformed  
930 with the steelwork. This approach also prevents excessive sag of the soft slab. After the state of the system  
931 is imported, the following changes are made to capture the response of the structure after the concrete has  
932 hardened:

- 933 • The modulus of elasticity of the concrete and rebar elements in the slab is changed to their final  
934 actual values. It is noted that no modifications need to be applied for the steelwork.
- 935 • The mesh tie constraint between the slab concrete elements and the top flanges of the steelwork is  
936 replaced by a frictional contact interaction. Additionally, since the structure under analysis is  
937 composite, elements which accurately model the behavior of shear studs are added.

938 All of the body forces applied during the initial implicit static analysis (i.e., the dead load of the structure)  
939 are maintained throughout the final explicit dynamic analysis.

940 To evaluate the capacity of the structure in the faulted state, the following steps were carried out in the  
941 final explicit dynamic analysis:

- 942 6. The stiffness of the elements located at the fracture location under consideration were slowly  
943 reduced. The stiffness was slowly reduced in order to minimize any dynamic effects. It is noted  
944 that the actual fracture and subsequent vibration of the structure is not modeled. This dynamic  
945 effect is accounted for using the  $DA_R$  factor as discussed before. If dynamic effects are found to  
946 be significant even if the stiffness is slowly reduced, the system must be allowed to oscillate until  
947 these effects are dampened.
- 948 7. Factored loads due to traffic are applied as surface tractions. For the Redundancy I load  
949 combination all loads are amplified by  $DA_R$ , for the Redundancy II load combination the dynamic  
950 load allowance (IM) is applied. These loads were applied very slowly to minimize any dynamic  
951 effects, as well. If dynamic effects are significant, the system must be allowed to oscillate until  
952 these effects are dampened.
- 953 8. An additional 15% of live load is gradually applied.

### 954 **F.3.2 Material Models**

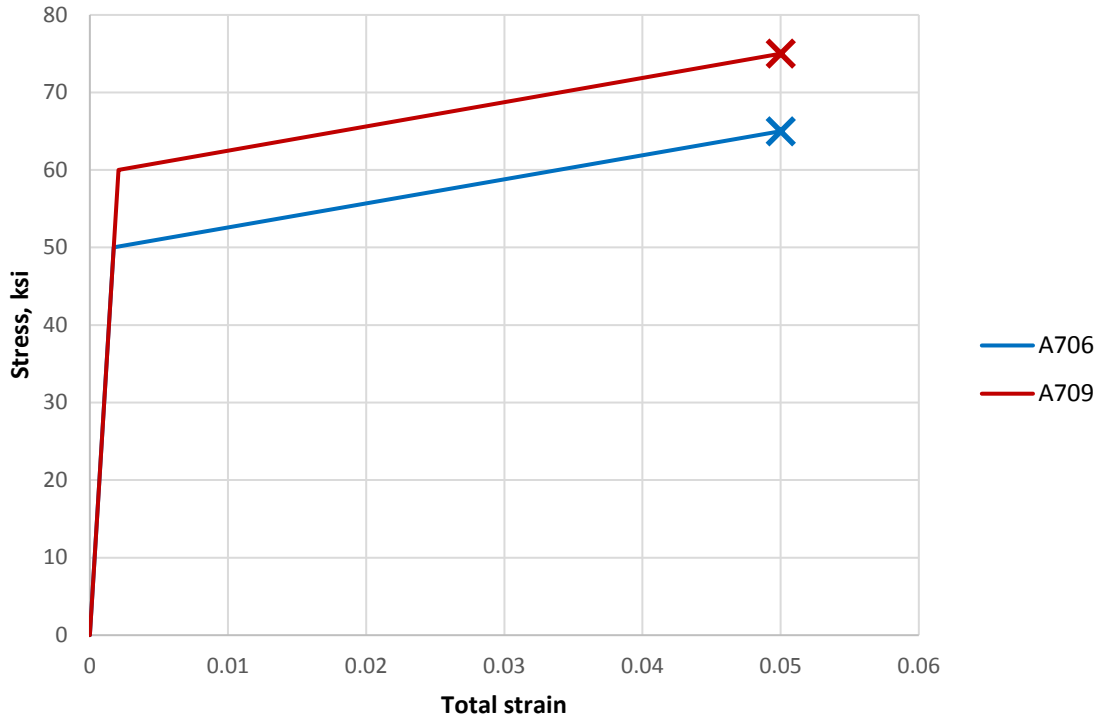
955 Three material models are needed in the finite element model. Two of these are utilized to model  
956 different steel types, and one is utilized to model the response of concrete. For the development of the steel  
957 material models, it is necessary to know the yield strength and ultimate strength of each steel type. In this  
958 example, since no test values are known to the Engineer, nominal values specified in the respective

959 standards are utilized. These are summarized in Table F-8. A mass density of 0.494 kcf was specified for  
 960 all steel types.

961 **Table F-8. Material properties for steel material models.**

Material	Nominal Yield Strength	Nominal Ultimate Strength	Standard
ASTM A709 Gr. 50	50 ksi	65 ksi	ASTM A709/A709M
ASTM A 706 Gr. 60	60 ksi	75 ksi	ASTM A706/A706M

962 The stress-strain relation for all steel components will follow an initial linear elastic steel with a Young's  
 963 modulus of 29,000 ksi and Poisson's ratio of 0.3. Once the nominal yield strength is reached, the stress-  
 964 strain relation is defined by Von Mises (J2) plasticity with kinematic linear hardening, until the nominal  
 965 ultimate strength is reached at a total strain of 0.05. Once the nominal ultimate strength or a total strain of  
 966 0.05 is reached, the material is assumed to fail. Figure F-26 shows the uniaxial material response for the  
 967 steel employed in this finite element model with the 'X' denoting the stress at the failure strain of 0.05.  
 968  
 969



970 **Figure F-26. Stress-strain curves of steel material models.**  
 971

972 The material model used in concrete is defined entirely by the specified compressive strength, which in  
 973 this case is 4 ksi. This quantity is also used to calculate the tensile strength, the total strain at compressive  
 974 strength,  $\epsilon_c$ , and the material parameter  $n$ . Table F-9 summarizes the calculation of these values. A mass  
 975 density of 0.150 kcf was specified for concrete.  
 976



Table F-9. Material properties for concrete material model.

Quantity	Symbol	Equation	Result
Young's modulus	$E_c$	$E_c = 33,000w_c^{1.5}\sqrt{f'_c} \leq 1,802.5\sqrt{f'_c}$	3,600 ksi
Tensile strength	$f_t$	$f_t = 0.158(f'_c)^{\frac{2}{3}}$ for $f'_c \leq 7.25\text{ksi}$ $f_t = 0.307 \ln(f'_c + 2.61) - 0.114$ for $f'_c > 7.25\text{ksi}$	0.398 ksi
Fracture energy	$G_t$	$5.9 \cdot 10^{-4}(f'_c + 1.16)^{0.18}$	$7.93 \cdot 10^{-4}$ kip/in
Total strain at compressive strength	$\varepsilon_c$	$\varepsilon_c = 0.00124\sqrt[4]{f'_c}$	0.00175
Material parameter	$n$	$n = 0.4f'_c + 1.0$	2.6

978

979

980

981

982

983

The concrete material model is initially linear elastic, defined by a Young's modulus of 3,600 ksi and Poisson's ratio of 0.2, followed by concrete damage plasticity. In tension, once the material reaches its tensile strength, set at 0.398 ksi in this case, a tensile stress-displacement relation characterized by a fracture energy,  $G_t$ , of  $7.93 \cdot 10^{-4}$  kip-in is followed. This fracture energy is applied through a bi-linear tensile stress-displacement relation as shown in Figure F-27, and defined by the following quantities:

984

$$f_{t1} = \frac{f_t}{5} = 0.0796 \text{ ksi}$$

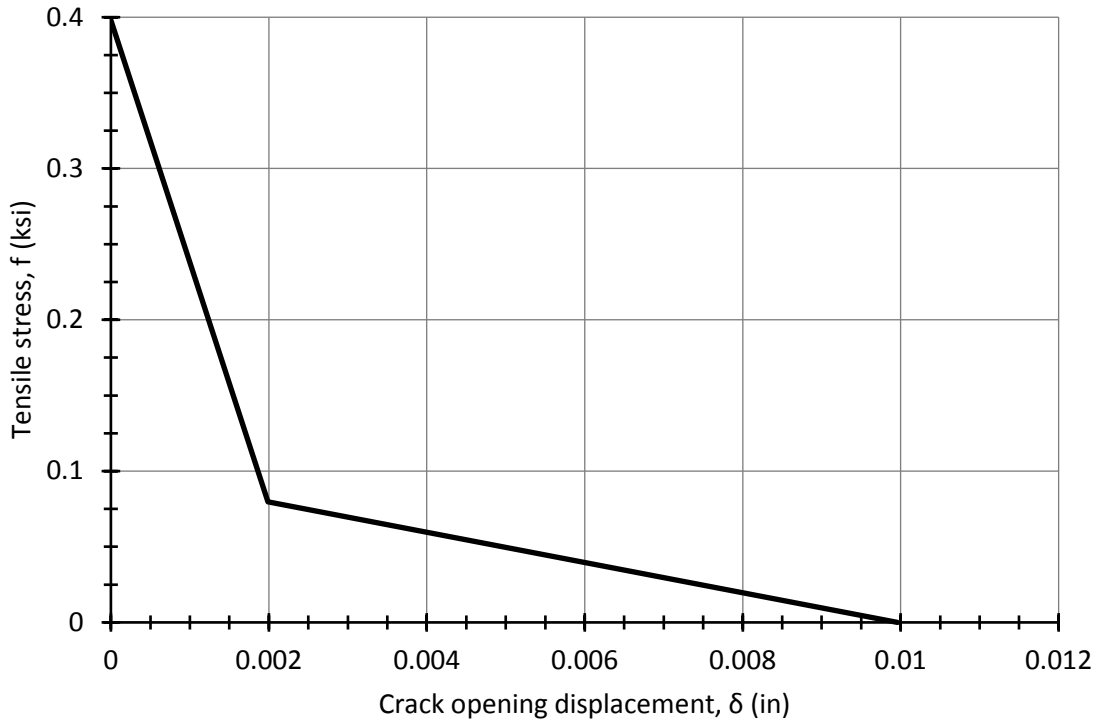
985

$$\delta_t = \frac{5G_t}{f_t} = 0.00996$$

986

$$\delta_{t1} = \frac{G_t}{f_t} = 0.00199$$

987



988  
989

**Figure F-27. Tensile stress-crack opening displacement curve for concrete material model.**

990 In compression the material follows the following stress-strain relations:

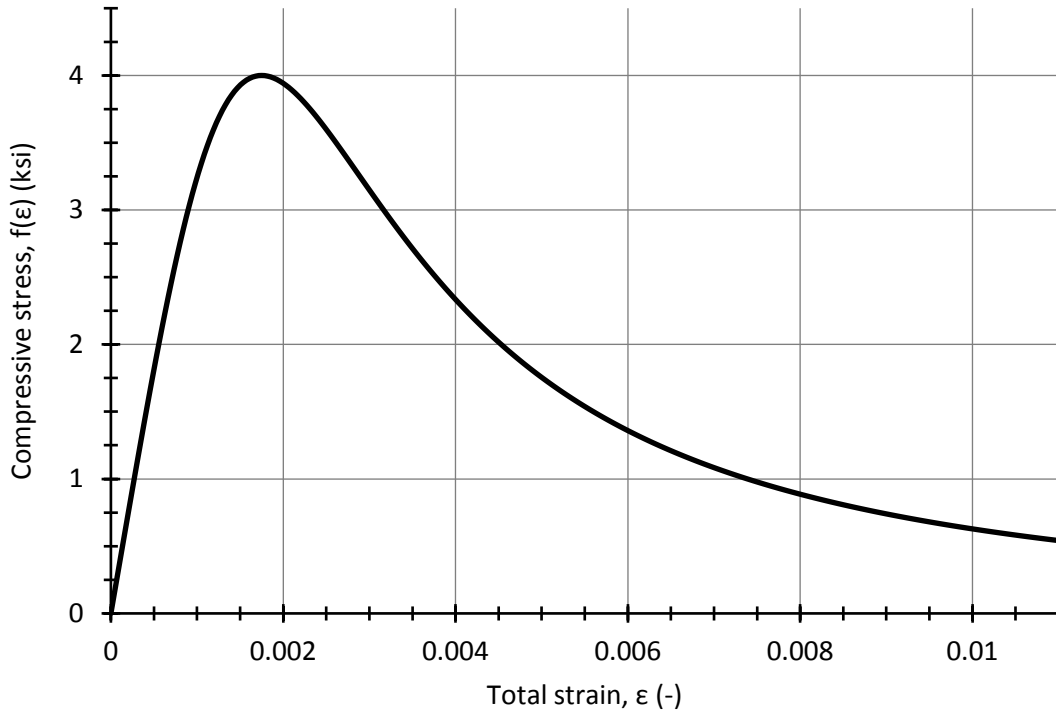
991

$$f(\varepsilon) = f'_c \left( \frac{\varepsilon}{\varepsilon_c} \right) \left[ \frac{n}{n - 1 + \left( \frac{\varepsilon}{\varepsilon_c} \right)^n} \right]$$

992

$$\varepsilon_{plastic} = \varepsilon - \frac{f(\varepsilon)}{E_c}$$

993 Where  $\varepsilon$  is total (elastic + plastic) strain,  $f(\varepsilon)$  is the compressive stress at a given total strain,  $f'_c$  is the  
 994 specified compressive strength,  $\varepsilon_c$  is the total strain at compressive strength,  $n$  is a material parameter,  
 995  $\varepsilon_{plastic}$  is the plastic strain and  $E_c$  is the concrete Young's modulus. Figure F-28 shows the resulting  
 996 compressive stress-strain relation.



997  
998

**Figure F-28. Compressive stress-strain curve for concrete material model.**

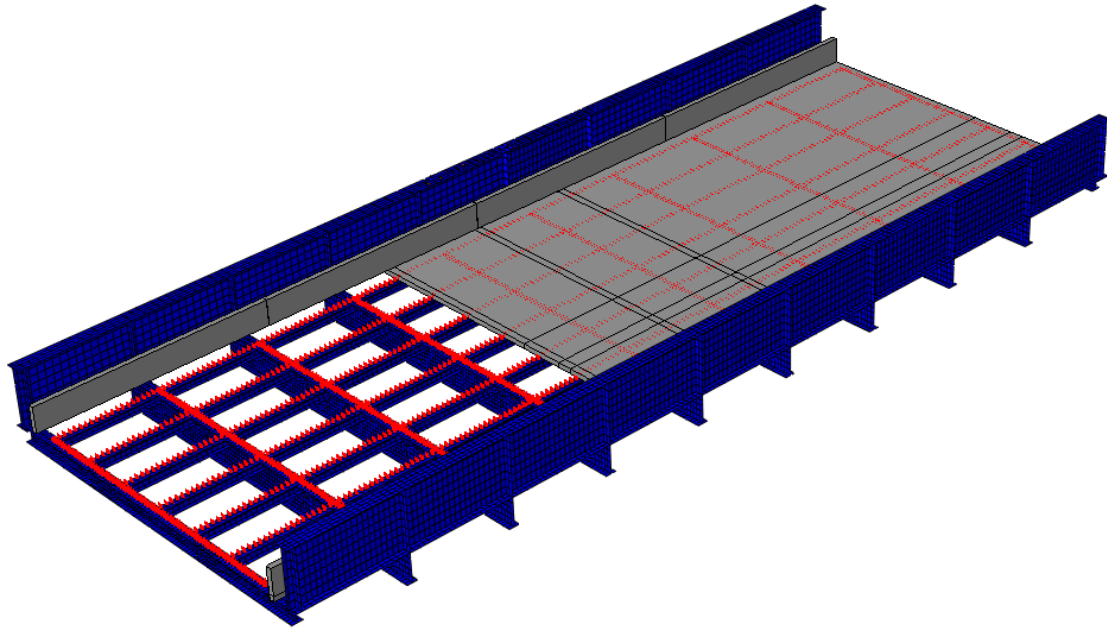
999 **F.3.3 Geometries, Meshes and Constraints**

1000 The geometry of the structure (see Figure F-29) is based on available design plans and is composed of  
1001 the following components that must be explicitly modeled:

- 1002 1. West and east plate girders.
- 1003 2. 10 floor beams.
- 1004 3. Seven stringers.
- 1005 4. A reinforced concrete slab with concrete railings.
- 1006 5. Shear studs.

1007 When generating the finite element model, splices, holes, access hatches, etc. are neglected. The  
1008 structure is assumed to be flat in the vertical plane, in other words, camber and superelevation are ignored.

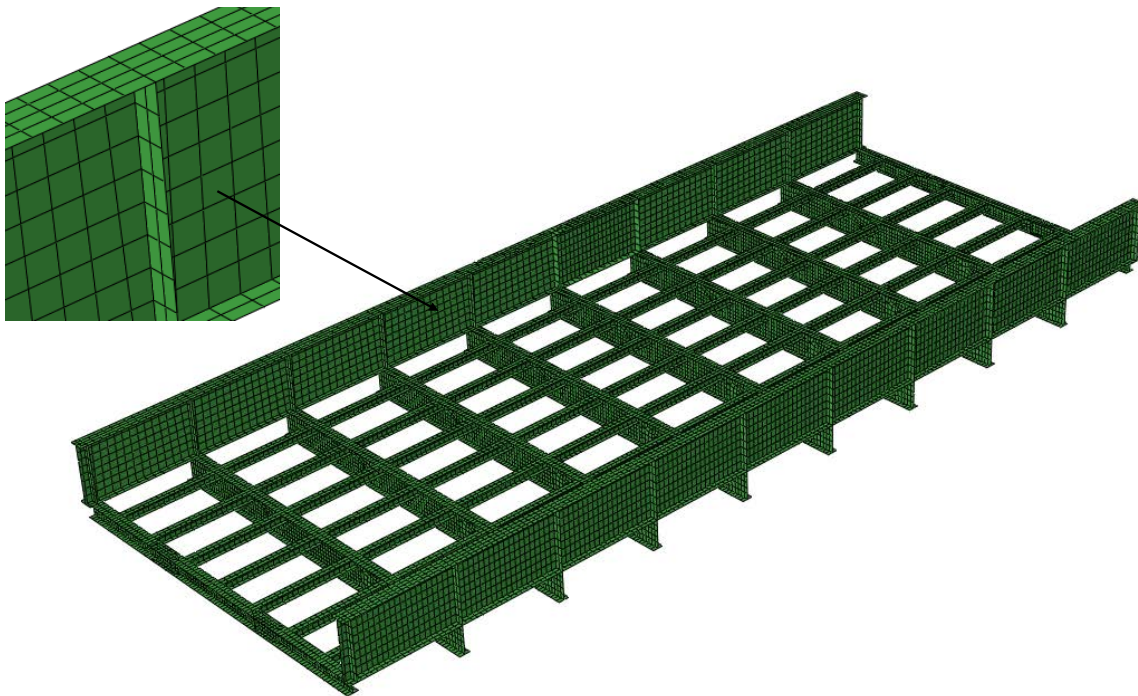
1009 Plate girders, floor beams and stringers are modeled with 4-node shell elements with reduced integration.  
1010 A minimum of four elements are used along flange widths and along web heights. Stiffening attachments  
1011 are modeled with shell elements as well. Figure F-30 shows two details of the mesh employed to model  
1012 the steel system. As shown in this figure, the plate girders, floor beams and stiffeners constitute a single  
1013 geometry.



1014  
1015  
1016

**Figure F-29. Through girder bridge geometries. Concrete slab and barriers (grey), steel system (blue), and shear studs (red).**

1017



1018  
1019

**Figure F-30. Mesh details of the steel system.**

1020 The reinforced concrete slab was modeled with two types of elements. Specifically, 8-node linear bricks  
1021 with reduced integration were used to model concrete and 2-node truss elements with linear displacement

1022 were used to model steel reinforcement. Eight solid concrete elements are used through the thickness of  
1023 the slab with maximum aspect ratio (length of longest edge divided by length of shortest edge) of 5, and  
1024 corner angles (angle at which two element edges meet) between 40 and 140 degrees. The length of the  
1025 truss elements used to model the reinforcement were approximately equal to the length of the longest edge  
1026 of the solid concrete elements. These truss elements were embedded within the solid concrete elements.  
1027 At the nodes of the embedded truss elements, the translational degrees of freedom are eliminated and the  
1028 nodal translations were constrained to interpolated values of the nodal translations of the host solid concrete  
1029 element. The railings were meshed with four elements along its height and two elements across its width,  
1030 it was attached to the slab by a mesh tie. The reinforcement of the concrete railing was neglected.

### 1031 **F.3.4 Slab-Structural Steel Interaction**

1032 As stated, the interaction between the bottom of the concrete slab and the top of the flanges of the  
1033 steelwork is modeled differently in the two steps described above. In the initial implicit static analysis,  
1034 when the elements comprising the slab and barriers have  $1/1,000^{\text{th}}$  of the modulus of elasticity to model the  
1035 “wet” condition, a mesh tie is used to slave the motion of the slab to the motion of the surface comprising  
1036 the top of the steel work. With this procedure, it is ensured that the slab deformation will conform to the  
1037 deformation of the steelwork while unrealistic sagging of the slab between supporting elements and tipping  
1038 of the barrier is prevented.

1039 In the final explicit dynamic analysis, when the stiffness of the elements comprising the slab and barriers  
1040 has been changed to their final real values, the mesh tie previously used is deleted and replaced by a contact  
1041 interaction and modeling of shear studs. The normal behavior of the contact interaction is modeled through  
1042 a penalty stiffness. The penalty stiffness is several orders of magnitude larger than the normal stiffness of  
1043 the underlying contacting elements and allows a very small penetration so a pressure can be calculated.  
1044 The tangential behavior of the contact interaction is modeled through an algorithm based on Coulomb  
1045 friction with a limit on the allowable shear. A friction coefficient of 0.55 and an interfacial shear strength  
1046 of 0.06 ksi are specified.

1047 The simplified stud model, as described in the Appendix A is used to model composite action between  
1048 the slab and the steelwork. In the simplified stud model, the shear studs were modeled using connector  
1049 elements which were used to define the axial and interfacial shear interaction between the shear studs and  
1050 concrete slab. Connector elements are special purpose elements with zero length. These elements model  
1051 discrete physical connections between deformable or rigid bodies, and are able to model linear or nonlinear  
1052 force-displacement behavior in their unconstrained relative motion components.

1053 The recommendations of Appendix A were used to define the shear and tensile behavior of shear studs.  
1054 The stiffness, strength, and displacement at failure for the different shear stud assemblies included in the  
1055 model are in Table F-10. In shear, the stud groups follows the shear force-displacement relation proposed  
1056 by Ollgaard et al. (1971) up to maximum shear displacement of 0.2 inches. In tension, the governing failure  
1057 mode is concrete break-out, and follows the characteristic triangular response for transversely grouped  
1058 shear studs which governing failure mode is concrete break-out or shear stud pullout, as described in the  
1059 recommendations of Appendix A. The tension-shear interaction equation presented in Appendix A is used  
1060 to combine the effects of shear and tension acting simultaneously on a shear stud group.  
1061

1062

**Table F-10. Shear stud group properties.**

Location	Shear		Tension		
	Strength (kips)	Max. Slip (in)	Initial Stiffness (kip/in)	Strength (kips)	Max. Displ. (in)
End floor beam	108	0.2	3000	11.6	0.04
Interior floor beam	108	0.2	3000	13.9	0.05
Stringer 1	72.2	0.2	2500	7.31	0.03
Stringers 2-7	72.2	0.2	2500	4.64	0.02

1063

1064 **F.3.5 Connection Failure Modeling**

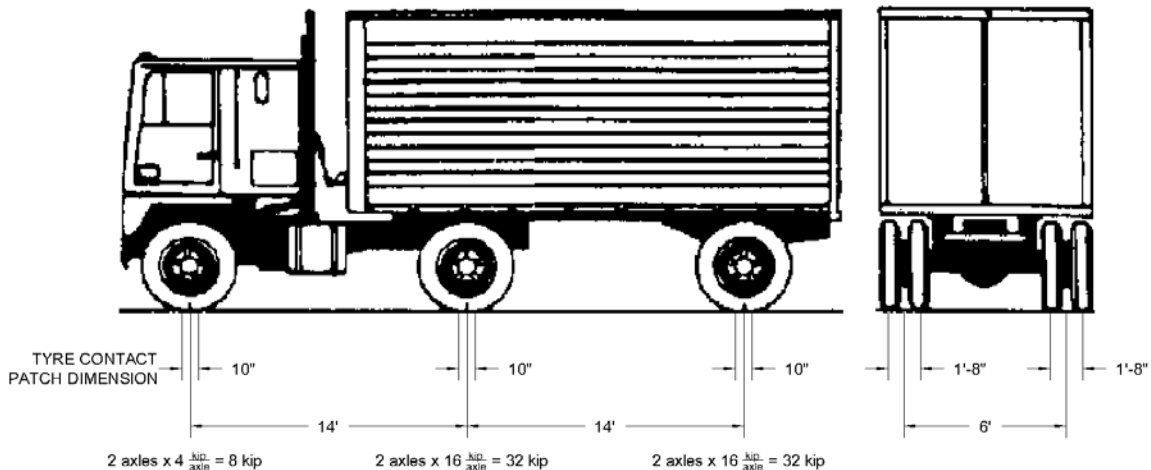
1065 When a connection is likely to fail before yielding of the member, in addition to the use of mesh ties to  
 1066 attach the components, an additional step may be necessary to capture connection failure. In this particular  
 1067 example, it was not necessary to include to model connection failure as the forces developed in the member  
 1068 did not exceed the capacity of the connections.

1069 **F.3.6 Substructure Flexibility Model**

1070 Details of the substructure were not available. Therefore, the substructure was not modeled in this case.  
 1071 In the case that such modeling is necessary, please refer to the proposed guide specification in Appendix E.

1072 **F.3.7 Loads and Boundary Conditions**

1073 Two types of loads were applied in the finite element models: body forces and surface tractions as  
 1074 required by the proposed guide specification in Appendix E. Body forces were applied for component dead  
 1075 loads (“DC” and “DW” per AASHTO designations). These are simply the product of mass, gravity and  
 1076 applicable load factors. Surfaces tractions were applied for traffic live loads (“LL” per AASHTO  
 1077 designation). The traffic live load is based on the HL-93 load model described in the AASHTO LRFD  
 1078 BDS, which is a combination of the truck loads, shown in Figure F-31, and a 0.64 klf load distributed over  
 1079 a width of 10 ft. The current structure does not include any bituminous pavement (i.e.: DW is zero).  
 1080



1081

1082

**Figure F-31. Truck load components and dimensions of the HL-93 vehicular live load model.**

1083 The Redundancy I and Redundancy II loading combinations were used to evaluate the structure in the  
 1084 faulted state. The load factors for these two combinations are as in Table F-11 are based on the provisions  
 1085 in Appendix E for bridges built to Section 12 in the AWS D1.5. The live load (LL) factors are modified by  
 1086 the appropriate multiple presence factors as described in Article 3.6.1.1.2 of the AASHTO LRFD BDS. It  
 1087 must be noted that dynamic amplification factor is equal to 0.4, which is applied to DC and LL in the  
 1088 Redundancy I load combination only. Also, the dynamic load allowance is 0.15 of the truck axle loads,  
 1089 and is only applied in the Redundancy II load combination.

1090 **Table F-11. Load factors used for Redundancy I and Redundancy II load combinations.**

Load Combination	Load Factors				Notes
	DC	LL	DA <sub>R</sub>	IM	
Redundancy I	1.05	0.85	0.40	N. A.	β = 1.5
Redundancy II	1.05	1.30	N. A.	0.15	β = 1.5

1091  
 1092 Longitudinally, the loads are positioned in the most critical positions in both the Redundancy I and  
 1093 Redundancy II load combinations. For the failure scenario considered in the current case (failure of the  
 1094 east girder at mid span as shown in Figure F-21), the most critical position of the truck axle loads which  
 1095 results in the truck facing south with its middle axis positioned at the failure plane, as shown in Figure F-32.  
 1096 The distributed load portion of the HL-93 load is applied along the span of the bridge.

1097 As described in the proposed guide specification in Appendix E, the transverse positioning of the HL-93  
 1098 live load model differs between the Redundancy I and Redundancy II load combinations, as illustrated in  
 1099 Figure F-32. Since the vehicular loads in the Redundancy I load combination are meant to represent the  
 1100 applied load at the instant in time in which the assumed member failure occurs, the HL-93 vehicular live  
 1101 load model is transversely positioned centered (both the 10 ft loaded width and the truck axle loads) within  
 1102 the marked (striped) lanes, in this case two lanes. Hence, as the bridge is striped for two lanes, there are  
 1103 two load cases for the Redundancy I load combination: two design lanes loaded, or one design lane loaded.

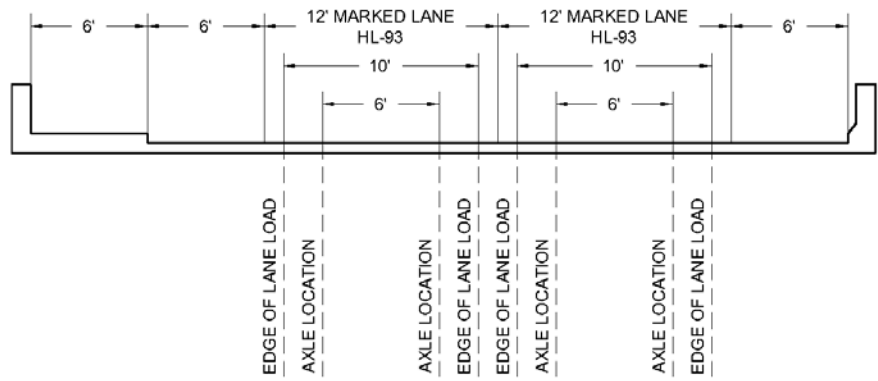
1104 On the other hand, the objective of the Redundancy II load combination is to evaluate the strength of the  
 1105 system after the failure of the primary steel tension member has occurred, so the number of design lanes is  
 1106 established in accordance with Article 3.6.1.1.1 in the AASHTO LRFD BDS, which in this case results in  
 1107 three design lanes with a width of 12 ft. In the Redundancy II load combination, the HL-93 vehicular live  
 1108 load model is transversely positioned (both the 10 ft loaded width and the truck axle loads) to produce  
 1109 extreme force effects within each design lane; however, the truck axle loads are transversely positioned  
 1110 such that the center of any wheel load is not closer than 2 ft from the edge of the design lane. Hence, there  
 1111 are three load cases for the Redundancy II load combination: three design lanes loaded, two design lanes  
 1112 loaded, or one design lane loaded.

1113 Component dead loads were linearly applied in the initial implicit static analysis. Traffic live loads were  
 1114 applied in the final explicit dynamic analysis. Their dynamic effects were minimized by applying them  
 1115 slowly through the use of smooth step, as in the following equation:

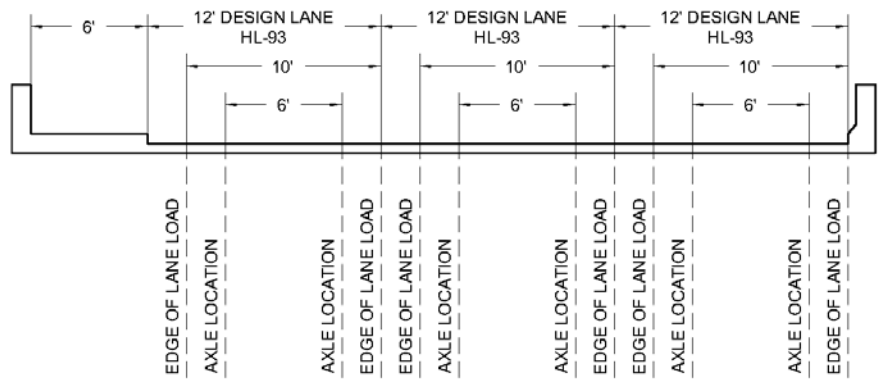
1116 
$$LR(t) = 6 \left(\frac{t}{T}\right)^5 - 15 \left(\frac{t}{T}\right)^4 + 10 \left(\frac{t}{T}\right)^3$$

1117 where  $LR(t)$  is the fraction of load at a load application time  $t$ , and  $T$  is the duration of the load application.  
 1118 The duration of the load application must be larger than the fundamental period of the structure to minimize  
 1119 oscillatory behavior in the final explicit dynamic analysis.

1120 Regarding prescribed boundary conditions, the structure is simply supported at the ends of the span.  
 1121 Based on the construction plans the bridge was allowed to translate longitudinally and transversely.  
 1122



TRANSVERSE LOAD POSITION FOR REDUNDANCY I



TRANSVERSE LOAD POSITION FOR REDUNDANCY II

1123  
1124

**Figure F-32. Transverse position of the HL-93 live load model.**

1125

1126 **F.3.8 Analysis of Results for Redundancy**

1127 Once the analysis is completed the obtained results are evaluated using the requirements described in  
 1128 Article 8 of the proposed guide specification in Appendix E. It was found that the structure did NOT meet  
 1129 the strength and serviceability requirements and is considered non-redundant against failure of the exterior  
 1130 tub girder. Specific details regarding the performance requirements and the results are summarized in Table  
 1131 F-12.  
 1132



1133

**Table F-12. Summary of the redundancy evaluation.**

Performance Requirement		Most Critical Load Combination	Result	Acceptable?
Strength Requirements	Strain Primary Steel Members	Redundancy I	Significant yielding (Maximum 31.9%)	<b>NO</b>
	Slab Concrete Crushing	Redundancy I	No concrete crushing in the slab	<b>YES</b>
Serviceability Requirements	Vertical Deflection	Only Redundancy II DL considered	137.1 in.	<b>NO</b>
Notes:				
1. In order to complete the evaluation, the displacements and reaction forces calculated at support locations should be used as factored demands to check against the nominal capacity of the supports and substructure members.				

1134

1135 **F.3.8.1 Minimum Strength Requirements**

1136 The strength requirements were not met by the system in the faulted state. The structure in the faulted  
1137 state did not meet the strength requirements when subjected to factored and amplified dead loads, under  
1138 either the Redundancy I load combination or the Redundancy II load combination. Therefore, the response  
1139 of the bridge in the faulted state with traffic loads (LL and IM) was not evaluated. Since the system did not  
1140 meet all of the strength requirements the east girder must remain a fracture critical member (FCM).

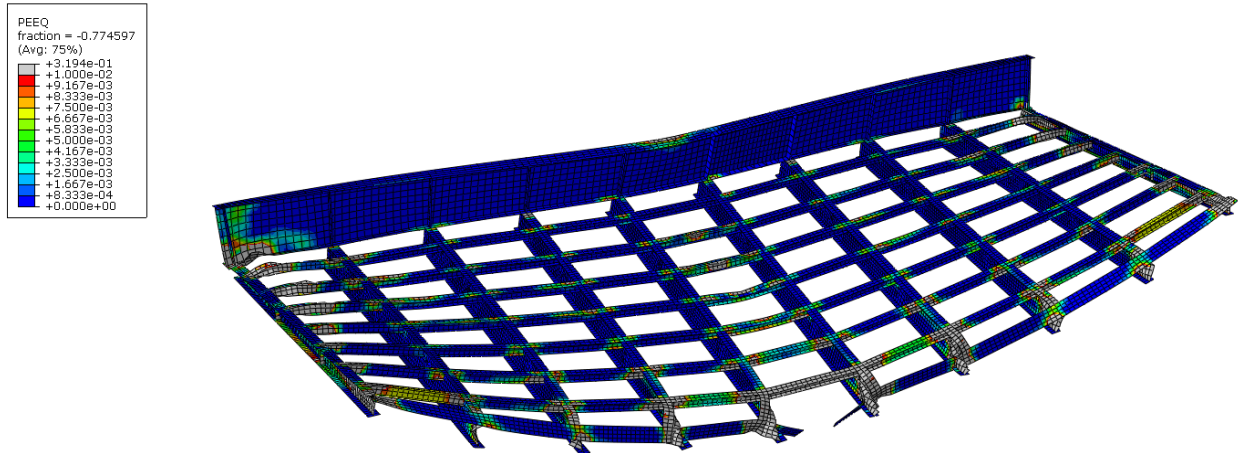
1141 The first set of strength requirements apply to any primary member of the superstructure, which in this  
1142 case are the tub girders, diaphragms, and concrete slab. These requirements are the following:

- 1143 • In a component, such as a web or a flange of a primary steel member, the average strain is less than  
1144 five times the material yield strain.
- 1145 • In a component, such as a web or a flange of a primary steel member, the average strain is less than  
1146 0.01.
- 1147 • A strain level of 0.05 is not reached anywhere in a primary steel member.
- 1148 • The combined flexural, torsional and axial force effects computed in primary compression  
1149 members are below the nominal compressive resistance of the member (these limit states are  
1150 predicted by the FEA).
- 1151 • If a compression strain greater than 0.003 is reached in the slab, the portion where that limit is  
1152 exceeded does not compromise the overall system load carrying capacity.
- 1153 • The system in the faulted condition is able to support an additional 15% of the factored live load.

1154 In this case, the load combination that resulted in the largest strain in steel primary members was  
1155 Redundancy I, although the resulting behaviors were similar for both Redundancy I and Redundancy II  
1156 load combinations. The largest plastic strain was 0.319 and took place on the top flange of the fractured  
1157 girder at the north support. Also, the average plastic strain of all stringers was greater than 0.01 at the  
1158 support, and the average plastic strain of floor beams 4-7 was greater than 0.01 at the span between stringer  
1159 7 and the fractured girder, as shown in Figure F-33. This is indicated by the elements that are grey in the  
1160 figure. Thus, the requirements regarding strain in primary steel members are exceeded.

1161

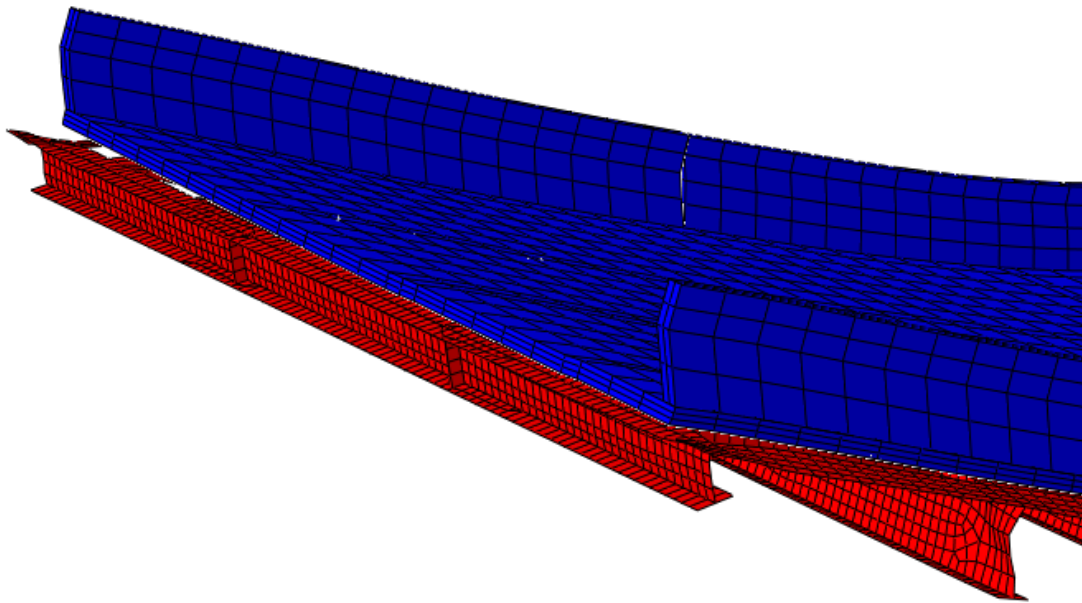
1162



1163  
1164

**Figure F-33. Equivalent plastic strain in primary steel members.**

1165 Regarding the concrete slab, concrete crushing and tension cracking is allowed and expected to take  
 1166 place. However, if the portion of the slab where a total compressive strain of 0.003 has been exceeded is  
 1167 large enough to compromise the overall system load carrying capacity or if significant hinging occurs, the  
 1168 structure should not be considered as sufficiently redundant. In this example, due to the presence of the  
 1169 concrete railings, there was no significant concrete crushing of the slab for both the Redundancy I and  
 1170 Redundancy II load combination. After the fracture occurred, the studs pulled out at two regions: (i) the  
 1171 region where fracture occurred, and (ii) the supports of the west girder (see Figure F-34). Throughout the  
 1172 rest of the slab no obvious stud pullout was observed and, as stated, there was no concrete crushing.  
 1173



1174  
1175

**Figure F-34. Pullout of the shear studs at the supports.**

1176 Although the substructure is not explicitly included in the finite element model, the reaction forces at  
 1177 support locations are calculated in the analysis. These should be taken as the factored demands that the

1178 substructure must be able to safely sustain, which are summarized in Table F-13. In this example, the  
 1179 Redundancy I load combination resulted in the largest vertical reaction forces. The unfactored nominal  
 1180 capacity of the abutments and the pier need to be checked against these load demands. Similarly the end  
 1181 supports must accommodate the horizontal displacements that are calculated in the analysis at the support  
 1182 locations. In this example, Redundancy I load combination resulted in particularly large transverse  
 1183 displacements which are summarized in Table F-14.

1184 **Table F-13. Calculated reaction forces for redundancy evaluation.**

Support	Girder	Reaction Force	Result for Redundancy I
South Abutment	West	Vertical	326.3 kips
	East	Vertical	489.5 kips
North Abutment	West	Vertical	327.1 kips
	East	Vertical	489.8 kips

1185

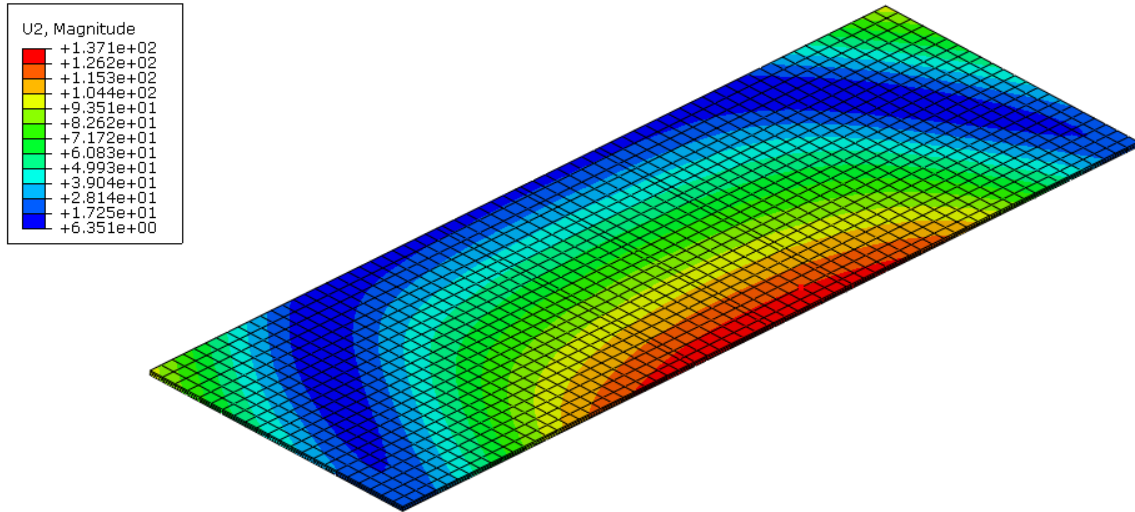
1186 **Table F-14. Calculated displacements at support locations for redundancy evaluation.**

Support	Girder	Displacement	Result for Redundancy I
South Abutment	West	Longitudinal	0 in.
		Transverse	0 in.
	East	Longitudinal	0 in.
		Transverse	0 in.
North Abutment	West	Longitudinal	1.1 in.
		Transverse	15.6 in.
	East	Longitudinal	4.2 in.
		Transverse	19.2 in.
Notes:			
1. Longitudinal direction is along the span direction. Positive longitudinal direction points south.			
2. Transverse direction is parallel to span direction. Positive transverse direction points east.			

1187

1188 *F.3.8.2 Minimum Serviceability Requirements*

1189 The only serviceability requirement in the Appendix E is that the increase of deflection after the failure  
 1190 of a primary steel tension member cannot be greater than L/50. This requirement is to be checked in the  
 1191 Redundancy II load combination under factored dead load only. In the current case, the limit is 31.4 inches,  
 1192 which was surpassed since the maximum additional deflection computed in the FEA was 137.1 inches. This  
 1193 is illustrated in Figure F-35.



1194  
1195  
1196

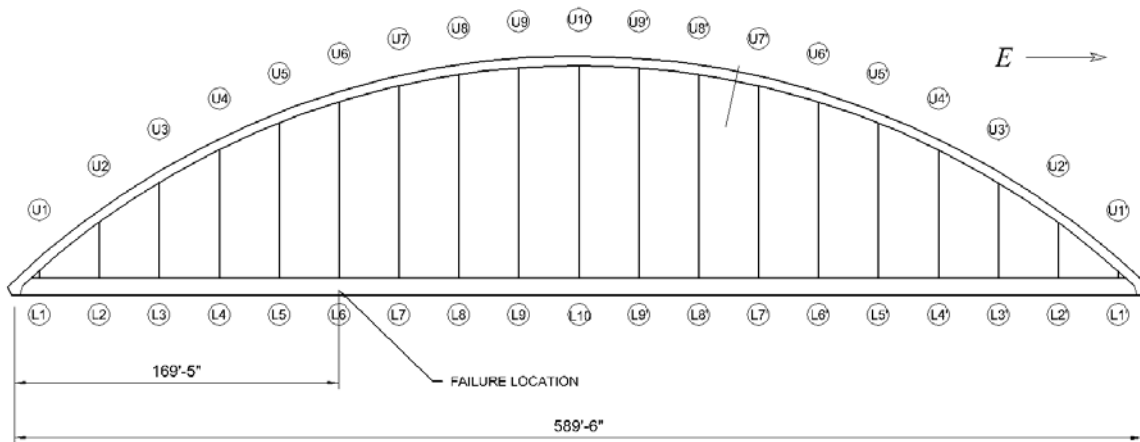
**Figure F-35. Deflection after failure of primary steel tension member for the through-girder bridge.**

1197 **F.3.9 Conclusions**

1198 Redundancy of a single span straight through girder bridge after the failure of the east plate girder was  
 1199 analyzed in accordance with the methodology described in the proposed guide specification in Appendix  
 1200 E. Based on the comparison between the obtained results and the minimum performance requirements, the  
 1201 structure is likely to fail and undergo significant serviceability loss after the failure of the east girder. Thus,  
 1202 the east girder must be designated as a fracture critical member (FCM).  
 1203

1204 F.4 Tied Arch Bridge

1205 The redundancy of a tied arch bridge is analyzed by developing a finite element model in accordance  
1206 with the methodology described in the proposed guide specification in Appendix E. It is assumed that the  
1207 structure does not possess any of the detrimental attributes described in the screening criteria and that it is  
1208 built to Section 12 of the AWS D1.5. In this case, the failing tension member is assumed to be southernmost  
1209 tie girder. The failure is assumed to take place at a location in which there is a discontinuity in the slab and  
1210 the stringers are relieved as this presents a worst-case condition since the beneficial participation from the  
1211 slab is reduced. Figure F-36 shows the location of the failure.  
1212



1213  
1214

**Figure F-36. Steelwork geometry and failure location.**

1215 The structure is a single straight span measuring 589.5 feet. Two curved boxes compose each of the  
1216 arches. The tie is comprised of an I shaped plate girder. The box section of each arch has 42” wide flanges  
1217 and 60” deep webs. The tie girders have 108” deep webs and 24” wide flanges, as shown in Figure F-37.  
1218 These dimensions change at the knuckles, which geometry is depicted in Figure F-40. The floor system is  
1219 comprised of floor beams which provide support to the stringers. The typical cross-section of the lower  
1220 assembly is shown in Figure F-39. Stability of the lower steel assembly is provided by lateral bracing and  
1221 diaphragms connecting the stringers. The framing of the lower assembly is shown in Figure F-38. Lateral  
1222 bracing of the arches is provided by struts as shown in Figure F-38. Location of the hangers is as shown in  
1223 Figure F-37 and a detail of the hanger anchorages is shown in Figure F-41.



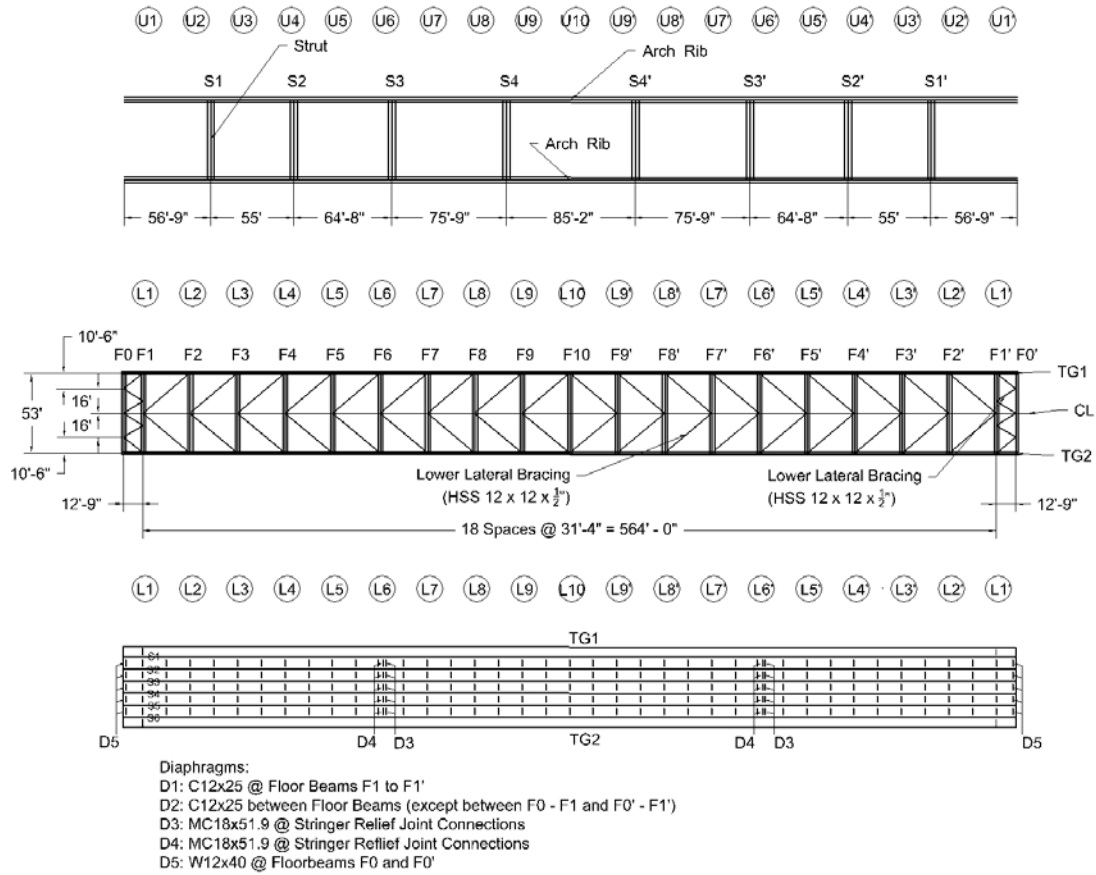


Figure F-38. Steel assembly of tied arch bridge (top views).

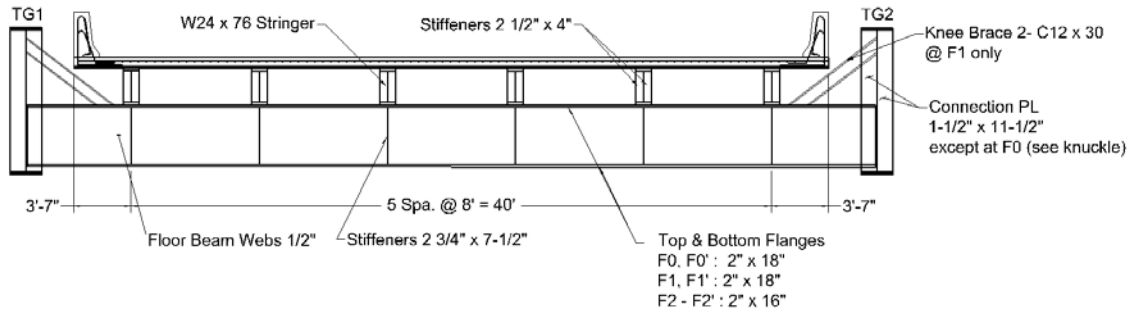


Figure F-39. Cross section of tied arch bridge, lower assembly.

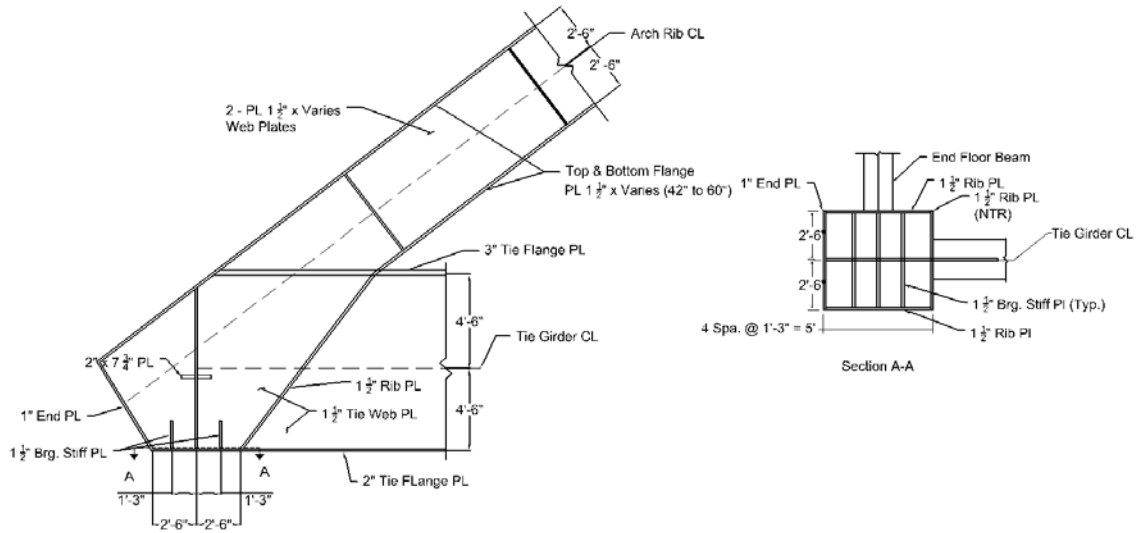


Figure F-40. Detail of knuckle of tied arch bridge.

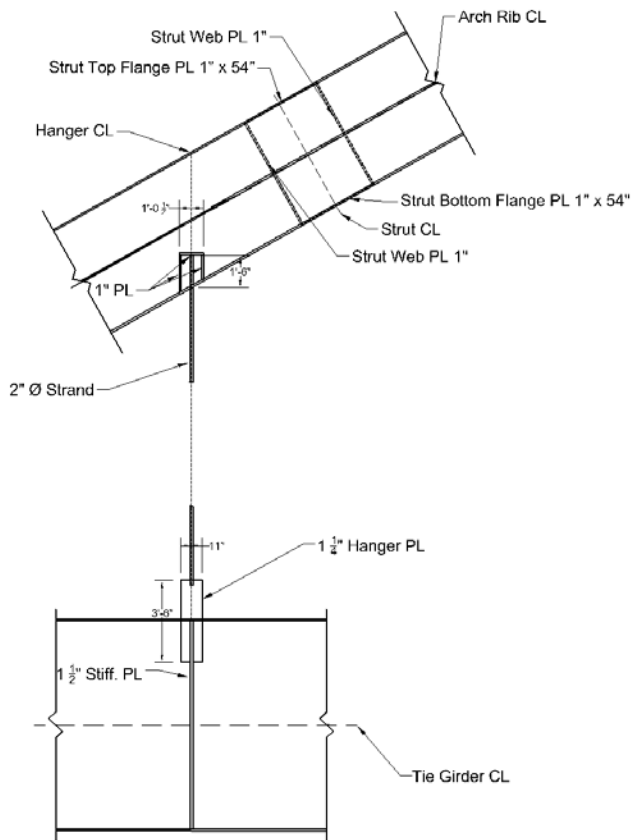


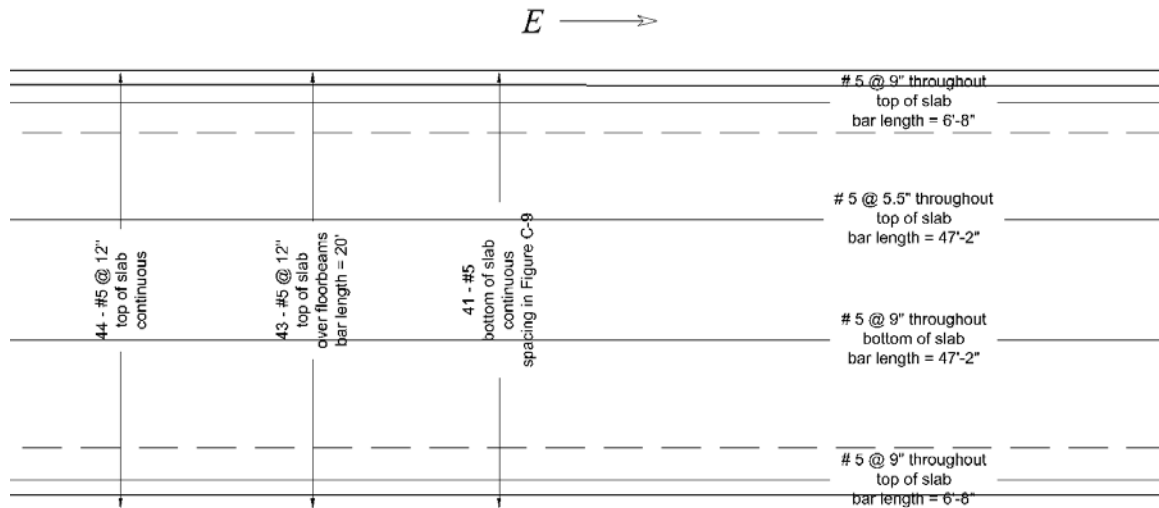
Figure F-41. Detail of hanger anchorage of tied arch bridge.

1231  
1232

1233  
1234



1235 The reinforced concrete slab is 44 feet wide between interior edges of concrete barriers (approximately  
 1236 30 feet wide between the outer exterior edges of concrete barriers) and is fully composite with the stringers'  
 1237 top flanges through shear studs. The end supports at the piers are pin supports, in which translations are  
 1238 fixed but rotations are free. The tie girders are fabricated in ASTM A709 HPS 70W steel, the suspenders'  
 1239 strand is ASTM A586 Grade 1 Class A and the rest of the steel components are fabricated ASTM A709  
 1240 Grade 50 steel. All concrete has a minimum specified compressive strength of 3.5 ksi and all rebar has 60  
 1241 ksi yield strength. In the analysis of this structure, the longitudinal and transverse slope of the slab will be  
 1242 neglected (i.e., the slab is assumed flat). Figure F-42 shows the reinforcement schedule of the slab and  
 1243 Figure F-43 shows the reinforcement details.  
 1244



1245 **Figure F-42. Schedule of reinforcement of the slab.**  
 1246



1249 **F.4.1 Analysis Procedure**

1250 The analysis is performed to establish if the system demonstrates acceptable performance in the faulted  
1251 condition. In the example, the term “faulted condition” specifically refers to the case in which a primary  
1252 steel tension member is assumed to have failed. For this analysis, load factors for both dead and live load  
1253 are applied as described in the proposed guide specification in Appendix E. In this example, the described  
1254 analysis procedure is composed of an initial implicit static analysis and a final explicit dynamic analysis,  
1255 into which the results from the initial implicit static analysis are imported. While it is not mandatory for  
1256 the Engineer to follow these particular steps, it has been found that this procedure optimizes the  
1257 computational time required.

1258 *F.4.1.1 Initial Implicit Static Analysis*

1259 Implicit static analysis was utilized to calculate the state of the structure prior to hardening of the concrete  
1260 in the slab. An implicit static analysis was used for the initial steps because, although non-linearity is  
1261 considered in the analysis, the bridge behavior is linear and inertial effects can be neglected as the bridge  
1262 is in the undamaged condition. As the slab does not carry any load and does not contribute to the stiffness  
1263 of the system before concrete hardening, two modifications are required in the finite element analysis during  
1264 this initial implicit static analysis as follows:

- 1265 • A very low stiffness is specified for the elements composing the slab, i.e., the elements modeling  
1266 concrete and rebar. A reduced stiffness of 1/1,000 of the respective modulus of elasticity of each  
1267 material was used. This is done so the load carried by the slab and rebar have negligible  
1268 contribution to the stiffness of the system. No modifications to the stiffness should be applied to  
1269 the steelwork.
- 1270 • Instead of defining contact interaction between the slab and the steelwork, a mesh tie was specified.  
1271 The nodal displacements of the concrete slab elements are tied to the displacements of the top  
1272 flanges of girders, floor beams, and stringers which occur due to dead load. As a result, the slab  
1273 deforms with the steelwork and does not ‘sag’ between the girders, floor beams, and stringers.

1274 It is worth noting that the remainder of the finite element modeling is identical between the initial implicit  
1275 static analysis and the final explicit dynamic analysis. The specific steps in the initial implicit static analysis  
1276 are described as follows:

- 1277 1. Apply load due to self-weight of the structural steel components as a body force.
- 1278 2. Apply load due to self-weight of the wet slab components as a body force.
- 1279 3. The system is then fixed in terms of position, that is, the displacement degrees of freedom are not  
1280 allowed to change.
- 1281 4. The elements composing the slab (elements modeling rebar and concrete) are then deactivated.
- 1282 5. The elements composing the slab are then reactivated. During this reactivation the strain in the  
1283 elements composing the slab is reset to zero.

1284 Steps 3 through 5 are necessary since even though very low stiffness was specified for the slab, these  
1285 elements do undergo strain. Setting the strains to zero eliminates “locked in” artificial stresses in later steps.

1286 *F.4.1.2 Final Explicit Dynamic Analysis*

1287 As contact algorithms, softening material behavior, and non-linear geometry are required to be part of  
1288 the finite element analysis, implicit solution procedures present unavoidable convergence problems in most  
1289 FEA solvers. In order to calculate the capacity of the bridge after sudden failure of a tension component, a  
1290 dynamic explicit analysis needs to be carried out. Therefore, the results obtained from the initial implicit  
1291 static analysis are imported into the final explicit dynamic analysis. In other words, the state of the system  
1292 (stresses, strains, displacements and forces) at the beginning of the final explicit dynamic analysis is defined  
1293 by the state of the system computed at the end of the initial implicit static analysis.

1294 As previously stated, during the initial implicit static analysis, the slab was modeled with largely reduced  
 1295 stiffness to reflect that it is not hardened and a mesh tie constraint was used to assure that the slab deformed  
 1296 with the steelwork. This approach also prevents excessive sag of the soft slab. After the state of the system  
 1297 is imported, the following changes are made to capture the response of the structure after the concrete has  
 1298 hardened:

- 1299 • The modulus of elasticity of the concrete and rebar elements in the slab is changed to their final  
 1300 actual values. It is noted that no modifications need to be applied for the steelwork.
- 1301 • The mesh tie constraint between the slab concrete elements and the top flanges of the steelwork is  
 1302 replaced by a frictional contact interaction. Additionally, since the structure under analysis is  
 1303 composite, elements which accurately model the behavior of shear studs are added.

1304 All of the body forces applied during the initial implicit static analysis (i.e., the dead load of the structure)  
 1305 are maintained throughout the final explicit dynamic analysis.

1306 To evaluate the capacity of the structure in the faulted state, the following steps were carried out in the  
 1307 final explicit dynamic analysis:

- 1308 6. The stiffness of the elements located at the fracture location under consideration were slowly  
 1309 reduced. The stiffness was slowly reduced in order to minimize any dynamic effects. It is noted  
 1310 that the actual fracture and subsequent vibration of the structure is not modeled. This dynamic  
 1311 effect is accounted for using the  $DA_R$  factor as discussed before. If dynamic effects are found to  
 1312 be significant even if the stiffness is slowly reduced, the system must be allowed to oscillate until  
 1313 these effects are dampened.
- 1314 7. Factored loads due to traffic are applied as surface tractions. For the Redundancy I load  
 1315 combination all loads are amplified by  $DA_R$ , for the Redundancy II load combination the dynamic  
 1316 load allowance (IM) is applied. These loads were applied very slowly to minimize any dynamic  
 1317 effects, as well. If dynamic effects are significant, the system must be allowed to oscillate until  
 1318 these effects are dampened.
- 1319 8. An additional 15% of live load is gradually applied.

#### 1320 F.4.2 Material Models

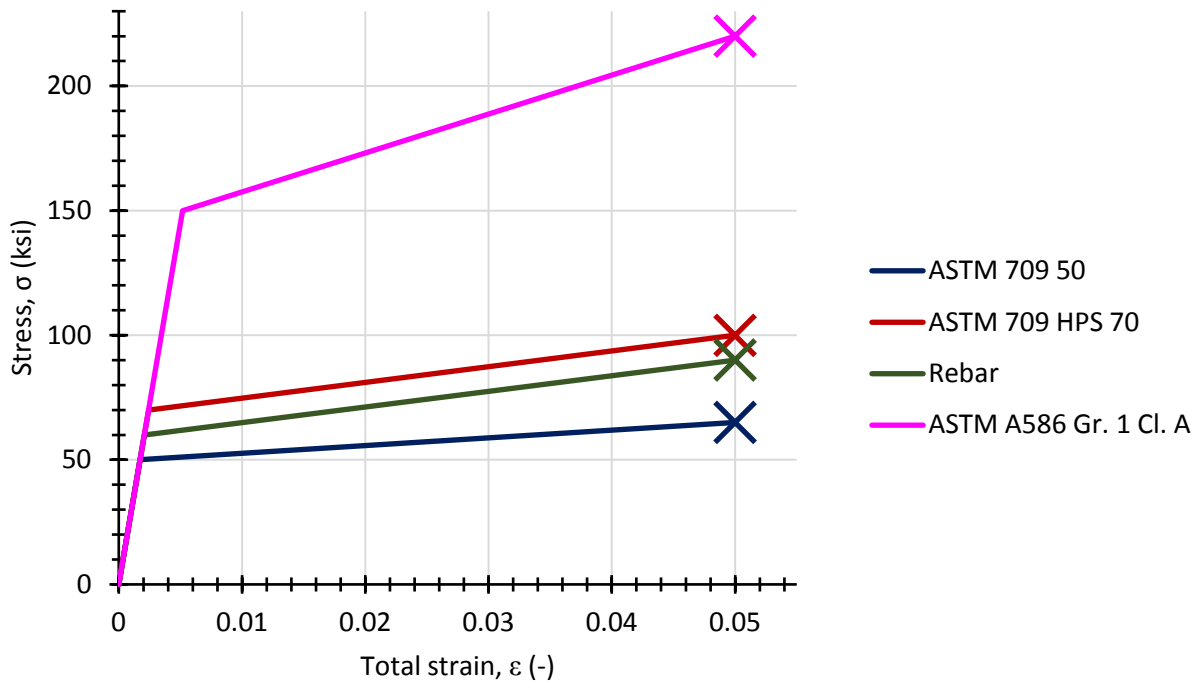
1321 Five material models are needed in the finite element model. Four of those are utilized to model different  
 1322 steel types, and one is utilized to model the response of concrete. For the development of the steel material  
 1323 models, it is necessary to know the yield strength and ultimate strength of each steel type. In this example,  
 1324 since no test values are known to the Engineer, nominal values specified in the respective standards are  
 1325 utilized. These are summarized in Table F-15. A mass density of 0.494 kcf was specified for all steel types.

1326 **Table F-15. Material properties for steel material models.**

Material	Nominal Yield Strength	Nominal Ultimate Strength	Standard
ASTM A709 HPS 70W	70 ksi	100 ksi	ASTM A709/A709M
ASTM A709 Gr. 50	50 ksi	65 ksi	ASTM A709/A709M
Grade 60 Rebar	60 ksi	90 ksi	ASTM A615/A615M
ASTM A586 Gr. 1 Cl. A	150 ksi	220 ksi	ASTM A586/A586M

1327  
 1328 The stress-strain relation for all steel components will follow an initial linear elastic steel with a Young's  
 1329 modulus of 29,000 ksi and Poisson's ratio of 0.3. Once the nominal yield strength is reached the stress-  
 1330 strain relation is defined by Von Mises (J2) plasticity with kinematic linear hardening, until the nominal  
 1331 ultimate strength is reached at a total strain of 0.05. Once the nominal ultimate strength or a total strain of

1332 0.05 is reached, the material is assumed to fail. Figure F-44 shows the uniaxial material response for the  
 1333 steel employed in this finite element model with the 'X' denoting the stress at the failure strain of 0.05.  
 1334



1335  
 1336 **Figure F-44. Stress-strain curves of steel material models.**

1337 The material model used in concrete is defined entirely by the specified compressive strength, which in  
 1338 this case is 3.5 ksi. This quantity is also used to calculate the tensile strength, the total strain at compressive  
 1339 strength,  $\epsilon_c$ , and the material parameter  $n$ . Table F-16 summarizes the calculation of these values. A mass  
 1340 density of 0.150 kcf was specified for concrete.

1341 **Table F-16. Material properties for concrete material model.**

Quantity	Symbol	Equation	Result
Young's modulus	$E_c$	$E_c = 33,000w_c^{1.5}\sqrt{f'_c} \leq 1,802.5\sqrt{f'_c}$	3,370 ksi
Tensile strength	$f_t$	$f_t = 0.158(f'_c)^{\frac{2}{3}}$ for $f'_c \leq 7.25\text{ksi}$ $f_t = 0.307 \ln(f'_c + 2.61) - 0.114$ for $f'_c > 7.25\text{ksi}$	0.364 ksi
Fracture energy	$G_t$	$5.9 \cdot 10^{-4}(f'_c + 1.16)^{0.18}$	$7.78 \cdot 10^{-4}$ kip/in
Total strain at compressive strength	$\epsilon_c$	$\epsilon_c = 0.00124^4\sqrt{f'_c}$	0.00170
Material parameter	$n$	$n = 0.4f'_c + 1.0$	2.4

1342

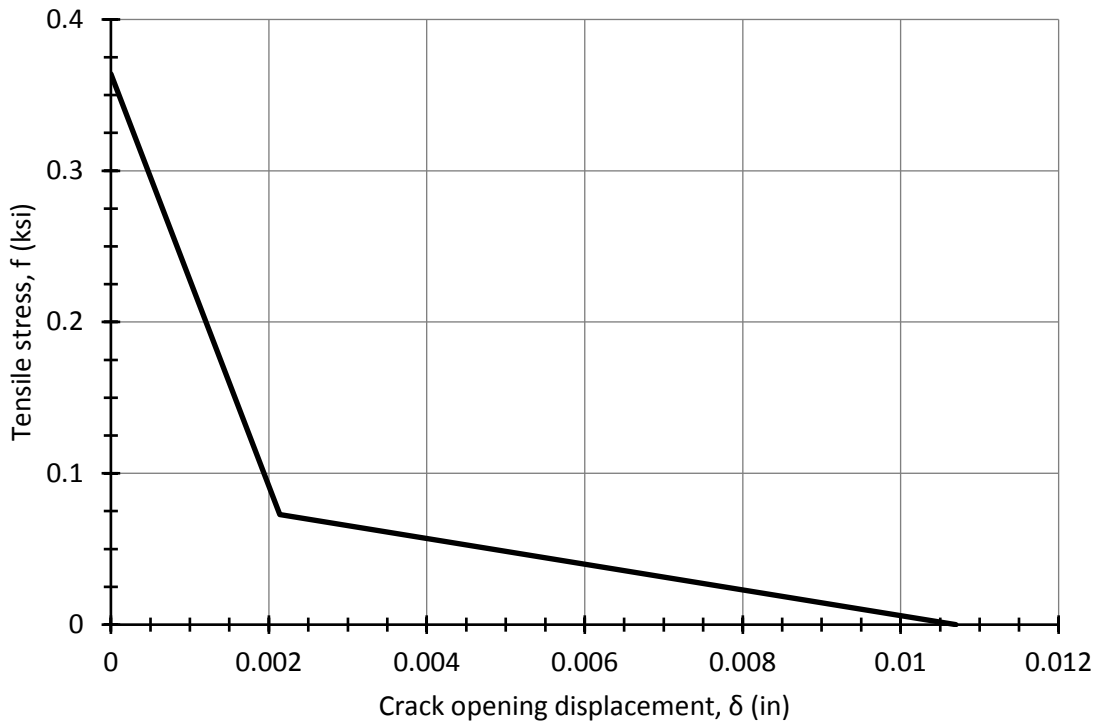
1343 The concrete material model is initially linear elastic, defined by a Young's modulus of 3,600 ksi and  
 1344 Poisson's ratio of 0.2, followed by concrete damage plasticity. In tension, once the material reaches its  
 1345 tensile strength, set at 0.364 ksi in this case, a tensile stress-displacement relation characterized by a fracture  
 1346 energy,  $G_t$ , of  $7.28 \cdot 10^{-4}$  kip-in is followed. This fracture energy is applied through a bi-linear tensile stress-  
 1347 displacement relation as shown in Figure F-45, and defined by the following quantities:

1348 
$$f_{t1} = \frac{f_t}{5} = 0.0728 \text{ ksi}$$

1349 
$$\delta_t = \frac{5G_t}{f_t} = 0.0107$$

1350 
$$\delta_{t1} = \frac{G_t}{f_t} = 0.00214$$

1351



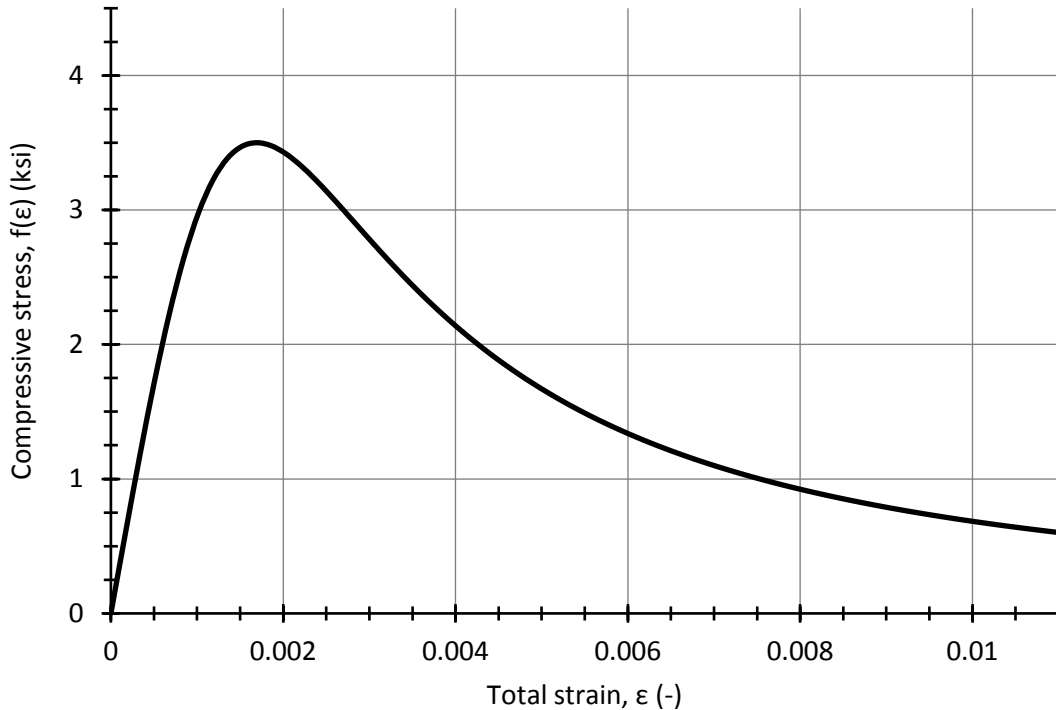
1352  
 1353 **Figure F-45. Tensile stress-crack opening displacement curve for concrete material model.**

1354 In compression the material follows the following stress-strain relations:

1355 
$$f(\varepsilon) = f'_c \left( \frac{\varepsilon}{\varepsilon_c} \right) \left[ \frac{n}{n - 1 + \left( \frac{\varepsilon}{\varepsilon_c} \right)^n} \right]$$

1356 
$$\varepsilon_{plastic} = \varepsilon - \frac{f(\varepsilon)}{E_c}$$

1357 where  $\varepsilon$  is total (elastic + plastic) strain,  $f(\varepsilon)$  is the compressive stress at a given total strain,  $f'_c$  is the  
 1358 specified compressive strength,  $\varepsilon_c$  is the total strain at compressive strength,  $n$  is a material parameter,  
 1359  $\varepsilon_{plastic}$  is the plastic strain and  $E_c$  is the concrete Young's modulus. Figure F-46 shows the resulting  
 1360 compressive stress-strain relation.



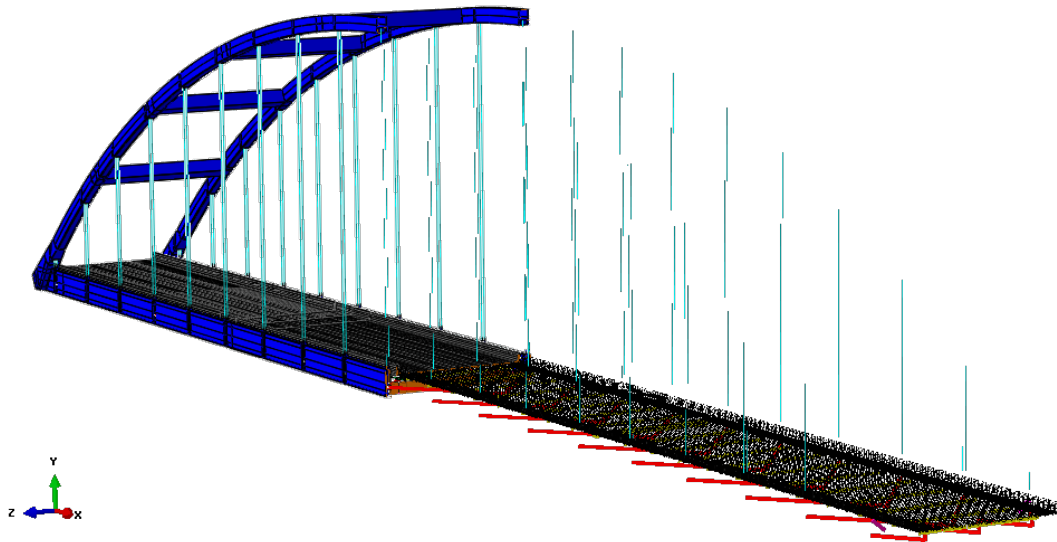
1361  
1362 **Figure F-46. Compressive stress-strain curve for concrete material model.**

1363 **F.4.3 Geometries, Meshes and Constraints**

1364 The geometry of the structure is based on available design plans and is composed of the following  
1365 components that must be explicitly modeled:

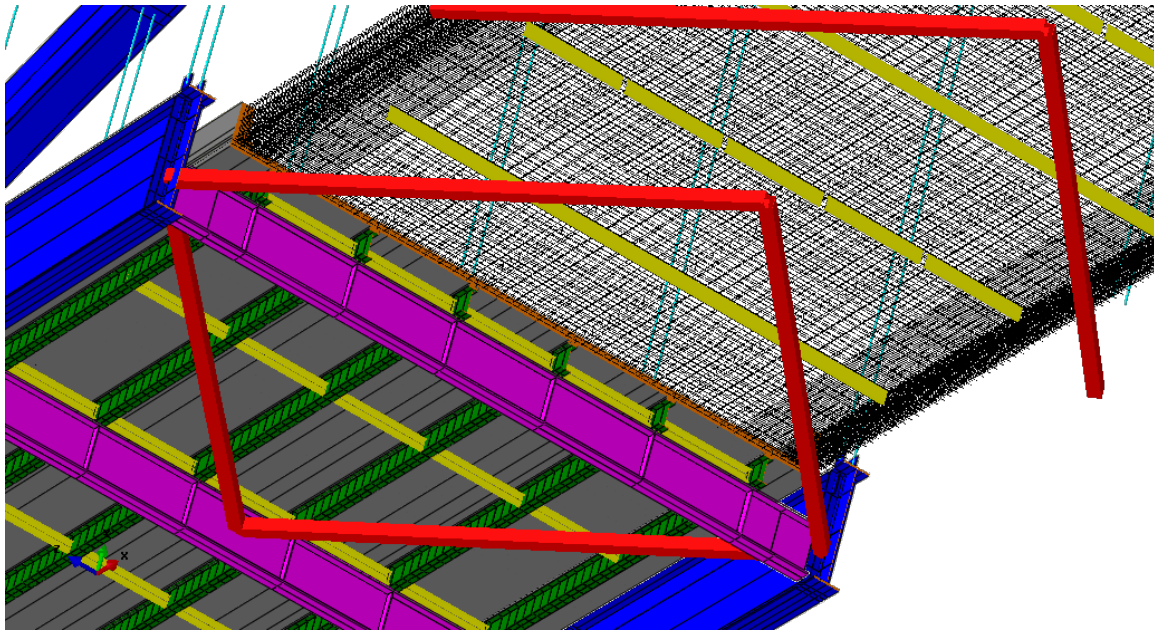
- 1366 1. A tied arch system composed of:
- 1367 a. Two arch ribs.
  - 1368 b. Two tie girders.
  - 1369 c. A set of eight struts.
  - 1370 d. Hanger anchorage system.
  - 1371 e. Arch knuckles.
- 1372 2. Floor beam system composed of 19 floor beams connected to the tie girders.
- 1373 3. Stringer system composed 6 stringers supported by the floor beam system.
- 1374 4. A hanger system composed of 76 hangers.
- 1375 5. A lower assembly bracing system composed of:
- 1376 a. W-bracing between floor beam F0 and F1, and F1' and F0', connected to the floor beams  
1377 and tie girders.
  - 1378 b. V-bracing among the rest of floor beams, connected to the floor beams and tie girders.
  - 1379 c. Diaphragms among stringers.
- 1380 6. A reinforced concrete slab with concrete barriers.

1381 When generating the finite element model, splices, holes, access hatches, etc. are neglected. The  
1382 structure is assumed to be flat in the vertical plane, in other words, camber and superelevation are ignored.  
1383 Figure F-47 shows the assembly of all bridge components and Figure F-48 shows a detail of the underside.



1384  
1385  
1386  
1387

**Figure F-47. Tied arch bridge geometries. Concrete slab and barriers (grey), tied arch system (blue), lateral bracing (red), diaphragms (yellow), floor beams (magenta), hangers (cyan), stringers (green), slab reinforcement (black).**



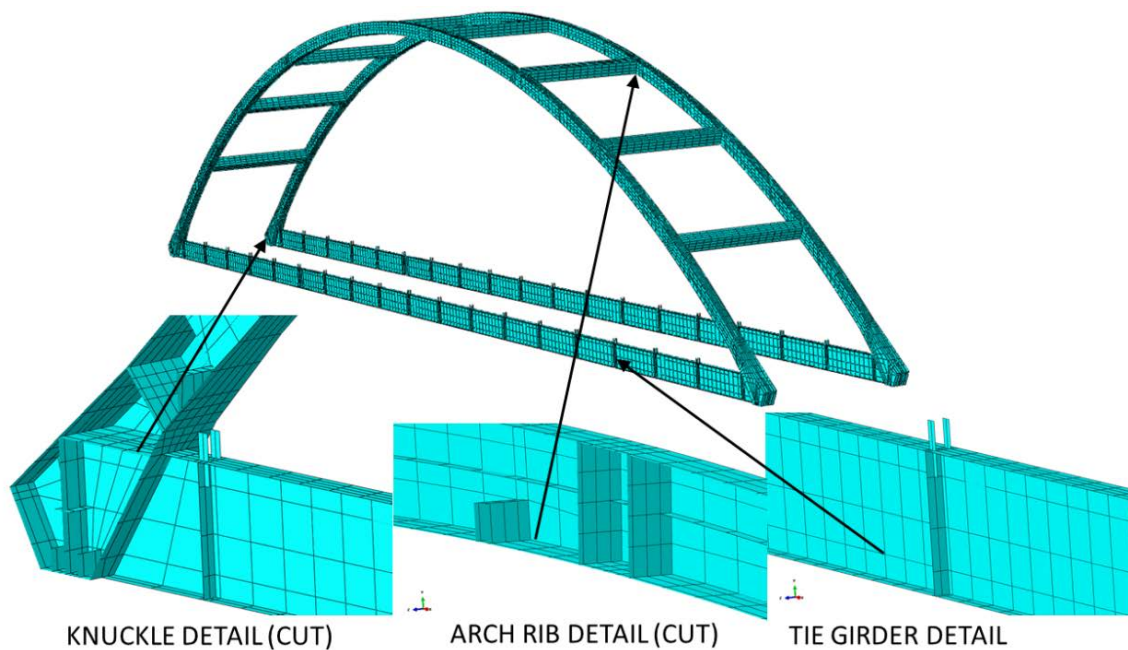
1388  
1389  
1390  
1391

**Figure F-48. Detail of the underside of the tied arch bridge geometries. Concrete slab and barriers (grey), tied arch system (blue), lateral bracing (red), diaphragms (yellow), floor beams (magenta), hangers (cyan), stringers (green), slab reinforcement (black).**

1392 The tied arch system (arch ribs, tie girders, struts, hanger anchorages and knuckles), floor beams,  
1393 stringers and diaphragms are modeled with 4-node shell elements with reduced integration. A minimum of  
1394 four elements are used along flange widths and along web heights. Stiffeners and connection plates are  
1395 modeled as shell elements as well. The arch ribs, tie girders, struts, hanger anchorages and knuckles

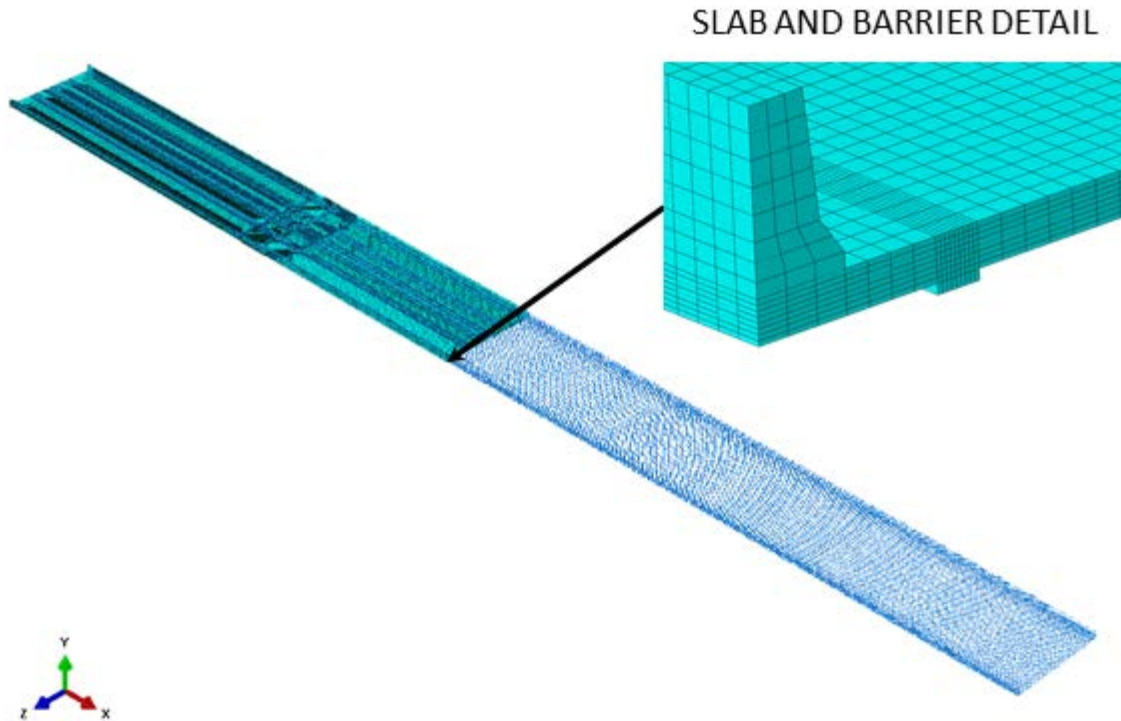


1396 constitute a single geometry. The maximum aspect ratio was kept below five and corner angles were kept  
1397 between 60 and 120 degrees. Figure F-49 shows two details of the mesh employed to model the tied arch  
1398 system. All lower assembly lateral bracing (W-bracing, V-bracing and diaphragms) and hangers are  
1399 modeled with 2-node linear shear-flexible (Timoshenko) beam elements. A minimum of three (3) elements  
1400 are used along the length of the elements. Mesh ties, which are constraints that slave the motion of a surface  
1401 or node set to the motion of a master surface or node set, are utilized to connect the all steel components.  
1402



1403  
1404 **Figure F-49. Mesh details of the tied arch system.**

1405 The slab is modeled with two types of elements. Specifically, 8-node linear bricks with reduced  
1406 integration are used to model concrete and 2-node truss elements with linear displacement to model steel  
1407 reinforcement. Eight solid concrete elements are used through the thickness of the slab with maximum  
1408 aspect ratio (length of longest edge divided by length of shortest edge) of 5, and corner angles (angle at  
1409 which two element edges meet) between 40 and 140 degrees. The length of the truss elements used to  
1410 model the reinforcement were approximately equal to the length of the longest edge of the solid concrete  
1411 elements. These truss elements are embedded within the solid concrete elements. At the nodes of the  
1412 embedded truss elements, the translational degrees of freedom are eliminated and the nodal translations  
1413 were constrained to interpolated values of the nodal translations of the host solid concrete element. The  
1414 reinforcement of the concrete barrier was neglected and it was meshed with four elements along its height  
1415 and two elements across its width, it was attached to the slab by a mesh tie. Figure F-50 shows the concrete  
1416 slab with the embedded truss elements and a detail of the mesh used for the concrete barrier and slab.



1417  
1418

*Figure F-50. Mesh details of the reinforced concrete slab and barriers.*

1419 **F.4.4 Slab-Structural Steel Interaction**

1420 As stated, the interaction between the bottom of the concrete slab and the top of the flanges of the  
 1421 steelwork is modeled differently in the two steps described above. In the initial implicit static analysis,  
 1422 when the elements comprising the slab and barriers have  $1/1,000^{\text{th}}$  of the modulus of elasticity to model the  
 1423 “wet” condition, a mesh tie is used to slave the motion of the slab to the motion of the surface comprising  
 1424 the top of the steel work. With this procedure, it is ensured that the slab deformation will conform to the  
 1425 deformation of the steelwork while unrealistic sagging of the slab between supporting elements and tipping  
 1426 of the barrier is prevented.

1427 In the final explicit dynamic analysis, when the stiffness of the elements comprising the slab and barriers  
 1428 has been changed to their final real values, the mesh tie previously used is deleted and replaced by a contact  
 1429 interaction and modeling of shear studs. The normal behavior of the contact interaction is modeled through  
 1430 a penalty stiffness. The penalty stiffness is several orders of magnitude larger than the normal stiffness of  
 1431 the underlying contacting elements and allows a very small penetration so a pressure can be calculated.  
 1432 The tangential behavior of the contact interaction is modeled through an algorithm based on Coulomb  
 1433 friction with a limit on the allowable shear. A friction coefficient of 0.55 and an interfacial shear strength  
 1434 of 0.06 ksi are specified.

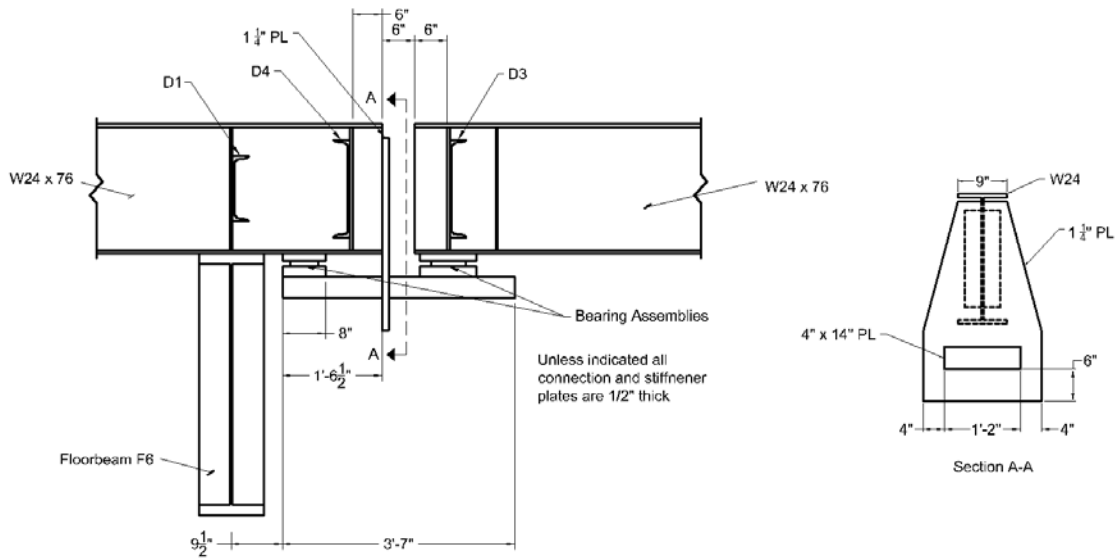
1435 The simplified stud model, as described in the Appendix A is used to model composite action between  
 1436 the slab and the steelwork. In the simplified stud model, the shear studs were modeled using connector  
 1437 elements which were used to define the axial and interfacial shear interaction between the shear studs and  
 1438 concrete slab. Connector elements are special purpose elements with zero length. These elements model  
 1439 discrete physical connections between deformable or rigid bodies, and are able to model linear or nonlinear  
 1440 force-displacement behavior in their unconstrained relative motion components.

1441 The recommendations of Appendix A were used to define the shear and tensile behavior of shear studs.  
 1442 The shear stud group is composed of three transversely grouped studs which shear strength is 53.0 kips,

1443 following the shear force-displacement relation proposed by Ollgaard et al. (1971) up to maximum shear  
 1444 displacement of 0.2 inches. In tension, the governing failure mode is concrete break-out, resulting in a  
 1445 initial stiffness of 2500 kip/in, and tensile strength of 9.23 kips, and a maximum tensile displacement at  
 1446 failure of 0.04 inches. The tensile behavior follows the characteristic triangular response for transversely  
 1447 grouped shear studs which governing failure mode is concrete break-out or shear stud pullout, as described  
 1448 in the recommendations of Appendix A. The tension-shear interaction equation presented in Appendix A  
 1449 is used to combine the effects of shear and tension acting simultaneously on a shear stud group.

1450 **F.4.5 Stringer Relief Joint Modeling**

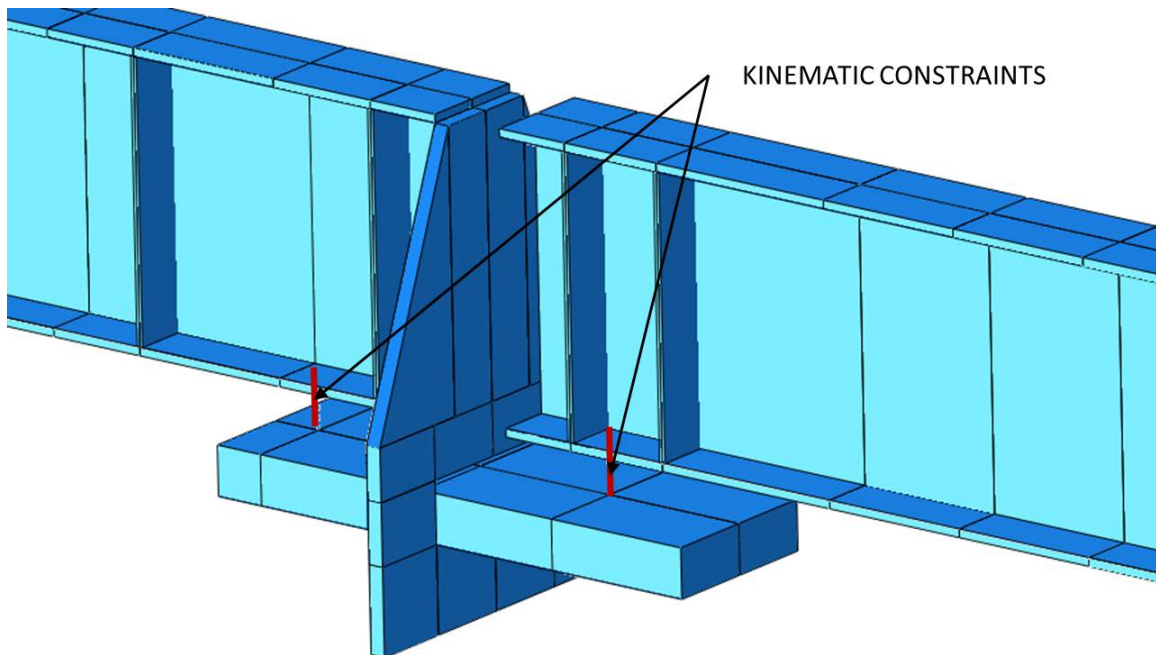
1451 The stringers of the tied arch bridge have relief joints next to floor beams F6 and F6' (see Figure F-38),  
 1452 at those locations the slab is discontinued as well. Figure F-51 shows the sketch of the relief joint. At the  
 1453 discontinuity, the slab may provide inferior load-path redundancy to other location in which the slab is  
 1454 continuous, and the relief joint may not provide sufficient capacity to make up for the loss of load-path  
 1455 redundancy in the slab. Hence, in this example, it was chosen as the critical location.  
 1456



1457  
 1458

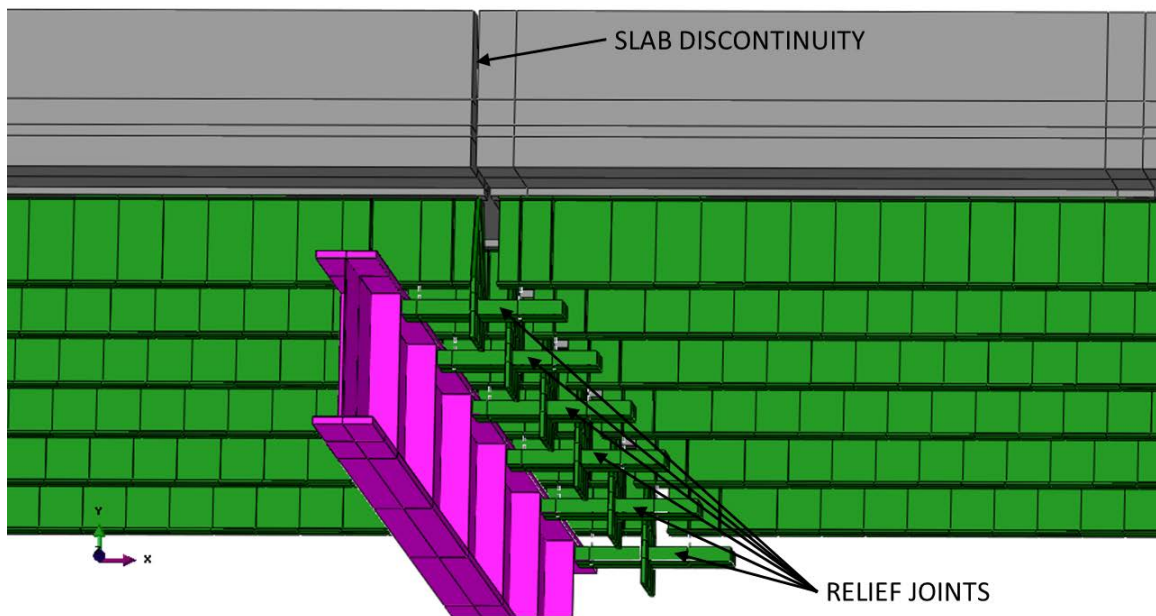
**Figure F-51. Sketch of the stringer relief joint.**

1459 The relief joint has complex behavior for which is not easy to obtain force/moment-displacement/rotation  
 1460 relations. In this example, all relief joints were explicitly modeled in the finite element analysis. The  
 1461 geometries of the joints were explicit included in the finite element model, except the bearing assemblies.  
 1462 The bearing assemblies were modeled with a kinematic constraint, which equals the translations between  
 1463 two points. Figure F-52 shows a detail of the relief joint as modeled in the finite element analysis, along  
 1464 with the location of the kinematic constrain. The discontinuity in the slab was included in the finite element  
 1465 model as well, as shown in Figure F-53



1466  
1467

*Figure F-52. Detail of stringer relief joint geometry in finite element models.*



1468  
1469  
1470

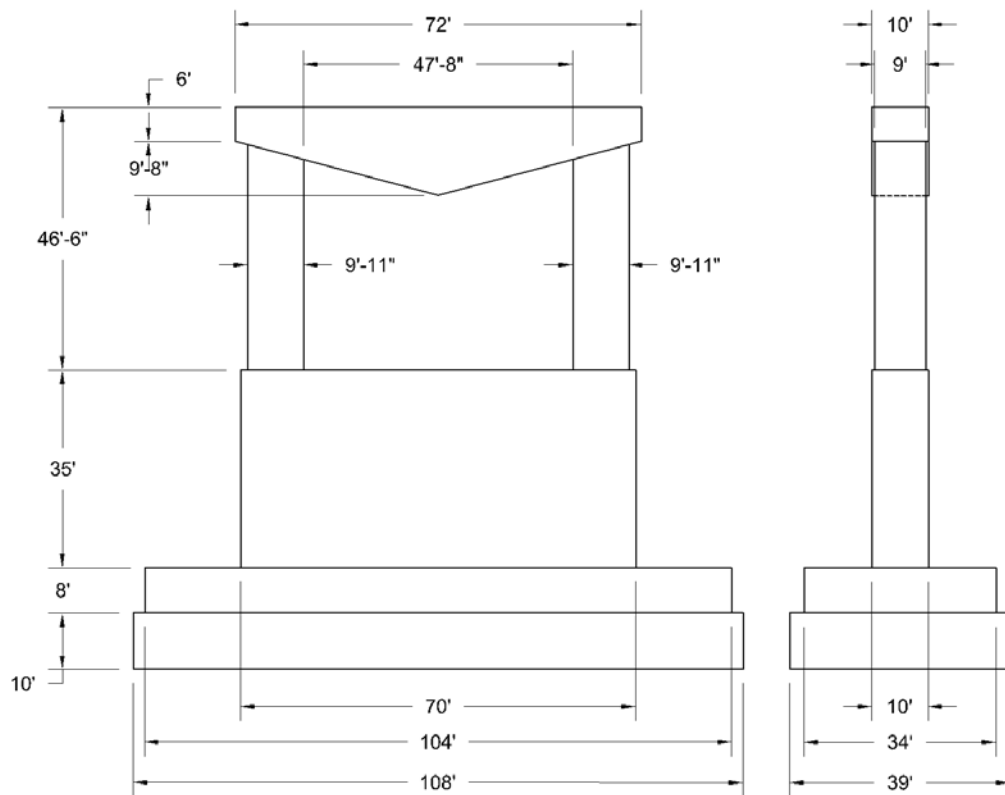
*Figure F-53. Detail of discontinuity in slab and stringer relief joints. Slabs (grey), stringers (green) and floor beam (magenta) are shown.*

1471 **F.4.6 Substructure Flexibility Model**

1472 In order to account for longitudinal and transverse flexibility of the substructure, connector elements  
 1473 were utilized. These elements allow for the definition of coupled force-deformation relations. The type  
 1474 that was determined to best capture the intended behavior was a Cartesian connector. These elements  
 1475 provide a connection between two nodes where the change in position is measured in three directions local

1476 to the connection. One of the nodes is fixed (or connected to ground) and the other node is the support  
 1477 point in the superstructure. The connector element is rigid in the vertical direction, and has a coupled linear  
 1478 elastic relation in the two horizontal directions (longitudinal and transverse).

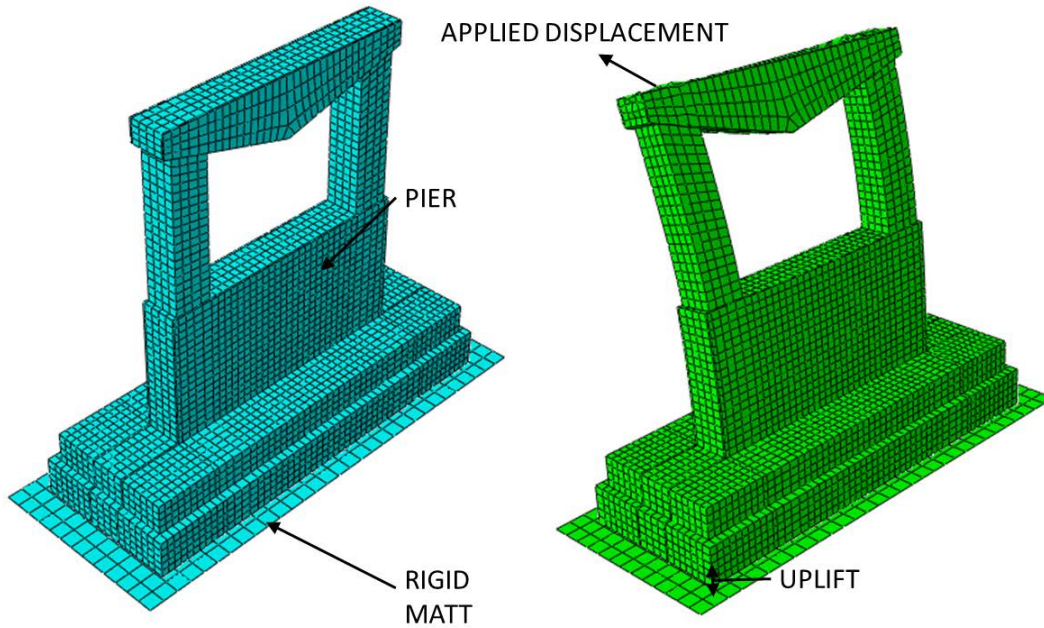
1479 In the current case, the structure is assumed to be pinned at the end spans; as a result, the vertical  
 1480 translation at the bearing location in the knuckles will be set to zero, while the horizontal stiffness of the  
 1481 pier will be incorporated through connector elements. In order to obtain the coupled elastic force-  
 1482 displacement relation, a simple finite element analysis of the pier is conducted. The geometry of the pier  
 1483 is drawn according to the design plans, as shown in Figure F-54 and meshed with 8-node linear bricks with  
 1484 reduced integration as shown in Figure F-55. The pier was modeled as linear elastic with modulus of  
 1485 elasticity of 1,800 ksi (in order to account for possible cracking due to combined compression and bending),  
 1486 Poisson's ratio of 0.2 and a density of 0.150 kcf. The base of the pier bears on a rigid mat, prohibiting  
 1487 sliding but allowing uplift as shown in Figure F-14.  
 1488



1489  
 1490

**Figure F-54. Geometry of the pier support.**





1491  
1492  
1493 **Figure F-55. Detail of mesh geometry used (left) and deformed configuration after application of displacement (right, displacements scale by a factor of 50).**

1494 During the first analysis step, dead loads are applied. These are due to (1) the self-weight of the pier,  
1495 applied as a body force, and (2) bearing of the superstructure on the pier, which were calculated to be 1750  
1496 kips at each bearing location. These are applied as surface tractions over a 60” by 60” patch, the size of the  
1497 patch is based on the size of the bearings. Once the first step is completed, displacements are applied at the  
1498 bearing locations so the reaction forces can be calculated. In this case, displacements of 10 inch were  
1499 applied in the longitudinal and transverse directions (positive and negative signs) so the reaction forces and  
1500 described in Table F-3 were obtained.

1501 **Table F-17. Reaction forces and displacements at support points.**

Pier Support			
$U_{TRANSVERSE}$	$U_{LONGIT.}$	$R_{TRANSVERSE}$	$R_{LONGIT.}$
in	in	kips	kips
10.0	-7.25E-10	222000	-
-10.0	7.03E-10	-222000	-
-6.89E-10	10.0	-	38400
7.02E-10	-10.0	-	-38400

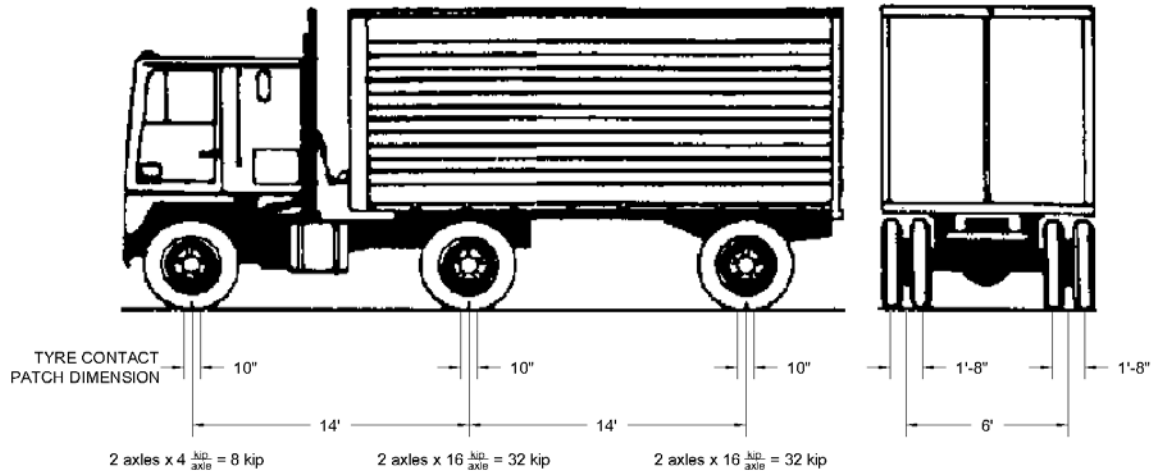
1502 These are used to build the force deformation relations shown hereof, which are incorporated as the  
1503 properties of the connector element in the global model to model the flexibility of the pier:  
1504

1505

$$\begin{bmatrix} F_{TRANSVERSE} \\ F_{LONGITUDINAL} \end{bmatrix}_{SUPPORT} = \begin{bmatrix} 22,200 & 0 \\ 0 & 3,840 \end{bmatrix} \frac{kips}{in} \begin{bmatrix} U_{TRANSVERSE} \\ U_{LONGITUDINAL} \end{bmatrix}_{SUPPORT}$$

1506 **F.4.7 Loads and Boundary Conditions**

1507 Two types of loads were applied in the finite element models: body forces and surface tractions as  
 1508 required by the proposed guide specification in Appendix E. Body forces were applied for component dead  
 1509 loads (“DC” and “DW” per AASHTO designations). These are simply the product of mass, gravity and  
 1510 applicable load factors. Surfaces tractions were applied for traffic live loads (“LL” per AASHTO  
 1511 designation). The traffic live load is based on the HL-93 load model described in the AASHTO LRFD  
 1512 BDS, which is a combination of the truck loads, shown in Figure F-56, and a 0.64 klf load distributed over  
 1513 a width of 10 ft. The current structure does not include any bituminous pavement (i.e., DW is zero).  
 1514



1515 **Figure F-56. Truck load components and dimensions of the HL-93 vehicular live load model.**  
 1516

1517 The Redundancy I and Redundancy II loading combinations were used to evaluate the structure in the  
 1518 faulted state. The load factors for these two combinations are as in Table F-18, based on the provisions in  
 1519 Appendix E for bridges built to Section 12 in the AWS D1.5. The live load (LL) factors are modified by  
 1520 the appropriate multiple presence factors as described in Article 3.6.1.1.2 of the AASHTO LRFD BDS. It  
 1521 must be noted that dynamic amplification factor is equal to 0.4, which is applied to DC and LL in the  
 1522 Redundancy I load combination only. Also, the dynamic load allowance is 0.15 of the truck axle loads,  
 1523 and is only applied in the Redundancy II load combination.

1524 **Table F-18. Load factors used for Redundancy I and Redundancy II load combinations.**

Load Combination	Load Factors				Notes
	DC	LL	DA <sub>R</sub>	IM	
Redundancy I	1.05	0.85	0.40	N. A.	β = 1.5
Redundancy II	1.05	1.30	N. A.	0.15	β = 1.5

1525 Longitudinally, the loads are positioned in the most critical positions in both the Redundancy I and  
 1526 Redundancy load combinations. For the failure scenario considered in the current case (failure of the  
 1527 southernmost tie girder at the stringer relief section, shown in Figure F-36 and Figure F-57, the most critical  
 1528 position of the truck axle loads which results in the truck facing west with its middle axis positioned at the  
 1529 failure plane, as shown in Figure F-57. The distributed load portion of the HL-93 load is applied along the  
 1530 entire span.  
 1531

1532 As described in the proposed guide specification in Appendix E, the transverse positioning of the HL-93  
 1533 live load model differs between the Redundancy I and Redundancy II load combinations, as illustrated in  
 1534 Figure F-58. Since the vehicular loads in the Redundancy I load combination are meant to represent the  
 1535 applied load at the instant in time in which the assumed member failure occurs, the HL-93 vehicular live  
 1536 load model is transversely positioned centered (both the 10 ft loaded width and the truck axle loads) within  
 1537 the marked (striped) lanes, in this case two lanes. Hence, as the bridge is striped for two lanes, there are  
 1538 two load cases for the Redundancy I load combination: two marked lanes loaded, or one marked lane  
 1539 loaded.

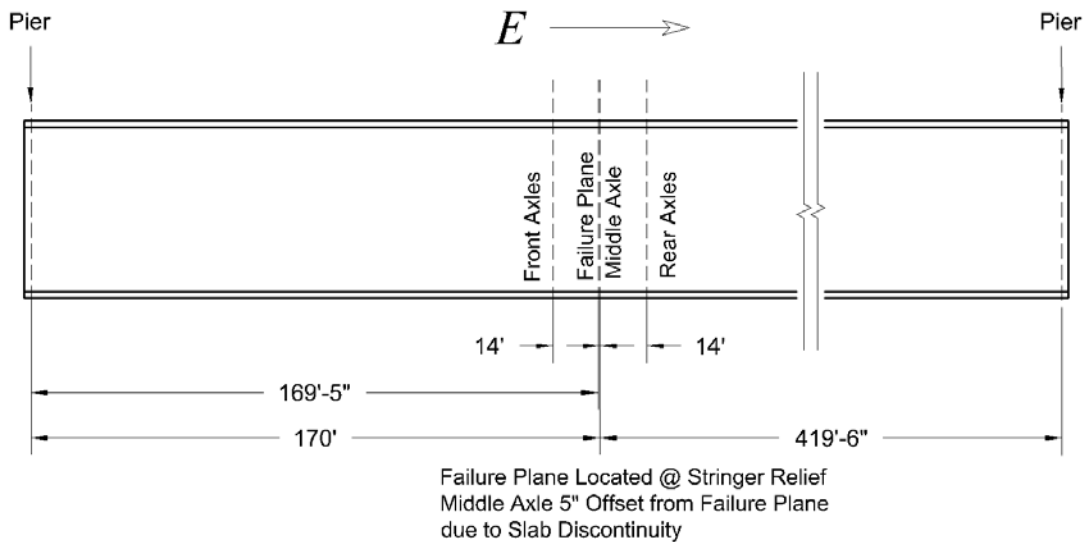
1540 On the other hand, the objective of the Redundancy II load combination is to evaluate the strength of the  
 1541 system after the failure of the primary steel tension member has occurred, so the number of design lanes is  
 1542 established in accordance with Article 3.6.1.1.1 in the AASHTO LRFD BDS, which in this case results in  
 1543 three design lanes with a width of 12 ft. In the Redundancy II load combination, the HL-93 vehicular live  
 1544 load model is transversely positioned (both the 10 ft loaded width and the truck axle loads) to produce  
 1545 extreme force effects within each design lane; however, the truck axle loads are transversely positioned  
 1546 such that the center of any wheel load is not closer than 2 ft from the edge of the design lane. Hence, there  
 1547 are three load cases for the Redundancy II load combination: three design lanes loaded, two design lanes  
 1548 loaded, or one design lane loaded.

1549 Component dead loads were linearly applied in the initial implicit static analysis. Traffic live loads were  
 1550 applied in the final explicit dynamic analysis. Their dynamic effects were minimized by applying them  
 1551 slowly through the use of smooth step, as in the following equation:

1552 
$$LR(t) = 6 \left(\frac{t}{T}\right)^5 - 15 \left(\frac{t}{T}\right)^4 + 10 \left(\frac{t}{T}\right)^3$$

1553 where  $LR(t)$  is the fraction of load at a load application time  $t$ , and  $T$  is the duration of the load application.  
 1554 The duration of the load application must be larger than the fundamental period of the structure to minimize  
 1555 oscillatory behavior in the final explicit dynamic analysis.

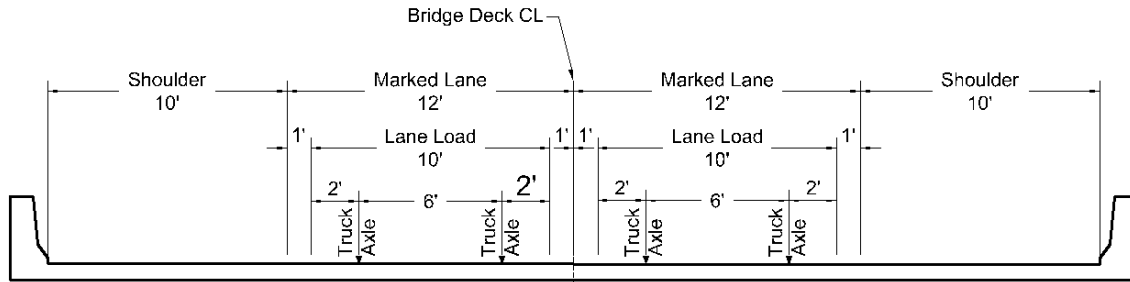
1556 Regarding prescribed boundary conditions, vertical translation is prescribed to be zero at all support  
 1557 location since uplift would not occur under the loading employed in the current case. Horizontal  
 1558 translations are discussed in Section F.4.6 as they are enforced through connector elements that model the  
 1559 flexibility of the substructure.  
 1560



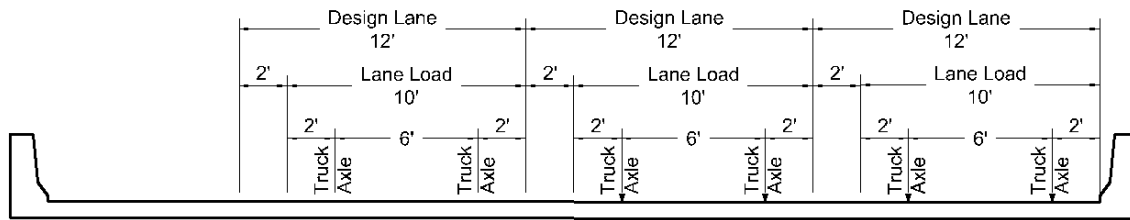
1561  
 1562

**Figure F-57. Longitudinal position of truck axles.**





TRANSVERSE LOAD POSITION FOR REDUNDANCY I



TRANSVERSE LOAD POSITION FOR REDUNDANCY II

**Figure F-58. Transverse position of traffic loads.**

1563  
1564

1565 **F.4.8 Analysis of Results for Redundancy**

1566 Once the analysis is completed the obtained results are evaluated using the requirements described in  
 1567 Article 8 of the proposed guide specification in Appendix E. It was found that the structure met the strength  
 1568 and serviceability requirements and is considered redundant against failure of the southernmost tie girder  
 1569 at the stringer relief joint. Specific details regarding the performance requirements and the results are  
 1570 summarized in Table F-19.

1571 **Table F-19. Summary of the redundancy evaluation after the failure of south tie girder.**

Performance Requirement		Most Critical Load Combination	Result	Acceptable?
Strength Requirements	Strain Primary Steel Members	Redundancy I 1 Lane	0.0055	<b>YES</b>
	Slab Concrete Crushing	-	No concrete crushing in the slab	<b>YES</b>
Serviceability Requirements	Vertical Deflection	Only Redundancy II DL considered	9.99 inches	<b>YES</b>

Notes:

1. The analysis showed that the structure was capable of resisting an additional 15% of the applied factored live load.
2. In order to complete the evaluation, the displacements and reaction forces calculated at support locations should be used as factored demands to check against the nominal capacity of the supports and substructure members.

1572

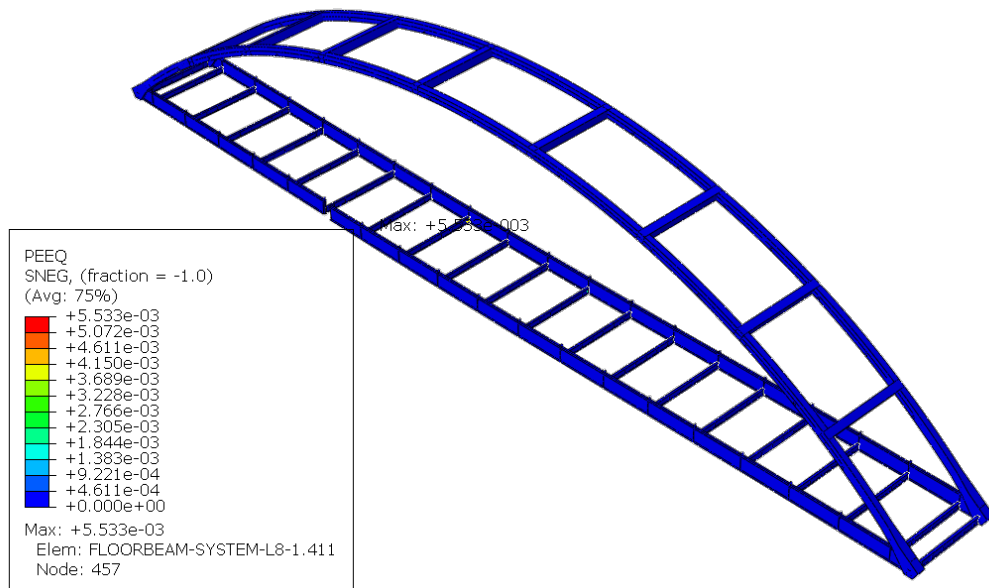
1573 *F.4.8.1 Minimum Strength Requirements*

1574 All of the strength requirements were met by the system in the faulted state while subjected to any one  
1575 of the load cases included in the Redundancy I and Redundancy II load combinations. Since the system  
1576 met all of the strength requirement it may be re-designated as a system redundant member (SRM) as soon  
1577 as the minimum serviceability requirements are met; otherwise it shall remain designated a fracture critical  
1578 member (FCM).

1579 The first set of strength requirements apply to any primary member of the superstructure, which in this  
1580 case are the tub girders, diaphragms, and concrete slab. These requirements are the following:

- 1581 • In a component, such as a web or a flange of a primary steel member, the average strain is less than  
1582 five times the material yield strain.
- 1583 • In a component, such as a web or a flange of a primary steel member, the average strain is less than  
1584 0.01.
- 1585 • A strain level of 0.05 is not reached anywhere in a primary steel member.
- 1586 • The combined flexural, torsional and axial force effects computed in primary compression  
1587 members are below the nominal compressive resistance of the member (these limit states are  
1588 predicted by the FEA).
- 1589 • If a compression strain greater than 0.003 is reached in the slab, the portion where that limit is  
1590 exceeded does not compromise the overall system load carrying capacity.
- 1591 • The system in the faulted condition is able to support an additional 15% of the factored live load.

1592 Very small and localized yielding was observed in the primary steel members, further critical buckling  
1593 loads were not reached in any primary steel member. The plastic strains calculated in the tie girders, tied  
1594 arch, and floor beams were below 0.01 after the failure of the southernmost tie girder for the Redundancy  
1595 I or Redundancy II load combinations; therefore, the strain requirements on primary steel members are met.  
1596 This is illustrated in Figure F-59, in which the equivalent plastic strain is shown for the most critical load  
1597 case: the Redundancy I load combination with one marked lane loaded. As the FEA accurately predicts  
1598 potential failure of primary steel compression member subjected to combined flexural, torsional, and axial  
1599 force effects, and quasi-static equilibrium is reached for both load combinations, the requirements of  
1600 primary steel compression members are met.  
1601



1602

1603

**Figure F-59. Location of maximum plastic equivalent strain in primary steel members.**

1604

1605

1606

1607

1608

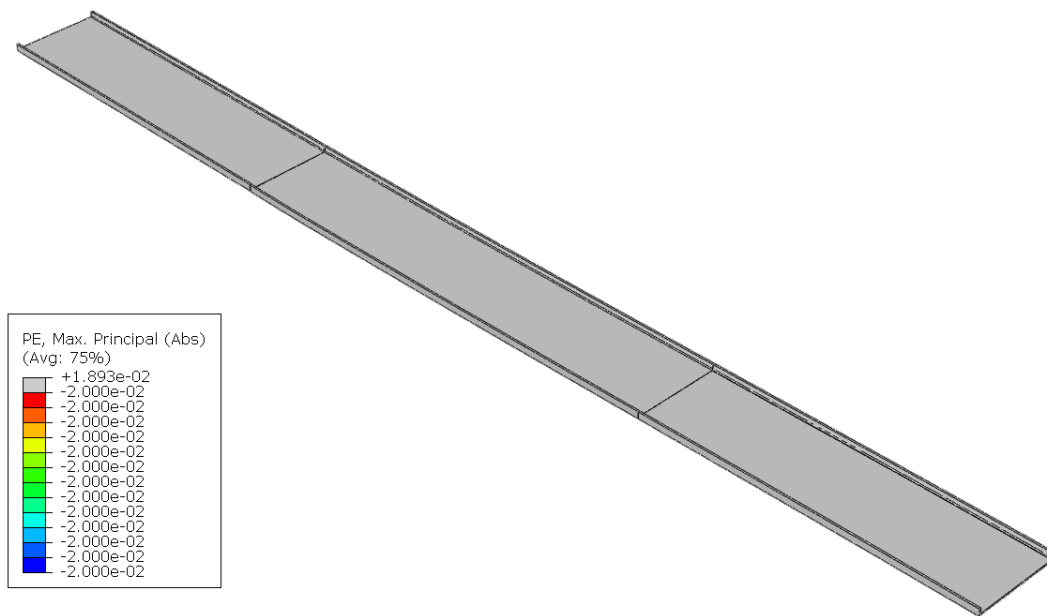
1609

1610

1611

1612

Regarding the concrete slab, concrete crushing and tension cracking is allowed and expected to take place. However, if the portion of the slab where a total compressive strain of 0.003 has been exceeded is large enough to compromise the overall system load carrying capacity or if significant hinging occurs, the structure should not be considered as sufficiently redundant. In this example, the Redundancy II load combination, with three design lanes loaded, resulted in the largest compressive strains in the slab, which were located in the haunches over the southernmost stringers near the failure location. However these strains do not reach 0.003 as shown in Figure F-60; thus, it was not enough to result in a reduction in load carrying capacity.



1613  
1614

**Figure F-60. Absence of concrete crushing in slab.**

1615 Although the substructure is not explicitly included in the finite element model, the reaction forces at  
 1616 support locations are calculated in the analysis. These should be taken as the factored demands that the  
 1617 substructure must be able to safely sustain, which are summarized in Table F-20. In this example, the  
 1618 Redundancy I load combination resulted in the largest vertical reaction forces. Similarly the largest  
 1619 longitudinal and transverse reaction forces take place under the Redundancy I load combination. The  
 1620 unfactored nominal capacity of the abutments and the pier need to be checked against these load demands.  
 1621 Similarly the pier and abutments must accommodate the horizontal displacements that are calculated in the  
 1622 analysis at the support locations. In this example, Redundancy I and Redundancy II load combinations  
 1623 resulted in similar small horizontal displacements which are summarized in Table F-21.  
 1624

1625

**Table F-20. Calculated reaction forces for redundancy evaluations.**

Support	Knuckle	Reaction Force	Redundancy I		Redundancy II		
			1 Lane	2 Lanes	1 Lane	2 Lanes	3 Lanes
East Pier	South	Vertical	2749 kips	2849 kips	2129 kips	2242 kips	2278 kips
		Longitudinal	-1594 kips	-1813 kips	-1045 kips	-1261 kips	-1444 kips
		Transverse	65.3 kips	74.8 kips	43.6 kips	56.5 kips	65.2 kips
	North	Vertical	2670 kips	2816 kips	1886 kips	2015 kips	2155 kips
		Longitudinal	-882 kips	-1211 kips	-421 kips	-621 kips	-888 kips
		Transverse	-11.5 kips	-22.6 kips	-2.71 kips	-11.9 kips	-20.0 kips
West Pier	South	Vertical	2754 kips	2831 kips	2096 kips	2253 kips	2297 kips
		Longitudinal	2184 kips	2386 kips	1496 kips	1753 kips	1936 kips
		Transverse	40.4 kips	41.1 kips	29.3 kips	28.5 kips	27.9 kips
	North	Vertical	2789 kips	2293 kips	1967 kips	2104 kips	2241 kips
		Longitudinal	292 kips	638 kips	-29.6 kips	130 kips	390 kips
		Transverse	-93.0 kips	-93.1 kips	69.5 kips	72.3 kips	72.7 kips
Notes:							
1. Positive longitudinal direction points east.							
2. Positive transverse direction points south.							

1626

1627

**Table F-21. Calculated displacements at support locations for redundancy evaluation.**

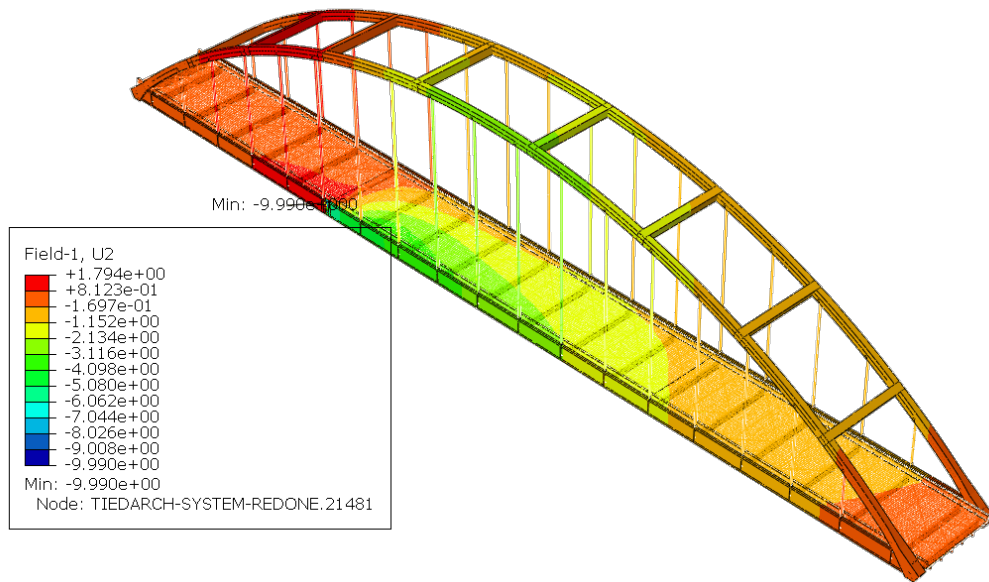
Support	Knuckle	Displacement	Redundancy I		Redundancy II		
			1 Lane	2 Lanes	1 Lane	2 Lanes	3 Lanes
East Pier	South	Longitudinal	0.415 in	0.472 in	0.272 in	0.328 in	0.375 in
		Transverse	-2.94E-3 in	-3.37E-3 in	-1.96E-3 in	-2.54E-3 in	-2.94E-3 in
	North	Longitudinal	0.230 in	0.316 in	0.110 in	0.162 in	0.231 in
		Transverse	5.18E-4 in	1.02E-3 in	1.21E-4 in	5.37E-4 in	9.02E-4 in
West Pier	South	Longitudinal	-0.569 in	-0.621 in	-0.390 in	-0.456 in	-0.504 in
		Transverse	-1.82E-3 in	-1.85E-3 in	-1.32E-3 in	-1.28E-3 in	-1.26E-3 in
	North	Longitudinal	-0.0760 in	-0.166 in	7.71E-3 in	-0.0338 in	-0.102 in
		Transverse	4.19E-3 in	4.20E-3 in	3.13E-3 in	3.26E-3 in	3.27E-3 in
Notes:							
1. Positive longitudinal direction points east.							
2. Positive transverse direction points south.							

1628

1629 Additionally, the system demonstrated a reserve margin of at least 15% of the applied live load in the  
1630 Redundancy I and II load combinations. Effectively, this requirement ensures the slope of the load vs  
1631 displacement curve for the system structure remains positive (i.e., there is still significant remaining reserve  
1632 capacity).

1633 *F.4.8.2 Minimum Serviceability Requirements*

1634 The only serviceability requirement in the Appendix E is that the increase of deflection after the failure  
1635 of a primary steel tension member cannot be greater than L/50. This requirement is to be checked in the  
1636 Redundancy II load combination under factored dead load only. In the current case, the limit is 135 inches,  
1637 which was not surpassed since the maximum additional deflection computed in the FEA was 9.99 inches.  
1638 This is illustrated in Figure F 20.  
1639



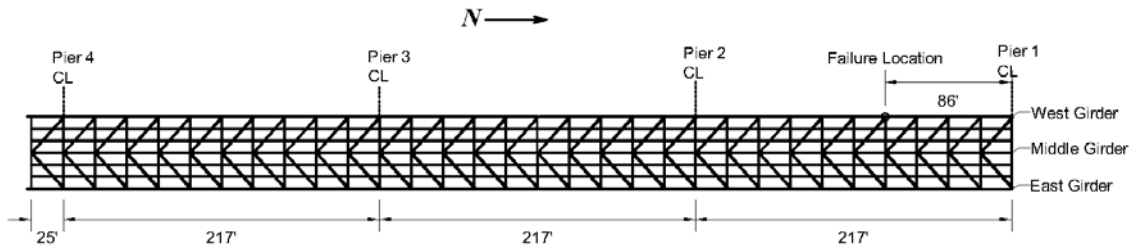
1640 **Figure F-61. Deflection after failure of primary steel tension member.**  
1641

1642 **F.4.9 Conclusions**

1643 The redundancy of a tied arch bridge after the failure of the southernmost tie girder at a stringer relief  
1644 joint was analyzed in accordance with the methodology described in the proposed guide specification in  
1645 Appendix E. Based on the comparison between the obtained results and the minimum performance  
1646 requirements, the structure is not likely to fail nor undergo a significant serviceability loss as result after  
1647 the failure of the tie girder at the stringer relief joint. Hence the tie girders may be re-designated as a system  
1648 redundant member (SRM), provided that it also passes an additional evaluation in which failure of the tie  
1649 girder is introduced near the knuckle.

1650 F.5 Continuous Three Span Three-Girder Bridge

1651 The redundancy of a continuous three span three-girder bridge is analyzed by developing a finite element  
1652 model in accordance with the methodology described in Appendix E. It is assumed that the structure does  
1653 not possess any of the detrimental attributes described in the screening criteria. The bridge is NOT built to  
1654 Section 12 of the AWS D1.5. In this case, the failing tension member is assumed to be the exterior  
1655 westernmost girder. The entire cross-section is assumed to have failed at a cross section located south of  
1656 the northernmost pier (Pier 1) as shown in Figure F-62.

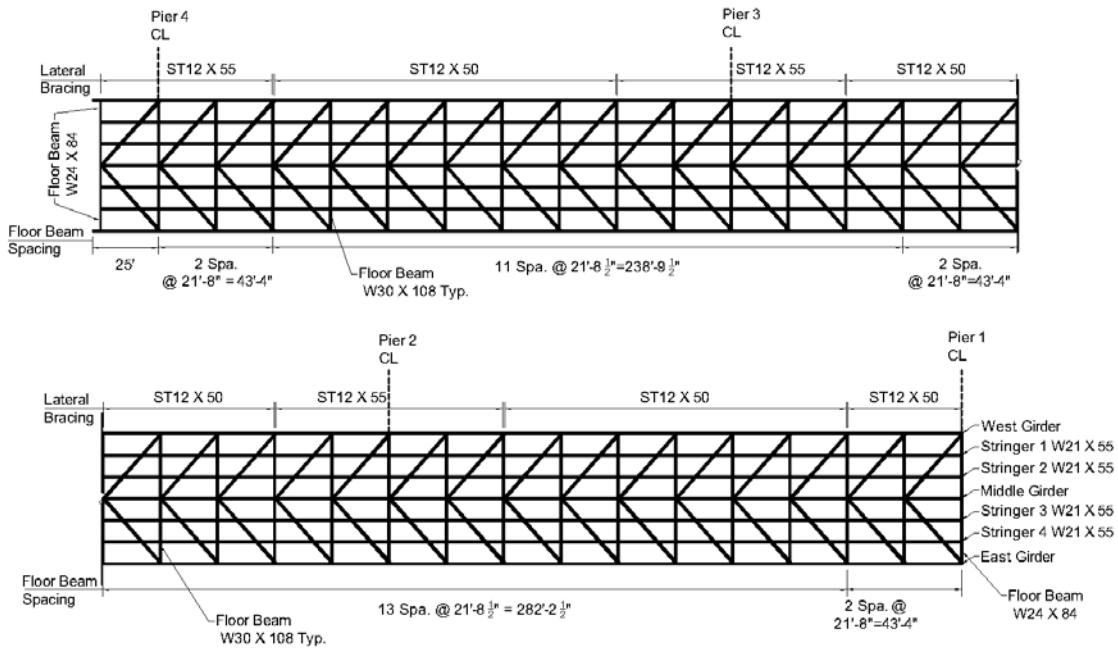


1657  
1658

**Figure F-62. Steelwork geometry and failure location.**

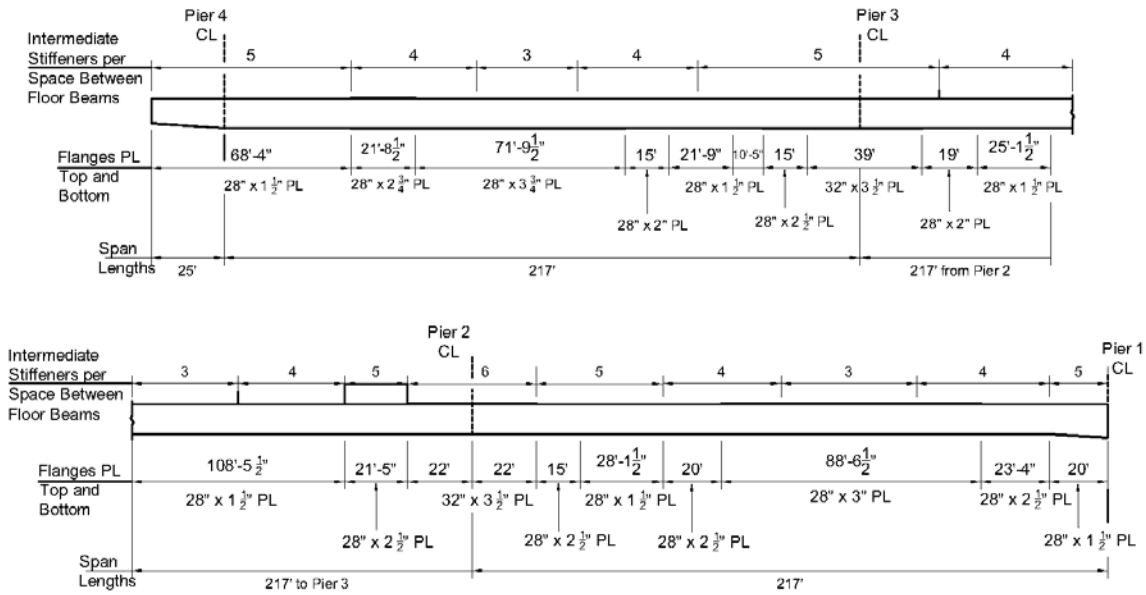
1659 The structure has three spans measuring 217 feet long each. The structure is straight with no skew. Three  
1660 welded plate girders conform the primary members. Attached to the girders there is a system of plate floor  
1661 beams which provided support to continuous stringers. Lateral stability of the girders is provided by K-  
1662 bracing connecting. Figure F-63 shows the steelwork framing plan. The girder schedules are described in  
1663 Figure F-64 for the exteriors (east and west) plate girders, and Figure F-65 for the middle girder. A sketch  
1664 of the typical connections among girders, floorbeams and bracing is shown in Figure F-66

1665 The reinforced concrete slab is 52 feet wide between interior edges of concrete barriers (approximately  
1666 56 feet wide between the outer exterior edges of concrete barriers) and is non-composite. The supports are  
1667 multi-rotational fixed bearings at all support points. All steel components are fabricated of ASTM A36,  
1668 with the exception of the flanges of the plate girders which are fabricated of ASTM A588. All concrete  
1669 has a minimum specified compressive strength of 4 ksi and all rebar has 60 ksi yield strength. In the analysis  
1670 of this structure, longitudinal and transverse slopes will be neglected. Figure F-67 shows the cross section  
1671 of the structure with the slab, barrier and reinforcement details.



1672  
1673

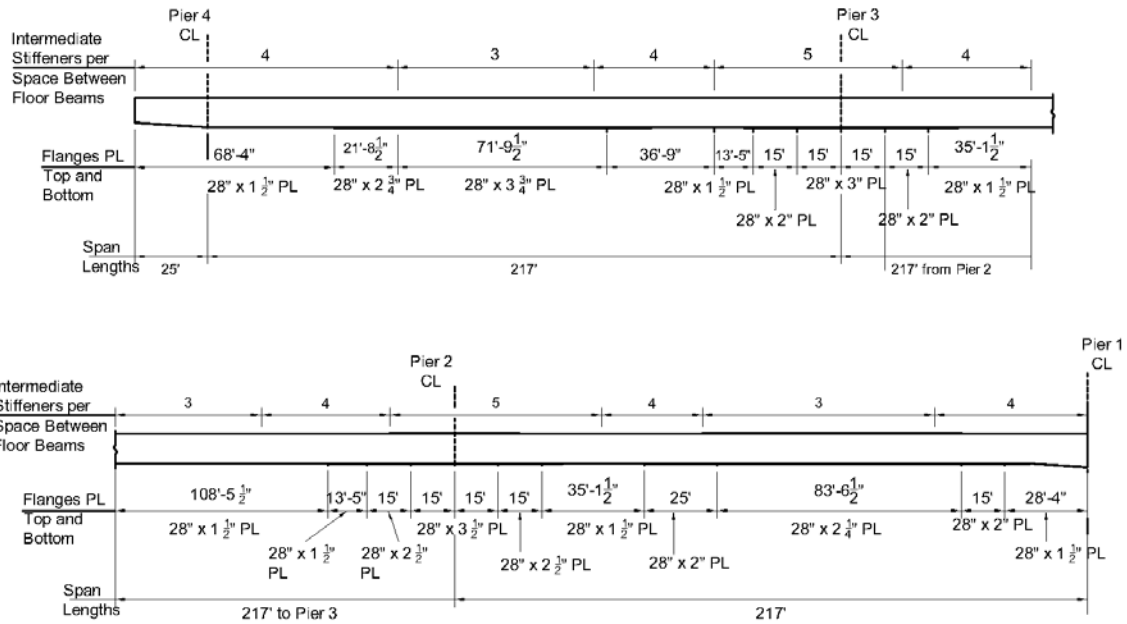
**Figure F-63. Assembly of steel components of the three-girder bridge.**



1674  
1675

**Figure F-64. Schedule of east and west plate girders.**

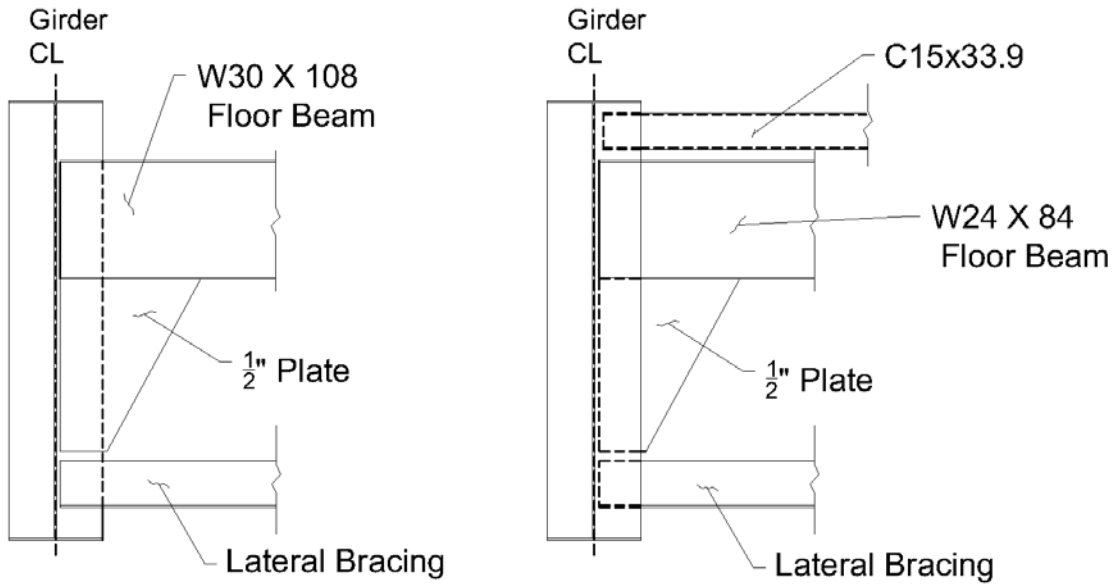




1676  
1677

**Figure F-65. Schedule of middle plate girder.**

1678



1679  
1680

**Figure F-66. Typical connection detail.**



1683 **F.5.1 Analysis Procedure**

1684 The analysis is performed to establish if the system demonstrates acceptable performance in the faulted  
1685 condition. In the example, the term “faulted condition” specifically refers to the case in which a primary  
1686 steel tension member is assumed to have failed. For this analysis, load factors for both dead and live load  
1687 are applied as described in the proposed guide specification in Appendix E. In this example, the described  
1688 analysis procedure is composed of an initial implicit static analysis and a final explicit dynamic analysis,  
1689 into which the results from the initial implicit static analysis are imported. While it is not mandatory for  
1690 the Engineer to follow these particular steps, it has been found that this procedure optimizes the  
1691 computational time required.

1692 *F.5.1.1 Initial Implicit Static Analysis*

1693 Implicit static analysis was utilized to calculate the state of the structure prior to hardening of the concrete  
1694 in the slab. An implicit static analysis was used for the initial steps because, although non-linearity is  
1695 considered in the analysis, the bridge behavior is linear and inertial effects can be neglected as the bridge  
1696 is in the undamaged condition. As the slab does not carry any load and does not contribute to the stiffness  
1697 of the system before concrete hardening, two modifications are required in the finite element analysis during  
1698 this initial implicit static analysis as follows:

- 1699 • A very low stiffness is specified for the elements composing the slab, i.e, the elements modeling  
1700 concrete and rebar. A reduced stiffness of 1/1,000 of the respective modulus of elasticity of each  
1701 material was used. This is done so the load carried by the slab and rebar have negligible  
1702 contribution to the stiffness of the system. No modifications to the stiffness should be applied to  
1703 the steelwork.
- 1704 • Instead of defining contact interaction between the slab and the steelwork, a mesh tie was specified.  
1705 The nodal displacements of the concrete slab elements are tied to the displacements of the top  
1706 flanges of girders, floor beams, and stringers which occur due to dead load. As a result, the slab  
1707 deforms with the steelwork and does not ‘sag’ between the girders, floor beams, and stringers.

1708 It is worth noting that the remainder of the finite element modeling is identical between the initial implicit  
1709 static analysis and the final explicit dynamic analysis. The specific steps in the initial implicit static analysis  
1710 are described as follows:

- 1711 1. Apply load due to self-weight of the structural steel components as a body force.
- 1712 2. Apply load due to self-weight of the wet slab components as a body force.
- 1713 3. The system is then fixed in terms of position, that is, the displacement degrees of freedom are not  
1714 allowed to change.
- 1715 4. The elements composing the slab (elements modeling rebar and concrete) are then deactivated.
- 1716 5. The elements composing the slab are then reactivated. During this reactivation the strain in the  
1717 elements composing the slab is reset to zero.

1718 Steps 3 through 5 are necessary since even though very low stiffness was specified for the slab, these  
1719 elements do undergo strain. Setting the strains to zero eliminates “locked in” artificial stresses in later steps.

1720 *F.5.1.2 Final Explicit Dynamic Analysis*

1721 As contact algorithms, softening material behavior, and non-linear geometry are required to be part of  
1722 the finite element analysis, implicit solution procedures present unavoidable convergence problems in most  
1723 FEA solvers. In order to calculate the capacity of the bridge after sudden failure of a tension component, a  
1724 dynamic explicit analysis needs to be carried out. Therefore, the results obtained from the initial implicit  
1725 static analysis are imported into the final explicit dynamic analysis. In other words, the state of the system  
1726 (stresses, strains, displacements and forces) at the beginning of the final explicit dynamic analysis is defined  
1727 by the state of the system computed at the end of the initial implicit static analysis.

1728 As previously stated, during the initial implicit static analysis, the slab was modeled with largely reduced  
 1729 stiffness to reflect that it is not hardened and a mesh tie constraint was used to assure that the slab deformed  
 1730 with the steelwork. This approach also prevents excessive sag of the soft slab. After the state of the system  
 1731 is imported, the following changes are made to capture the response of the structure after the concrete has  
 1732 hardened:

- 1733 • The modulus of elasticity of the concrete and rebar elements in the slab is changed to their final  
 1734 actual values. It is noted that no modifications need to be applied for the steelwork.
- 1735 • The mesh tie constraint between the slab concrete elements and the top flanges of the steelwork is  
 1736 replaced by a frictional contact interaction. In this case, since the structure is non-composite, the  
 1737 only interaction between the slab and the steel members' top flanges is frictional contact, i.e., no  
 1738 elements that model the behavior of shear studs are added.

1739 All of the body forces applied during the initial implicit static analysis (i.e., the dead load of the structure)  
 1740 are maintained throughout the final explicit dynamic analysis.

1741 To evaluate the capacity of the structure in the faulted state, the following steps were carried out in the  
 1742 final explicit dynamic analysis:

- 1743 6. The stiffness of the elements located at the fracture location under consideration were slowly  
 1744 reduced. The stiffness was slowly reduced in order to minimize any dynamic effects. It is noted  
 1745 that the actual fracture and subsequent vibration of the structure is not modeled. This dynamic  
 1746 effect is accounted for using the  $DA_R$  factor as discussed before. If dynamic effects are found to  
 1747 be significant even if the stiffness is slowly reduced, the system must be allowed to oscillate until  
 1748 these effects are dampened.
- 1749 7. Factored loads due to traffic are applied as surface tractions. For the Redundancy I load  
 1750 combination all loads are amplified by  $DA_R$ , for the Redundancy II load combination the dynamic  
 1751 load allowance (IM) is applied. These loads were applied very slowly to minimize any dynamic  
 1752 effects, as well. If dynamic effects are significant, the system must be allowed to oscillate until  
 1753 these effects are dampened.
- 1754 8. An additional 15% of live load is gradually applied.

## 1755 F.5.2 Material Models

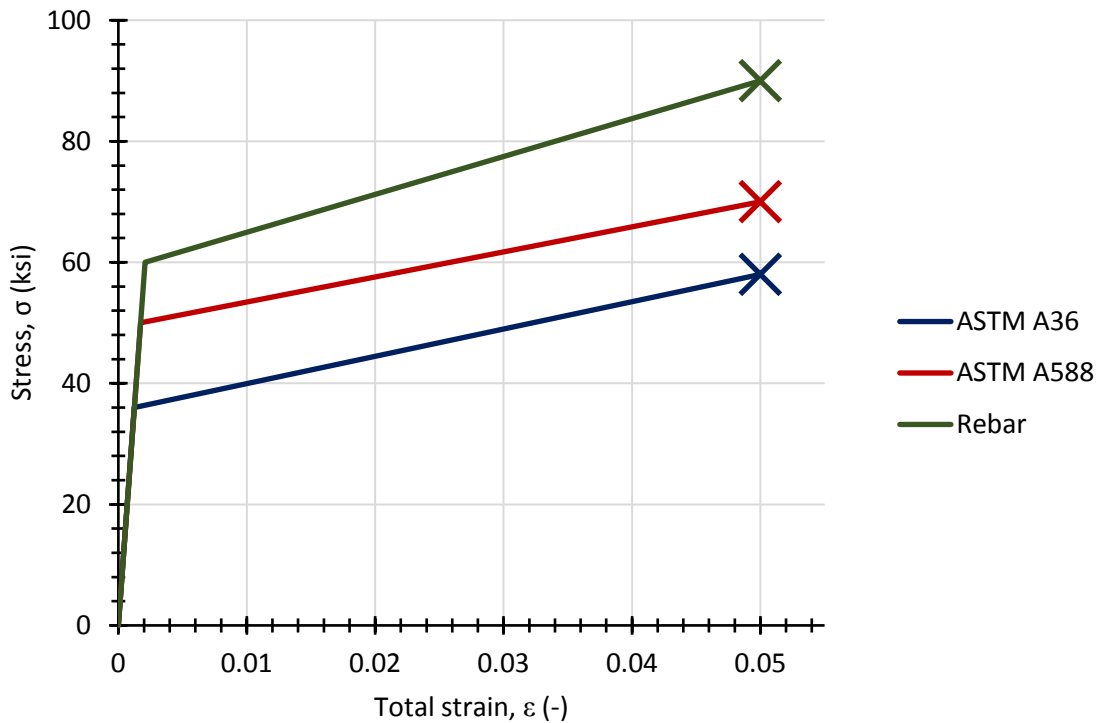
1756 Four material models are needed in the finite element model. Three of those are utilized to model  
 1757 different steel types, and one is utilized to model the response of concrete. For the development of the steel  
 1758 material models, it is necessary to know the yield strength and ultimate strength of each steel type. In this  
 1759 example, since no test values are known to the Engineer, nominal values specified in the respective  
 1760 standards are utilized. These are summarized in Table F-22. A mass density of 0.494 kcf was specified for  
 1761 all steel types.

1762 **Table F-22. Material properties for steel material models.**

Material	Nominal Yield Strength	Nominal Ultimate Strength	Standard
ASTM A36	36 ksi	58 ksi	ASTM A36/A36M
ASTM A588	50 ksi	70 ksi	ASTM A588/A588M
Grade 60 Rebar	60 ksi	90 ksi	ASTM A615/A615M

1763 The stress-strain relation for all steel components will follow an initial linear elastic steel with a Young's  
 1764 modulus of 29,000 ksi and Poisson's ratio of 0.3. Once the nominal yield strength is reached the stress-  
 1765 strain relation is defined by Von Mises (J2) plasticity with kinematic linear hardening, until the nominal  
 1766 ultimate strength is reached at a total strain of 0.05. Once the nominal ultimate strength or a total strain of  
 1767

1768 0.05 is reached, the material is assumed to fail. Figure F-68 shows the uniaxial material response for the  
 1769 steel employed in this finite element model with the 'X' denoting the stress at the failure strain of 0.05.  
 1770



1771  
 1772 **Figure F-68. Stress-strain curves of steel material models.**

1773 The material model used in concrete is defined entirely by the specified compressive strength which in  
 1774 this case is 4 ksi. This quantity is also used to calculate the tensile strength, the total strain at compressive  
 1775 strength,  $\epsilon_c$ , and the material parameter  $n$ . Table F-23 summarizes the calculation of these values. A mass  
 1776 density of 0.150 kcf was specified for concrete.

1777 **Table F-23. Material properties for concrete material model.**

Quantity	Symbol	Equation	Result
Young's modulus	$E_c$	$E_c = 33,000w_c^{1.5}\sqrt{f'_c} \leq 1,802.5\sqrt{f'_c}$	3,600 ksi
Tensile strength	$f_t$	$f_t = 0.158(f'_c)^{\frac{2}{3}}$ for $f'_c \leq 7.25ksi$ $f_t = 0.307 \ln(f'_c + 2.61) - 0.114$ for $f'_c > 7.25ksi$	0.398 ksi
Fracture energy	$G_t$	$5.9 \cdot 10^{-4}(f'_c + 1.16)^{0.18}$	$7.93 \cdot 10^{-4}$ kip/in
Total strain at compressive strength	$\epsilon_c$	$\epsilon_c = 0.00124^4\sqrt{f'_c}$	0.00175
Material parameter	$n$	$n = 0.4f'_c + 1.0$	2.6

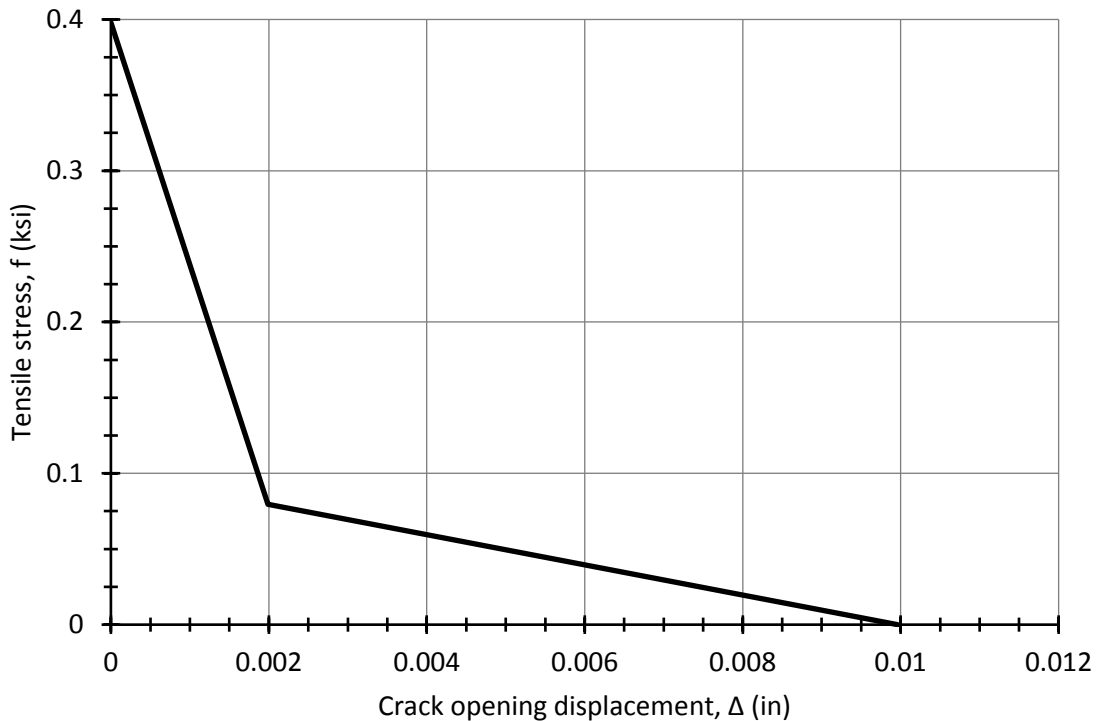
1779 The concrete material model is initially linear elastic, defined by a Young's modulus of 3,600 ksi and  
 1780 Poisson's ratio of 0.2, followed by concrete damage plasticity. In tension, once the material reaches its  
 1781 tensile strength, set at 0.398 ksi in this case, a tensile stress-displacement relation characterized by a fracture  
 1782 energy,  $G_t$ , of  $7.93 \cdot 10^{-4}$  kip-in is followed. This fracture energy is applied through a bi-linear tensile stress-  
 1783 displacement relation as shown in Figure F-69, and defined by the following quantities:

1784 
$$f_{t1} = \frac{f_t}{5} = 0.0796 \text{ ksi}$$

1785 
$$\delta_t = \frac{5G_t}{f_t} = 0.00996$$

1786 
$$\delta_{t1} = \frac{G_t}{f_t} = 0.00199$$

1787



1788  
 1789 **Figure F-69. Tensile stress-crack opening displacement curve for concrete material model.**

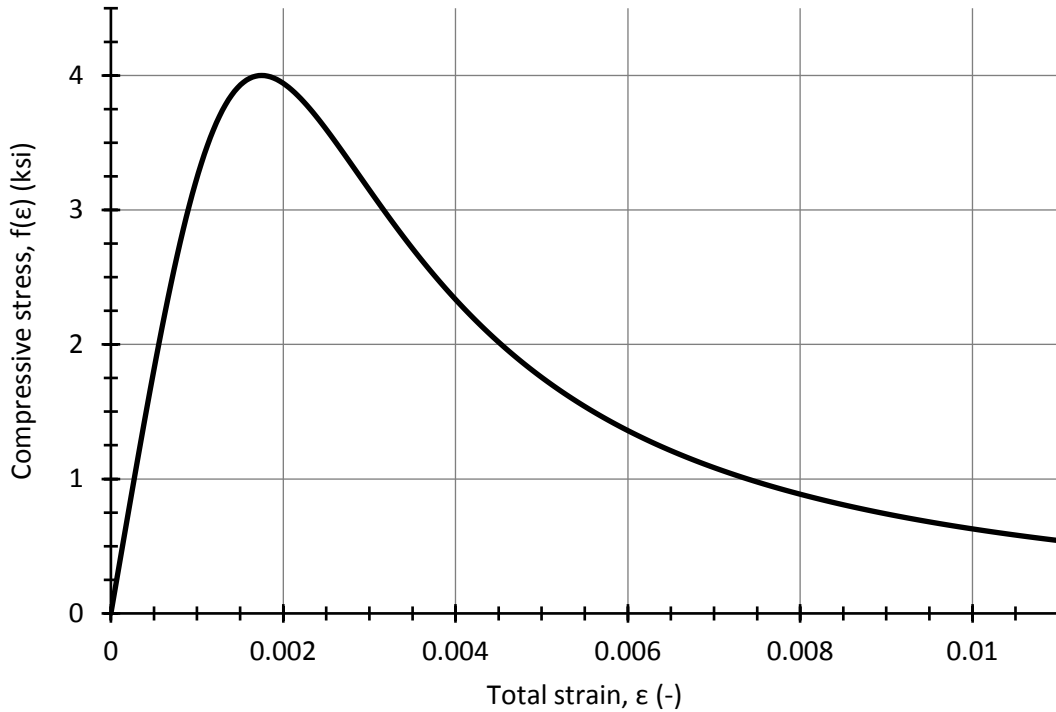
1790 In compression the material follows the following stress-strain relations:

1791 
$$f(\varepsilon) = f'_c \left( \frac{\varepsilon}{\varepsilon_c} \right) \left[ \frac{n}{n - 1 + \left( \frac{\varepsilon}{\varepsilon_c} \right)^n} \right]$$

1792 
$$\varepsilon_{plastic} = \varepsilon - \frac{f(\varepsilon)}{E_c}$$

1793 Where  $\varepsilon$  is total (elastic + plastic) strain,  $f(\varepsilon)$  is the compressive stress at a given total strain,  $f'_c$  is the  
 1794 specified compressive strength,  $\varepsilon_c$  is the total strain at compressive strength,  $n$  is a material parameter,  
 1795  $\varepsilon_{plastic}$  is the plastic strain and  $E_c$  is the concrete Young's modulus. Figure F-70 shows the resulting  
 1796 compressive stress-strain relation.

1797



1798  
1799

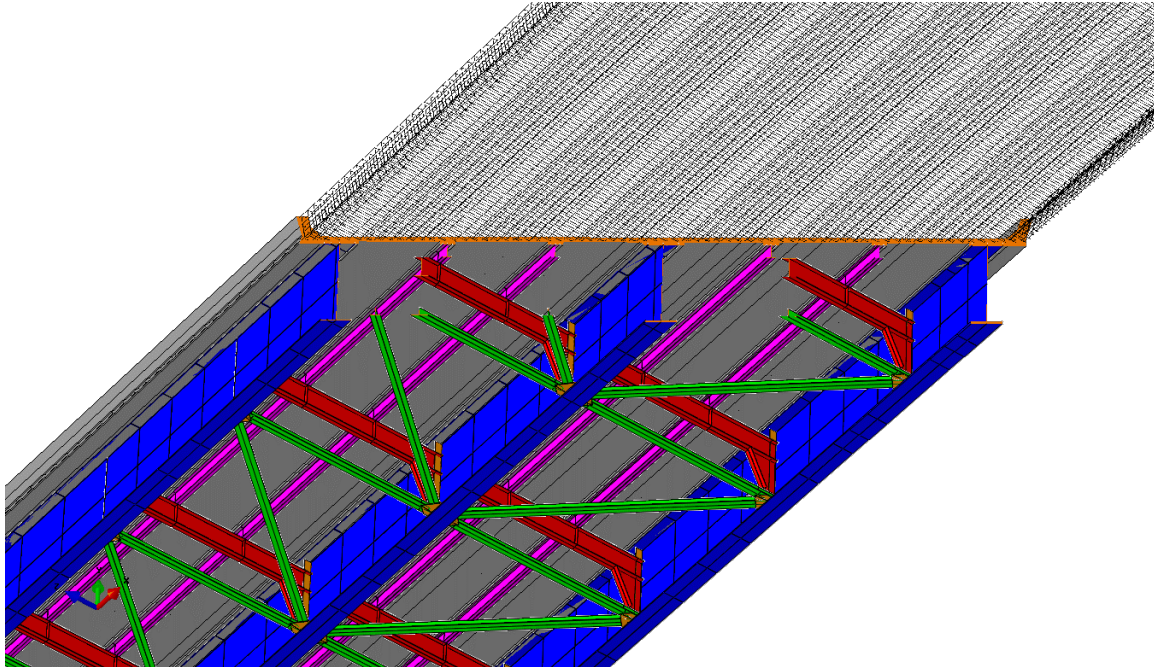
**Figure F-70. Compressive stress-strain curve for concrete material model.**

1800 **F.5.3 Geometries, Meshes and Constraints**

1801 The geometry of the structure is based on available design plans and is composed of the following  
1802 components that must be explicitly modeled:

- 1803 1. Three plate girders.  
1804 2. A system of 64 floor beam.  
1805 3. Four continuous stringers supported on the floor beams.  
1806 4. A system of lateral braces.  
1807 5. Stiffener plates and connection plates.  
1808 6. A reinforced concrete slab with concrete barriers.

1809 When generating the finite element model, splices, holes, access hatches, etc. are neglected. The  
1810 structure is assumed to be flat in the vertical plane, in other words, camber and superelevation are ignored.  
1811 Figure F-71 shows the assembly of all bridge components looking up from the below the bridge.



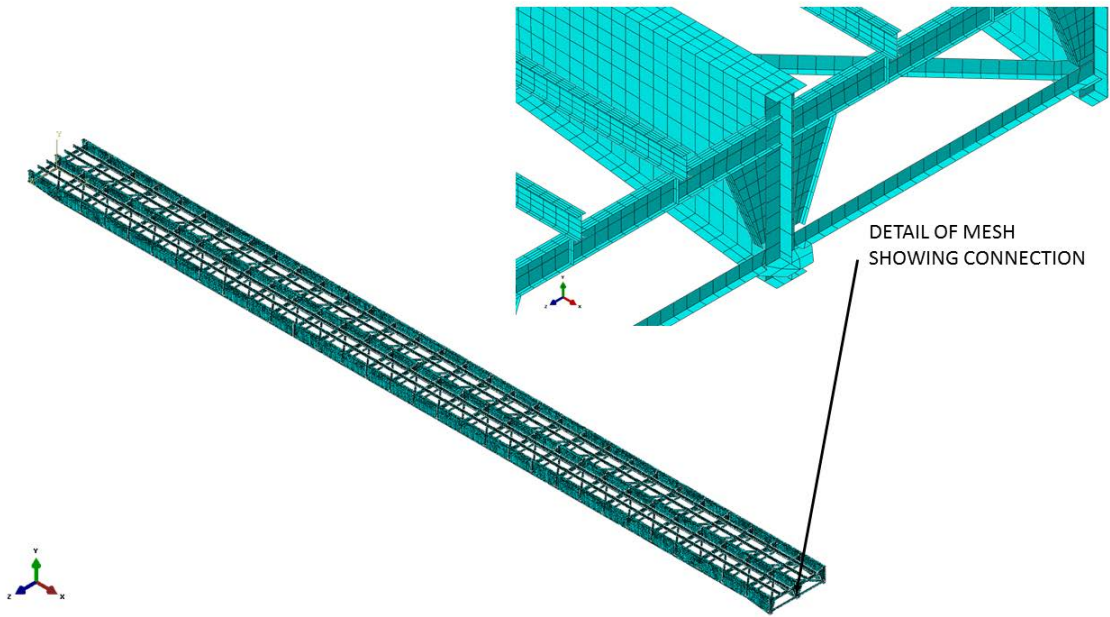
1812  
1813  
1814  
1815

**Figure F-71. Three-girder bridge geometries, detailed bottom view. Concrete slab and barriers (grey), plate girdes (blue), K-bracing (green), stringers (magenta), floor beams (red), slab reinforcement (black) and stiffeners and connection details (orange).**

1816 All steel components are modeled with 4-node shell elements with reduced integration. A minimum of  
1817 four elements are used along flange widths and along web heights, except at bracing elements, where one  
1818 element was used. The maximum aspect ratio was kept below five and corner angles were kept between  
1819 60 and 120 degrees. Figure F-72 shows a detail of the mesh employed to model the plate girders,  
1820 diaphragm, floor beam, stringers, and stiffeners. Mesh ties, which are constraints that slave the motion of  
1821 a surface or node set to the motion of a master surface or node set, are utilized to connect the various steel  
1822 components.

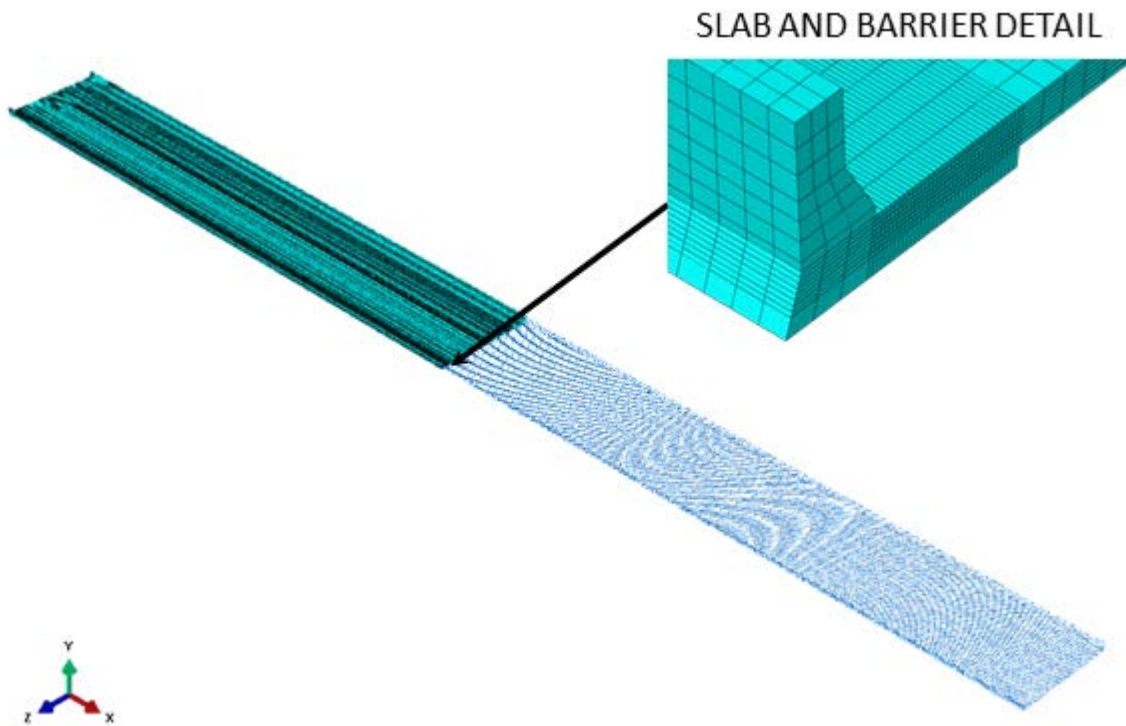
1823 The slab is modeled with two types of elements. Specifically, 8-node linear bricks with reduced  
1824 integration are used to model concrete and 2-node truss elements with linear displacement to model steel  
1825 reinforcement. Eight solid concrete elements are used through the thickness of the slab with maximum  
1826 aspect ratio (length of longest edge divided by length of shortest edge) of 5, and corner angles (angle at  
1827 which two element edges meet) between 40 and 140 degrees. The length of the truss elements used to  
1828 model the reinforcement were approximately equal to the length of the longest edge of the solid concrete  
1829 elements. These truss elements are embedded within the solid concrete elements. At the nodes of the  
1830 embedded truss elements, the translational degrees of freedom are eliminated and the nodal translations  
1831 were constrained to interpolated values of the nodal translations of the host solid concrete element. Figure  
1832 F-73 shows the concrete slab with the embedded truss elements and a detail of the mesh used for the  
1833 concrete barrier and slab.





1834  
1835

**Figure F-72. Mesh details of the steel component of the three-girder bridge.**



1836  
1837

**Figure F-73. Mesh details of the reinforced concrete slab and barriers.**

1838 **F.5.4 Slab-Structural Steel Interaction**

1839 As stated, the interaction between the bottom of the concrete slab and the top of the flanges of the  
 1840 steelwork is modeled differently in the two steps described above. In the initial implicit static analysis,  
 1841 when the elements comprising the slab and barriers have 1/1,000<sup>th</sup> of the modulus of elasticity to model the  
 1842 “wet” condition, a mesh tie is used to slave the motion of the slab to the motion of the surface comprising  
 1843 the top of the steel work. With this procedure, it is ensured that the slab deformation will conform to the  
 1844 deformation of the steelwork while unrealistic sagging of the slab between supporting elements and tipping  
 1845 of the barrier is prevented.

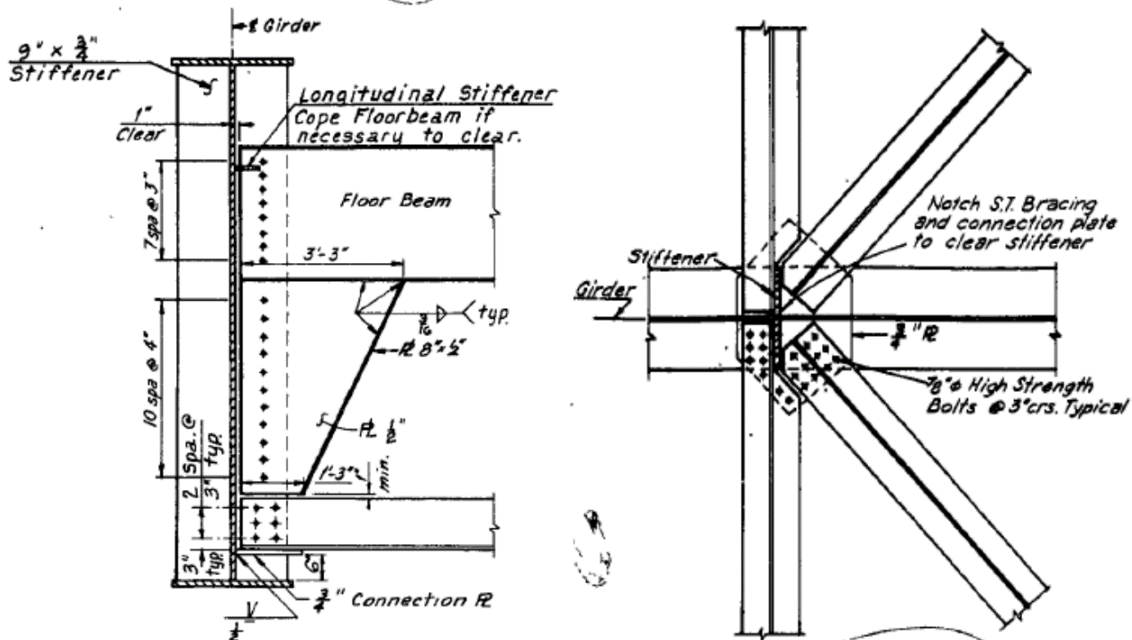
1846 In the final explicit dynamic analysis, when the stiffness of the elements comprising the slab and barriers  
 1847 has been changed to their final real values, the mesh tie previously used is deleted and replaced by a contact  
 1848 interaction and modeling of shear studs. The normal behavior of the contact interaction is modeled through  
 1849 a penalty stiffness. The penalty stiffness is several orders of magnitude larger than the normal stiffness of  
 1850 the underlying contacting elements and allows a very small penetration so a pressure can be calculated.  
 1851 The tangential behavior of the contact interaction is modeled through an algorithm based on Coulomb  
 1852 friction with a limit on the allowable shear. A friction coefficient of 0.55 and an interfacial shear strength  
 1853 of 0.06 ksi are specified.

1854 **F.5.5 Connection Modeling**

1855 When a connection is likely to fail before yielding of the member, in addition to the use of mesh ties to  
 1856 attach the components, an additional step may be necessary to capture connection failure. In this particular  
 1857 example, it was opted to model every component of the connections between floor beams, girders and  
 1858 bracing. Typical connections are shown in Figure F-74.

1859 The main motive was to capture the flexibility of the connection, the eccentricity of bracing elements at  
 1860 the connection, and possible failure of the braces at the connection. Mesh tie constraints were utilized to  
 1861 attach the components; in a mesh tie constraint the displacement of a slave region is constrain to the  
 1862 displacement of a master region. In this case, the entire stiffener and connection plate is the master region,  
 1863 while the slave regions are the portions of the connected elements that are bolted to the connection as shown  
 1864 in Figure F-75.

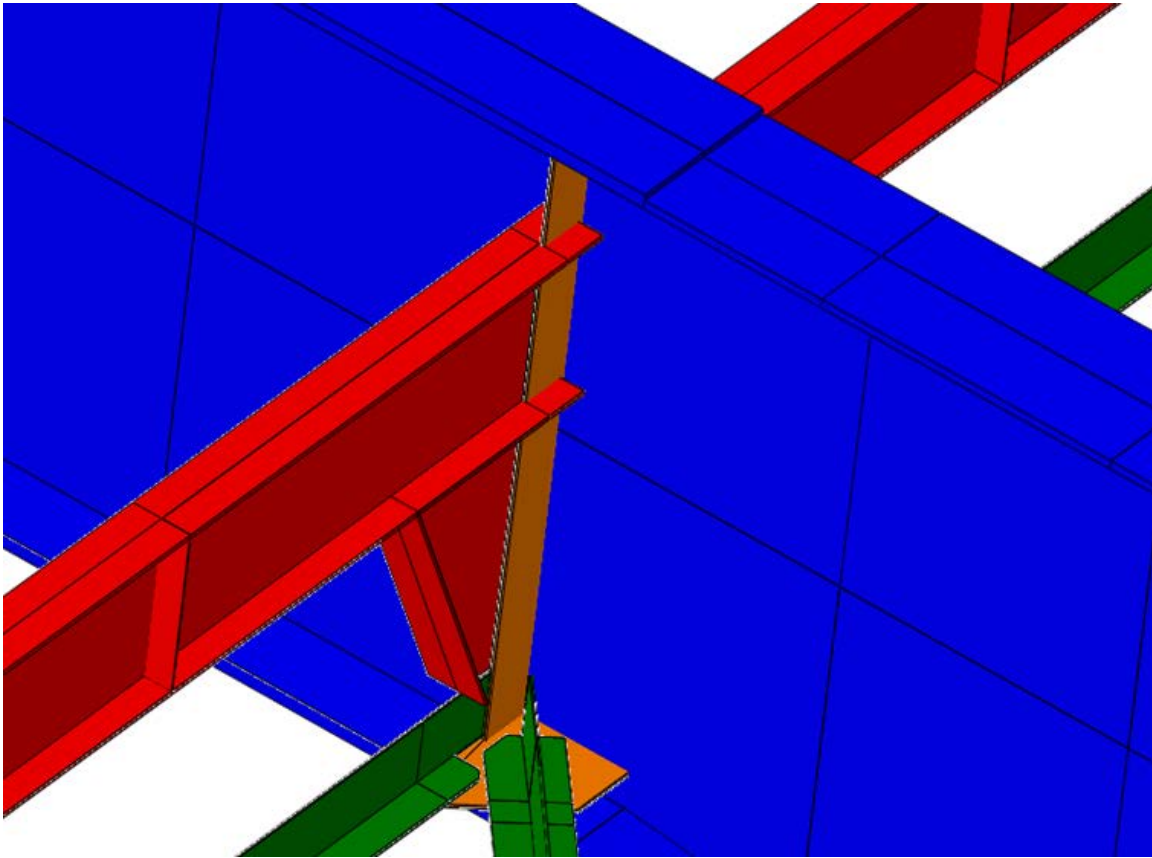
1865



1866

1867  
1868

*Figure F-74. Connection details. Longitudinal stiffener was not included in finite element model.*

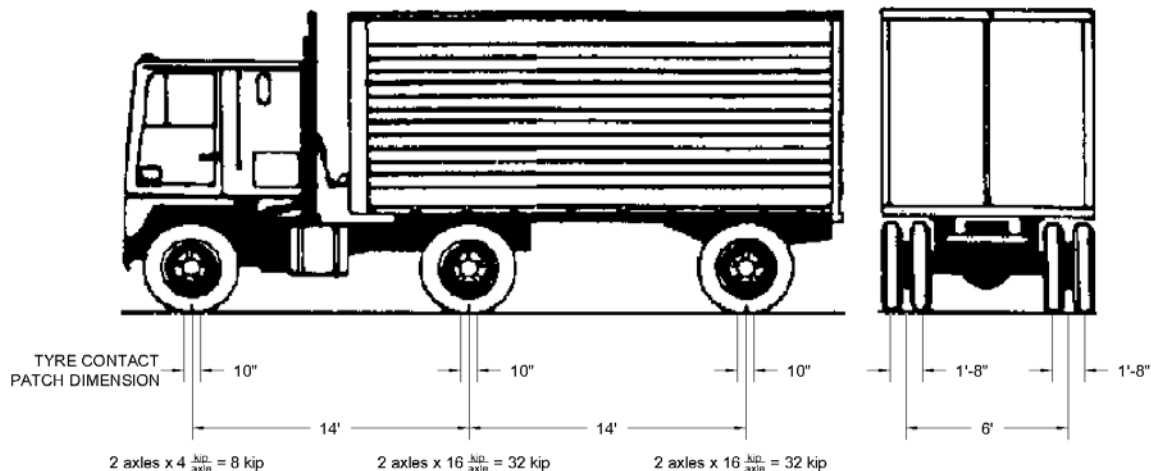


1869  
1870  
1871

*Figure F-75. Detail of connection as modeled in finite element model. Stiffener and connection plate shown in orange. Bracing (green), girder (blue) and floor beam (red) shown as well.*

## 1872 **F.5.6 Loads and Boundary Conditions**

1873 Two types of loads were applied in the finite element models: body forces and surface tractions as  
1874 required by the proposed guide specification in Appendix E. Body forces were applied for component dead  
1875 loads (“DC” and “DW” per AASHTO designations). These are simply the product of mass, gravity and  
1876 applicable load factors. Surfaces tractions were applied for traffic live loads (“LL” per AASHTO  
1877 designation). The traffic live load is based on the HL-93 load model described in the AASHTO LRFD  
1878 BDS, which is a combination of the truck loads, shown in Figure F-76, and a 0.64 klf load distributed over  
1879 a width of 10 ft. The current structure does not include any bituminous pavement (i.e., DW is zero).



1880  
1881 **Figure F-76. Truck load components and dimensions of the HL-93 vehicular live load model.**

1882 The Redundancy I and Redundancy II loading combinations were used to evaluate the structure in the  
 1883 faulted state. The load factors for these two combinations are as in Table F-24, based on the provisions in  
 1884 Appendix E for bridges NOT built to Section 12 in the AWS D1.5. It must be noted that dynamic  
 1885 amplification factor is equal to 0.4, which is applied to DC and LL in the Redundancy I load combination  
 1886 only. Also, the dynamic load allowance is 0.15 of the truck axle loads, and is only applied in the  
 1887 Redundancy II load combination. :

1888 **Table F-24. Load factors used for Redundancy I and Redundancy II load combinations.**

Load Combination	Load Factors				Notes
	DC	LL	DA <sub>R</sub>	IM	
Redundancy I	1.15	1.00	0.40	N. A.	$\beta = 2.5$
Redundancy II	1.15	1.50	N. A.	0.15	$\beta = 2.5$

1889  
1890 Longitudinally, the loads are positioned in the most critical positions in both the Redundancy I and  
 1891 Redundancy load combinations. For the failure scenario considered in the current case (failure of the  
 1892 exterior westernmost girder at 86 feet south or Pier 1, shown in Figure F-62 and Figure F-77), the most  
 1893 critical position of the truck axle loads which results in the truck facing north with its middle axis positioned  
 1894 at the failure plane, as shown in Figure F-57. The distributed load portion of the HL-93 load is applied  
 1895 along the entire span.

1896 As described in the proposed guide specification in Appendix E, the transverse positioning of the HL-93  
 1897 live load model differs between the Redundancy I and Redundancy II load combinations, as illustrated in  
 1898 Figure F-58. Since the vehicular loads in the Redundancy I load combination are meant to represent the  
 1899 applied load at the instant in time in which the assumed member failure occurs, the HL-93 vehicular live  
 1900 load model is transversely positioned centered (both the 10 ft loaded width and the truck axle loads) within  
 1901 the marked (striped) lanes, in this case three lanes. Hence, as the bridge is striped for three lanes, there are  
 1902 three load cases for the Redundancy I load combination: three marked lanes loaded, two marked lanes  
 1903 loaded, or one marked lane loaded.

1904 On the other hand, the objective of the Redundancy II load combination is to evaluate the strength of the  
 1905 system after the failure of the primary steel tension member has occurred, so the number of design lanes is  
 1906 established in accordance with Article 3.6.1.1.1 in the AASHTO LRFD BDS, which in this case results in  
 1907 four design lanes with a width of 12 ft. In the Redundancy II load combination, the HL-93 vehicular live

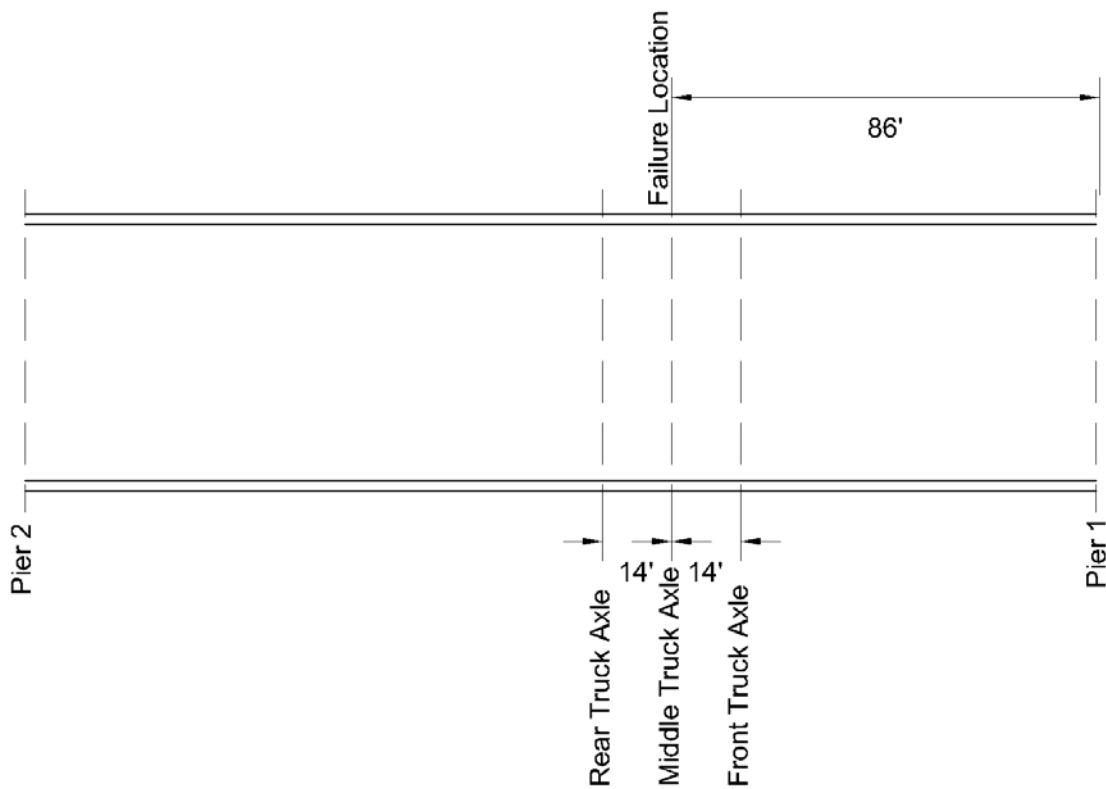
1908 load model is transversely positioned (both the 10 ft loaded width and the truck axle loads) to produce  
 1909 extreme force effects within each design lane; however, the truck axle loads are transversely positioned  
 1910 such that the center of any wheel load is not closer than 2 ft from the edge of the design lane. Hence, there  
 1911 are four load cases for the Redundancy II load combination: four design lanes loaded, three design lanes  
 1912 loaded, two design lanes loaded, or one design lane loaded.

1913 Component dead loads were linearly applied in the initial implicit static analysis. Traffic live loads were  
 1914 applied in the final explicit dynamic analysis. Their dynamic effects were minimized by applying them  
 1915 slowly through the use of smooth step, as in the following equation:

1916 
$$LR(t) = 6 \left(\frac{t}{T}\right)^5 - 15 \left(\frac{t}{T}\right)^4 + 10 \left(\frac{t}{T}\right)^3$$

1917 where  $LR(t)$  is the fraction of load at a load application time  $t$ , and  $T$  is the duration of the load application.  
 1918 The duration of the load application must be larger than the fundamental period of the structure to minimize  
 1919 oscillatory behavior in the final explicit dynamic analysis.

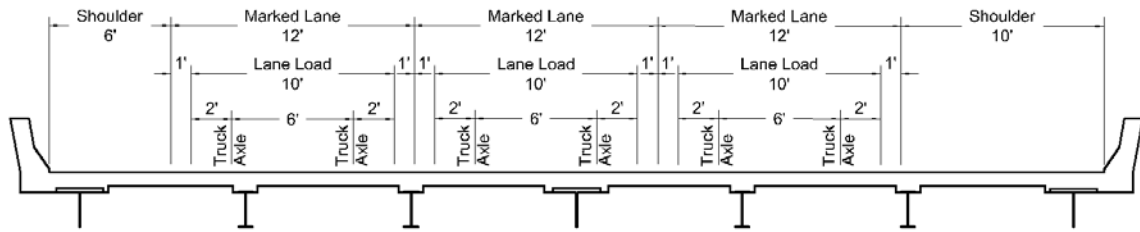
1920



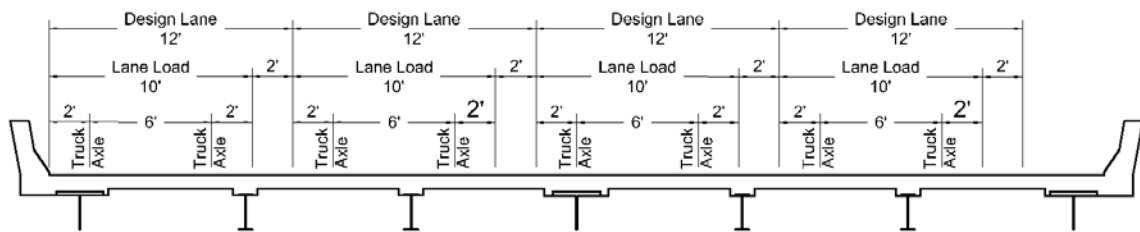
1921  
 1922

**Figure F-77. Longitudinal position of truck axles.**

1923



TRANSVERSE LOAD POSITION FOR REDUNDANCY I



TRANSVERSE LOAD POSITION FOR REDUNDANCY II

1924  
1925

**Figure F-78. Transverse position of traffic loads. Fracture is girder is leftmost girder.**

1926 **F.5.7 Analysis of Results for Redundancy**

1927 Once the analysis is completed the obtained results are evaluated using the requirements described in  
 1928 Article 8 of the proposed guide specification in Appendix E. It was found that the structure met the strength  
 1929 and serviceability requirements and is considered redundant against failure of the exterior westernmost  
 1930 girder. Specific details regarding the performance requirements and the results are summarized in Table  
 1931 F-25.  
 1932

1933

**Table F-25. Summary of the redundancy evaluation.**

Performance Requirement		Most Critical Load Combination	Result	Acceptable?
Strength Requirements	Strain Primary Steel Members	Redundancy I 3 Lanes	0.0022	<b>YES</b>
	Slab Concrete Crushing	-	No concrete crushing in the slab	<b>YES</b>
Serviceability Requirements	Vertical Deflection	Only Redundancy II DL considered	10.3 inches	<b>YES</b>
Notes: 1. The analysis showed that the structure was capable of resisting an additional 15% of the applied factored live load. 2. In order to complete the evaluation, the displacements and reaction forces calculated at support locations should be used as factored demands to check against the nominal capacity of the supports and substructure members.				

1934

1935 *F.5.7.1 Minimum Strength Requirements*

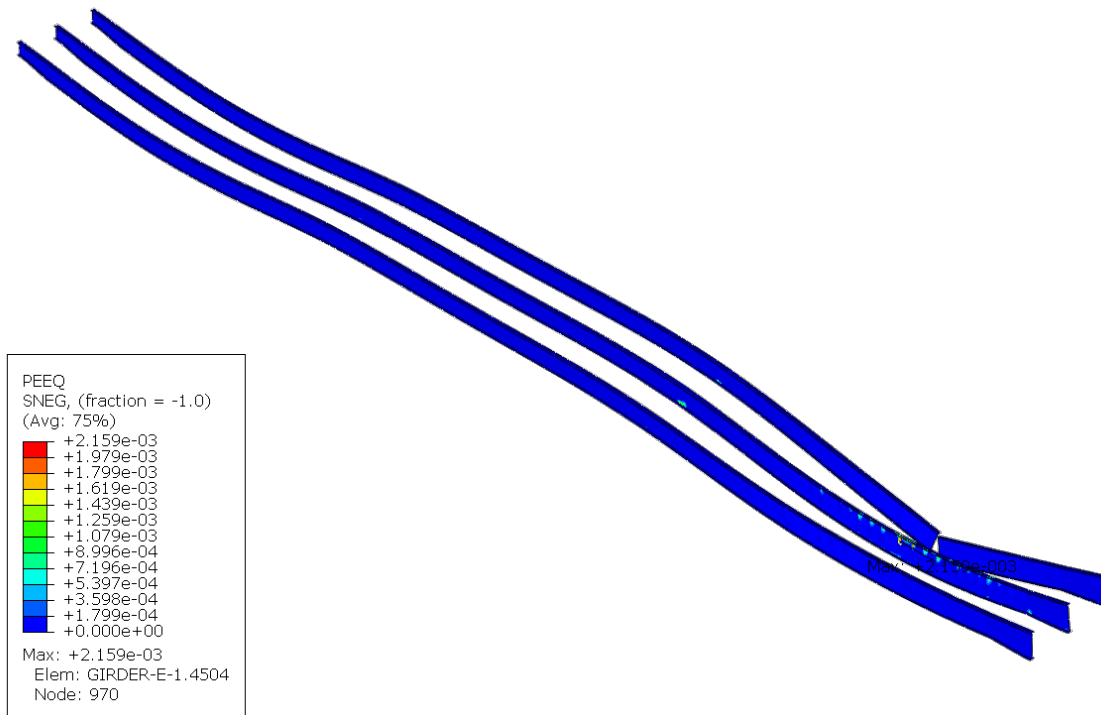
1936 All of the strength requirements were met by the system in the faulted state while subjected to any one  
 1937 of the load cases included in the Redundancy I and Redundancy II load combinations. Since the system  
 1938 met all of the strength requirement it may be re-designated as a system redundant member (SRM) as soon  
 1939 as the minimum serviceability requirements are met; otherwise it shall remain designated a fracture critical  
 1940 member (FCM).

1941 The first set of strength requirements apply to any primary member of the superstructure, which in this  
 1942 case are the girders, and concrete slab. These requirements are the following:

- 1943 • In a component, such as a web or a flange of a primary steel member, the average strain is less than  
 1944 five times the material yield strain.
- 1945 • In a component, such as a web or a flange of a primary steel member, the average strain is less than  
 1946 0.01.
- 1947 • A strain level of 0.05 is not reached anywhere in a primary steel member.
- 1948 • The combined flexural, torsional and axial force effects computed in primary compression  
 1949 members are below the nominal compressive resistance of the member (these limit states are  
 1950 predicted by the FEA).
- 1951 • If a compression strain greater than 0.003 is reached in the slab, the portion where that limit is  
 1952 exceeded does not compromise the overall system load carrying capacity.
- 1953 • The system in the faulted condition is able to support an additional 15% of the factored live load.

1954 Very small and localized yielding was observed in the primary steel members, further critical buckling  
 1955 loads were not reached in any primary steel member. The plastic strains calculated in the girders were  
 1956 below 0.01 after the failure of the southernmost tie girder for the Redundancy I or Redundancy II load  
 1957 combinations; therefore, the strain requirements on primary steel members are met. This is illustrated in  
 1958 Figure F-79, in which the equivalent plastic strain is shown for the most critical load case: the Redundancy  
 1959 I load combination with three marked lanes loaded. As the FEA accurately predicts potential failure of  
 1960 primary steel compression member subjected to combined flexural, torsional, and axial force effects, and  
 1961 quasi-static equilibrium is reached for both load combinations, the requirements for primary steel  
 1962 compression members are met.

1963



1964  
1965

**Figure F-79. Location of maximum plastic equivalent strain in primary steel members.**

1966      Regarding the concrete slab, concrete crushing and tension cracking is allowed and expected to take  
 1967 place. However, if the portion of the slab where a total compressive strain of 0.003 has been exceeded is  
 1968 large enough to compromise the overall system load carrying capacity or if significant hinging occurs, the  
 1969 structure should not be considered as sufficiently redundant. In this example, the Redundancy II load  
 1970 combination, with four design lanes loaded, resulted in the largest compressive strains in the slab, which  
 1971 were located in the haunches over the middle girder near the failure location. However these strains do not  
 1972 reach 0.003 as shown in Figure F-80; thus, it was not enough to result in a reduction in load carrying  
 1973 capacity.  
 1974



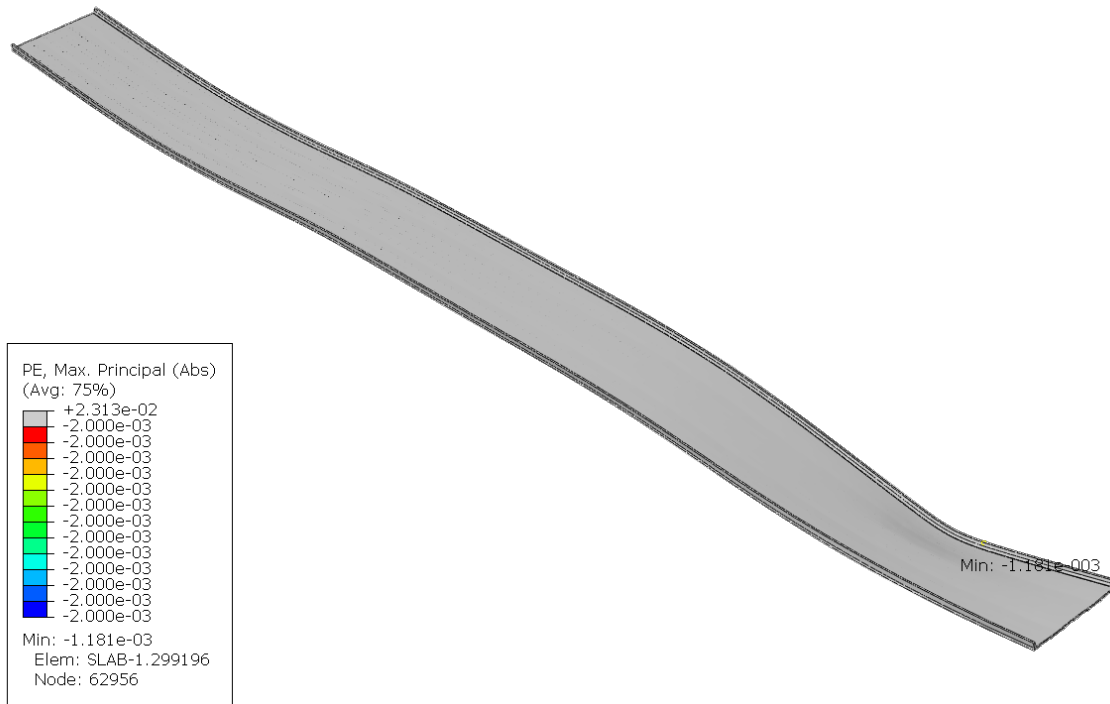


**Figure F-80. Absence of concrete crushing in slab.**

1975  
1976

1977

1978 Although the substructure is not explicitly included in the finite element model, the reaction forces at  
 1979 support locations are calculated in the analysis. These should be taken as the factored demands that the  
 1980 substructure must be able to safely sustain, which are summarized in Table F 20. In this case, the largest  
 1981 vertical reaction forces were calculated for the Redundancy I load combination. The calculated longitudinal  
 1982 and transverse reaction forces are small for both loading combinations. The unfactored nominal capacity  
 1983 of the members of the substructure needs to be checked against these load demands. Similarly these  
 1984 elements of the substructure must accommodate the horizontal displacements that are calculated in the  
 1985 analysis at the support locations. In this example, Redundancy I and Redundancy II load combinations  
 1986 resulted in similar small horizontal displacements which are summarized in Table F 21.

1987

**Table F-26. Calculated reaction forces for redundancy evaluation. All results in kips.**

Support	Girder	Reaction Force	Redundancy I			Redundancy II			
			1 Lane	2 Lanes	3 Lanes	1 Lane	2 Lanes	3 Lanes	4 Lanes
Pier 1	West	Vertical	298	321	315	235	275	276	254
		Longit.	7.90	-10.4	-51.6	12.6	-3.46	-25.8	-55.6
		Transv.	-2.48	3.54	19.9	-7.78	-5.77	3.34	18.7
	Middle	Vertical	902	957	989	726	788	830	811
		Longit.	12.8	2.05	-50.2	16.4	9.62	-7.60	-58.6
		Transv.	-1.96	-0.818	1.46	-5.22	-4.58	-3.22	-0.508
	East	Vertical	315	343	397	178	194	237	297
		Longit.	7.69	7.94	-15.5	7.95	9.54	8.95	-17.2
		Transv.	-0.267	-6.18	-17.4	-0.0554	-3.43	-10.4	-19.3
Pier 2	West	Vertical	1410	1441	1424	1115	1181	1173	1102
		Longit.	-8.90	-0.241	30.3	-11.6	-3.52	6.70	33.8
		Transv.	-1.65	1.43	2.82	1.99	4.74	6.30	4.10
	Middle	Vertical	1805	1893	1941	1350	1443	1511	1492
		Longit.	-6.17	-2.33	28.4	-7.70	-3.90	3.68	33.5
		Transv.	2.17	-1.85	-6.80	7.34	4.82	1.61	-4.23
	East	Vertical	1108	1147	1211	738	761	815	892
		Longit.	-4.22	-2.30	17.8	-4.75	-3.31	0.114	20.1
		Transv.	3.18	2.25	-5.91	5.65	7.33	6.30	-1.44
Pier 3	West	Vertical	1068	1060	1059	738	725	722	735
		Longit.	-0.512	0.888	-1.55	-0.621	-0.313	0.892	-1.35
		Transv.	2.88	3.07	3.25	3.74	3.32	1.97	1.60
	Middle	Vertical	1446	1433	1427	1022	1007	999.2	1004
		Longit.	-0.285	0.872	-0.127	-0.456	-0.167	1.10	0.266
		Transv.	2.84	3.56	6.22	3.53	3.95	3.97	6.40
	East	Vertical	1150	1137	1128	827	814	803	795
		Longit.	-0.117	0.665	0.959	-0.312	-0.0765	1.06	1.48
		Transv.	1.87	2.25	2.16	2.55	2.59	2.11	2.65
Pier 4	West	Vertical	559	561	563	400	403	404	404
		Longit.	-3.57	1.36	17.2	-4.84	-1.70	4.39	17.69
		Transv.	-2.18	-1.91	0.486	-4.19	-4.35	-3.24	-1.13
	Middle	Vertical	734	737	738	526	530	530	530
		Longit.	-3.15	0.864	14.0	-4.28	-1.68	3.47	14.7
		Transv.	-2.25	-2.64	-1.86	-3.99	-4.48	-3.81	-2.35
	East	Vertical	561	563	564	402	405	406	407
		Longit.	-2.14	0.443	9.58	-2.92	-1.25	2.14	10.4
		Transv.	-2.02	-2.55	-3.28	-3.50	-3.79	-3.27	-3.10

Notes:  
 1. Positive longitudinal direction points north.  
 2. Positive transverse direction points east.

1991  
1992

**Table F-27. Calculated displacements at support locations for redundancy evaluation. All results in inches.**

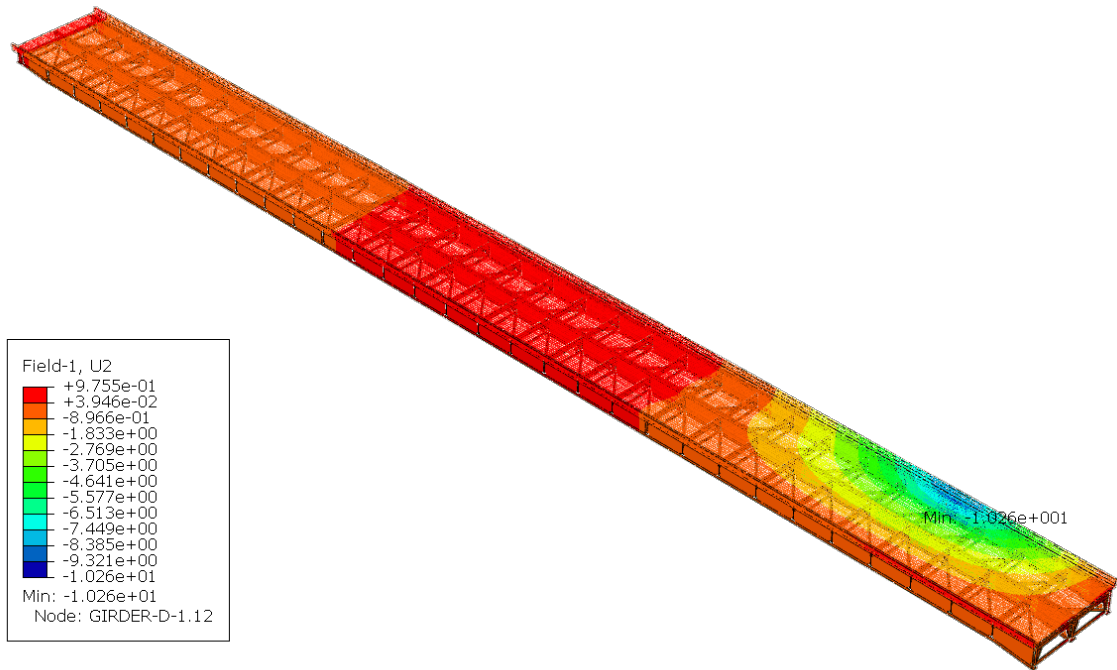
Support	Girder	Reaction Force	Redundancy I			Redundancy II			
			1 Lane	2 Lanes	3 Lanes	1 Lane	2 Lanes	3 Lanes	4 Lanes
Pier 1	West	Longit.	-0.0451	0.0594	0.295	-0.0719	0.0198	0.147	0.318
		Transv.	3.13E-3	-4.47E-3	-0.0252	9.84E-3	7.30E-3	-4.22E-3	-0.0236
	Middle	Longit.	-0.0844	-0.0135	0.331	-0.108	-0.0632	0.0500	0.385
		Transv.	2.61E-3	1.09E-3	-1.94E-3	6.94E-3	6.08E-3	4.29E-3	6.75E-4
	East	Longit.	-0.0719	-0.0742	0.145	-0.074	-0.0891	-0.0836	0.161
		Transv.	3.71E-4	8.56E-3	0.0241	7.67E-5	4.74E-3	0.0145	0.0267
Pier 2	West	Longit.	0.0748	2.02E-3	-0.254	0.0972	0.0295	-0.0563	-0.284
		Transv.	3.25E-3	-2.81E-3	-5.55E-3	-3.92E-3	-9.32E-3	-0.0124	-8.07E-3
	Middle	Longit.	0.0610	0.0231	-0.281	0.0762	0.0386	-0.0364	-0.332
		Transv.	-4.48E-3	3.81E-3	0.0140	-0.0151	-9.93E-3	-3.33E-3	8.71E-3
	East	Longit.	0.0620	0.0337	-0.262	0.0699	0.0486	-1.67E-3	-0.295
		Transv.	-7.27E-3	-5.14E-3	0.0135	-0.0129	-0.0168	-0.0144	3.29E-3
Pier 3	West	Longit.	3.69E-3	-6.39E-3	0.0112	4.46E-3	2.25E-3	-6.41E-3	9.74E-3
		Transv.	-4.54E-3	-4.84E-3	-5.12E-3	-5.89E-3	-5.23E-3	-3.10E-3	-2.52E-3
	Middle	Longit.	2.42E-3	-7.39E-3	1.08E-3	3.87E-3	1.41E-3	-9.29E-3	-2.25E-3
		Transv.	-4.71E-3	-5.91E-3	-0.0103	-5.86E-3	-6.57E-3	-6.60E-3	-0.0106
	East	Longit.	1.49E-3	-8.49E-3	-0.0122	3.98E-3	9.76E-4	-0.0135	-0.0188
		Transv.	-3.53E-3	-4.25E-3	-4.07E-3	-4.80E-3	-4.89E-3	-3.97E-3	-5.00E-3
Pier 4	West	Longit.	0.0222	-8.42E-3	-0.107	0.0301	0.0106	-0.0273	-0.110
		Transv.	2.89E-3	2.53E-3	-6.44E-4	5.54E-3	5.76E-3	4.29E-3	1.49E-3
	Middle	Longit.	0.0232	-6.36E-3	-0.103	0.0315	0.0124	-0.0255	-0.108
		Transv.	3.15E-3	3.70E-3	2.61E-3	5.60E-3	6.29E-3	5.35E-3	3.31E-3
	East	Longit.	0.024	-4.99E-3	-0.108	0.0328	0.0141	-0.0241	-0.117
		Transv.	3.23E-3	4.07E-3	5.23E-3	5.59E-3	6.05E-3	5.22E-3	4.95E-3
Notes:									
1. Positive longitudinal direction points north.									
2. Positive transverse direction points east.									

1993  
1994  
1995  
1996  
1997

Additionally, the system demonstrated a reserve margin of at least 15% of the applied live load in the Redundancy I and II load combinations. Effectively, this requirement ensures the slope of the load vs displacement curve for the system structure remains positive (i.e., there is still significant remaining reserve capacity).

1998 **F.5.7.2 Minimum Serviceability Requirements**

1999 The only serviceability requirement in the Appendix E is that the increase of deflection after the failure  
2000 of a primary steel tension member cannot be greater than  $L/50$ . This requirement is to be checked in the  
2001 Redundancy II load combination under factored dead load only. In the current case, the limit is 52 inches,  
2002 which was not surpassed since the maximum additional deflection computed in the FEA was 10.3 inches.  
2003 This is illustrated in Figure F-81.  
2004



2005 **Figure F-81. Deflection after failure of primary steel tension member.**  
2006

2007 **F.5.8 Conclusions**

2008 The redundancy of a straight continuous three-span three-girder bridge after the failure of the exterior  
2009 girder was analyzed in accordance with the methodology described in the proposed guide specification in  
2010 Appendix E. Based on the comparison between the calculated results and the minimum performance  
2011 requirements, the structure is not likely to fail nor undergo a significant serviceability loss as result after  
2012 the failure of the exterior tub girder. Hence, the westernmost girder may be re-designated as a system  
2013 redundant member (SRM).